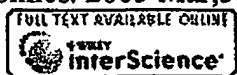


Best Available Copy

Exhibit 1



A transcriptomic and proteomic analysis of the effect of CpG-ODN on human THP-1 monocytic leukemia cells.

Kuo CC, Kuo CW, Liang CM, Liang SM.

Institute of BioAgricultural Sciences, Academia Sinica, Taipei, Taiwan.

The CpG motif of bacterial DNA (CpG-DNA) is a potent immunostimulating agent whose mechanism of action is not yet clear. Here, we used both DNA microarray and proteomic approaches to investigate the effects of oligodeoxynucleotides containing the CpG motif (CpG-ODN) on gene transcription and protein expression profiles of CpG-ODN responsive THP-1 cells. Microarray analysis revealed that 2 h stimulation with CpG-ODN up-regulated 50 genes and down-regulated five genes. These genes were identified as being associated with inflammation, antimicrobial defense, transcriptional regulation, signal transduction, tumor progression, cell differentiation, proteolysis and metabolism. Longer stimulation (8 h) with CpG-ODN enhanced transcriptional expression of 58 genes. Among these 58 genes, none except one, namely WNT1 inducible signaling pathway protein 2, was the same as those induced after 2 h stimulation. Proteomic analysis by two-dimensional gel electrophoresis, followed by mass spectrometry identified several proteins up-regulated by CpG-ODN. These proteins included heat shock proteins, modulators of inflammation, metabolic proteins and energy pathway proteins. Comparison of microarray and proteomic expression profiles showed poor correlation. Use of more reliable and sensitive analyses, such as reverse transcriptase polymerase chain reaction, Western blotting and functional assays, on several genes and proteins, nonetheless, confirmed that there is indeed good correlation between mRNA and protein expression after CpG-ODN treatment. This study also revealed that several anti-apoptotic and neuroprotective related proteins, not previously reported, are activated by CpG-DNA. These findings have extended our knowledge on the activation of cells by CpG-DNA and may contribute to further understanding of mechanisms that link innate immunity with acquired immune response(s).

PMID: 15693060 [PubMed - indexed for MEDLINE]

Type IV collagenase (M(r) 72,000) expression in human prostate: benign and malignant tissue.

Stearns ME, Wang M.

Department of Pathology, Medical College of Pennsylvania, Philadelphia 19129.

The expression of type IV collagenase (M(r) 72,000) has been examined in tissues from patients with benign prostatic hyperplasia (6 patients) and varying Gleason grades of malignant prostate cancer (18 patients). Immunoperoxidase labeling indicated that expression of the type IV collagenase was weak or nonexistent in benign tissue but consistently strong in the glandular and ductal epithelial cells of prostate tumors diagnosed at Gleason grades 1-8. In moderate to advanced cancer (i.e., Gleason grades 2 to 8), invasive tumor foci in the stromal tissue produced relatively modest amounts of type IV collagenase. The normal stromal tissue (i.e., fibroblasts) uniformly failed to produce detectable levels of type IV collagenase in the 24 patients examined. Northern and quantitative slot blot hybridization assays demonstrated that collagenase type IV mRNA levels were low in benign tissue and high in malignant tumors. In contrast, the stromal cells did not express significant amounts of type IV collagenase mRNA. Enzyme-linked immunosorbent assays demonstrated that the amounts of type IV collagenase protein correlated directly with the mRNA levels in the tumor tissue. The studies suggest that type IV collagenase may be selectively overexpressed by malignant, preinvasive prostatic epithelial cells.

PMID: 7679051 [PubMed - indexed for MEDLINE]

Genome-wide Study of Gene Copy Numbers, Transcripts, and Protein Levels in Pairs of Non-invasive and Invasive Human Transitional Cell Carcinomas*

Torben F. Ørntoft^{‡§}, Thomas Thykjaer[¶], Frederic M. Waldman^{||}, Hans Wolf^{**}, and Jullo E. Celis^{‡‡}

Gain and loss of chromosomal material is characteristic of bladder cancer, as well as malignant transformation in general. The consequences of these changes at both the transcription and translation levels is at present unknown partly because of technical limitations. Here we have attempted to address this question in pairs of non-invasive and invasive human bladder tumors using a combination of technology that included comparative genomic hybridization, high density oligonucleotide array-based monitoring of transcript levels (5600 genes), and high resolution two-dimensional gel electrophoresis. The results showed that there is a gene dosage effect that in some cases superimposes on other regulatory mechanisms. This effect depended ($p < 0.015$) on the magnitude of the comparative genomic hybridization change. In general (18 of 23 cases), chromosomal areas with more than 2-fold gain of DNA showed a corresponding increase in mRNA transcripts. Areas with loss of DNA, on the other hand, showed either reduced or unaltered transcript levels. Because most proteins resolved by two-dimensional gels are unknown it was only possible to compare mRNA and protein alterations in relatively few cases of well focused abundant proteins. With few exceptions we found a good correlation ($p < 0.005$) between transcript alterations and protein levels. The implications, as well as limitations, of the approach are discussed. *Molecular & Cellular Proteomics* 1:37–45, 2002.

Aneuploidy is a common feature of most human cancers (1), but little is known about the genome-wide effect of this

phenomenon at both the transcription and translation levels. High throughput array studies of the breast cancer cell line BT474 has suggested that there is a correlation between DNA copy numbers and gene expression in highly amplified areas (2), and studies of individual genes in solid tumors have revealed a good correlation between gene dose and mRNA or protein levels in the case of *c-erb-B2*, *cyclin d1*, *ems1*, and *N-myc* (3–5). However, a high cyclin D1 protein expression has been observed without simultaneous amplification (4), and a low level of *c-myc* copy number increase was observed without concomitant *c-myc* protein overexpression (6).

In human bladder tumors, karyotyping, fluorescent *in situ* hybridization, and comparative genomic hybridization (CGH)¹ have revealed chromosomal aberrations that seem to be characteristic of certain stages of disease progression. In the case of non-invasive pTa transitional cell carcinomas (TCCs), this includes loss of chromosome 9 or parts of it, as well as loss of Y in males. In minimally invasive pT1 TCCs, the following alterations have been reported: 2q–, 11p–, 1q+, 11q13+, 17q+, and 20q+ (7–12). It has been suggested that these regions harbor tumor suppressor genes and oncogenes; however, the large chromosomal areas involved often contain many genes, making meaningful predictions of the functional consequences of losses and gains very difficult.

In this investigation we have combined genome-wide technology for detecting genomic gains and losses (CGH) with gene expression profiling techniques (microarrays and proteomics) to determine the effect of gene copy number on transcript and protein levels in pairs of non-invasive and invasive human bladder TCCs.

EXPERIMENTAL PROCEDURES

Material—Bladder tumor biopsies were sampled after informed consent was obtained and after removal of tissue for routine pathology examination. By light microscopy tumors 335 and 532 were staged by an experienced pathologist as pTa (superficial papillary).

¹ The abbreviations used are: CGH, comparative genomic hybridization; TCC, transitional cell carcinoma; LOH, loss of heterozygosity; PA-FABP, psoriasis-associated fatty acid-binding protein; 2D, two-dimensional.

From the [‡]Department of Clinical Biochemistry, Molecular Diagnostic Laboratory and ^{**}Department of Urology, Aarhus University Hospital, Skejby, DK-8200 Aarhus N, Denmark, [‡]AAROS Applied Biotechnology ApS, Gustav Wiedsvej 10, DK-8000 Aarhus C, Denmark, ^{||}UCSF Cancer Center and Department of Laboratory Medicine, University of California, San Francisco, CA 94143-0808, and ^{‡‡}Institute of Medical Biochemistry and Danish Centre for Human Genome Research, Ole Worms Allé 170, Aarhus University, DK-8000 Aarhus C, Denmark

Received, September 26, 2001, and in revised form, November 7, 2001

Published, MCP Papers in Press, November 13, 2001, DOI 10.1074/mcp.M100019-MCP200

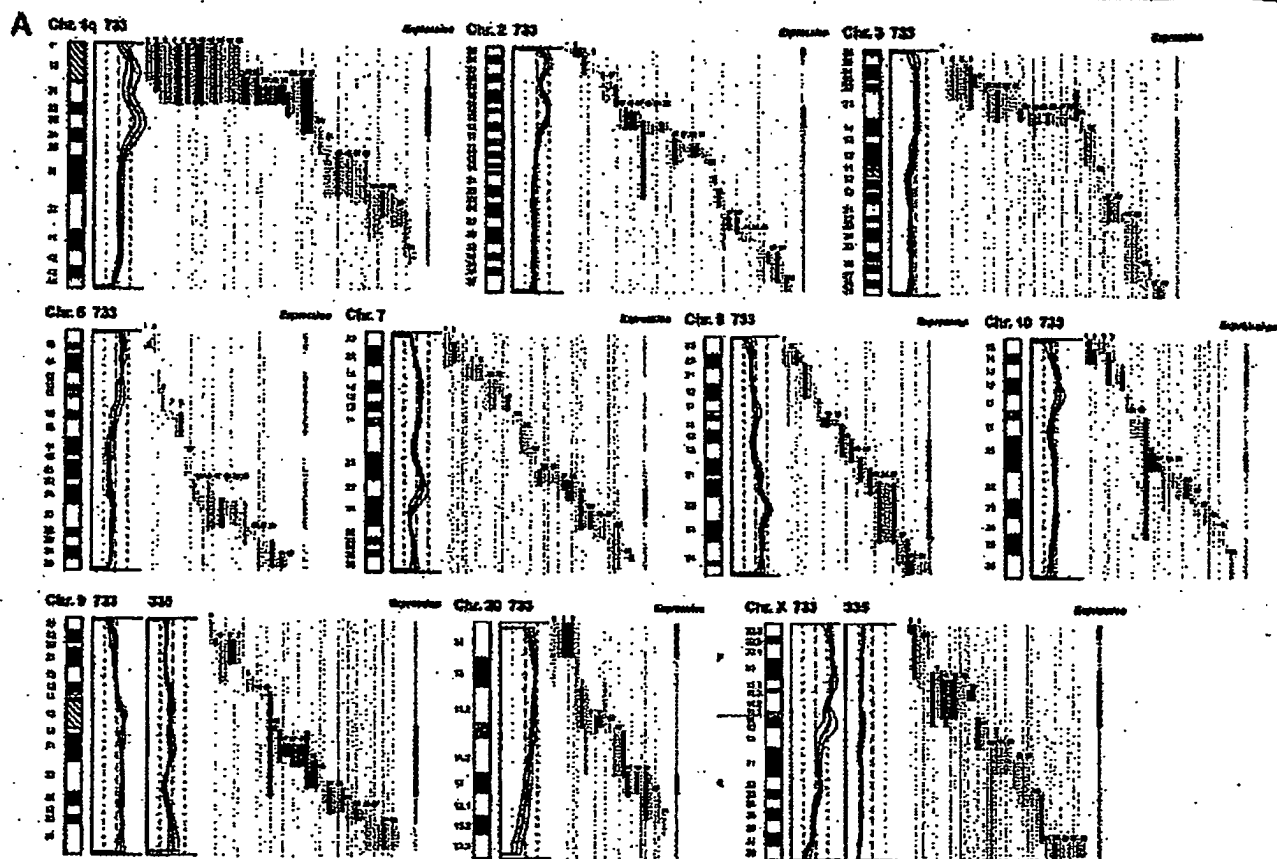


Fig. 1. DNA copy number and mRNA expression level. Shown from left to right are chromosome (Chr.), CGH profiles, gene location and expression level of specific genes, and overall expression level along the chromosome. **A**, expression of mRNA in invasive tumor 733 as compared with the non-invasive counterpart tumor 335. **B**, expression of mRNA in invasive tumor 827 compared with the non-invasive counterpart tumor 532. The average fluorescent signal ratio between tumor DNA and normal DNA is shown along the length of the chromosome (left). The bold curve in the ratio profile represents a mean of four chromosomes and is surrounded by thin curves indicating one standard deviation. The central vertical line (broken) indicates a ratio value of 1 (no change), and the vertical lines next to it (dotted) indicate a ratio of 0.5 (left) and 2.0 (right). In chromosomes where the non-invasive tumor 335 used for comparison showed alterations in DNA content, the ratio profile of that chromosome is shown to the right of the invasive tumor profile. The colored bars represent one gene each, identified by the running numbers above the bars (the name of the gene can be seen at www.MDL.DK/sdata.html). The bars indicate the purported location of the gene, and the colors indicate the expression level of the gene in the invasive tumor compared with the non-invasive counterpart; >2-fold increase (black), >2-fold decrease (blue), no significant change (orange). The bar to the far right, entitled Expression shows the resulting change in expression along the chromosome; the colors indicate that at least half of the genes were up-regulated (black), at least half of the genes down-regulated (blue), or more than half of the genes are unchanged (orange). If a gene was absent in one of the samples and present in another, it was regarded as more than a 2-fold change. A 2-fold level was chosen as this corresponded to one standard deviation in a double determination of ~1800 genes. Centromeres and heterochromatic regions were excluded from data analysis.

grade I and II, respectively, tumors 733 and 827 were staged as pT1 (invasive into submucosa), 733 was staged as solid, and 827 was staged as papillary, both grade III.

mRNA Preparation—Tissue biopsies, obtained fresh from surgery, were embedded immediately in a sodium-guanidinium thiocyanate solution and stored at -80°C . Total RNA was isolated using the RNeasy B RNA isolation method (WAK-Chemie Medical GmbH). poly(A)⁺ RNA was isolated by an oligo(dT) selection step (Oligotex mRNA kit; Qiagen).

cRNA Preparation—1 μg of mRNA was used as starting material. The first and second strand cDNA synthesis was performed using the SuperScript[®] choice system (Invitrogen) according to the manufacturer's instructions but using an oligo(dT) primer containing a T7 RNA polymerase binding site. Labeled cRNA was prepared using the MEGAscript[®] *in vitro* transcription kit (Ambion). Biotin-labeled CTP and

UTP (Enzo) was used, together with unlabeled NTPs in the reaction. Following the *in vitro* transcription reaction, the unincorporated nucleotides were removed using RNeasy columns (Qiagen).

Array Hybridization and Scanning—Array hybridization and scanning was modified from a previous method (13). 10 μg of cRNA was fragmented at 94°C for 35 min in buffer containing 40 mM Tris acetate, pH 8.1, 100 mM KOAc, 30 mM MgOAc. Prior to hybridization, the fragmented cRNA in a 6 \times SSPE-T hybridization buffer (1 M NaCl, 10 mM Tris, pH 7.6, 0.005% Triton), was heated to 85°C for 5 min, subsequently cooled to 40°C , and loaded onto the Affymetrix probe array cartridge. The probe array was then incubated for 16 h at 40°C at constant rotation (60 rpm). The probe array was exposed to 10 washes in 6 \times SSPE-T at 25°C followed by 4 washes in 0.5 \times SSPE-T at 50°C . The biotinylated cRNA was stained with a streptavidin-phycoerythrin conjugate, 10 $\mu\text{g}/\text{ml}$ (Molecular Probes) in 6 \times SSPE-T

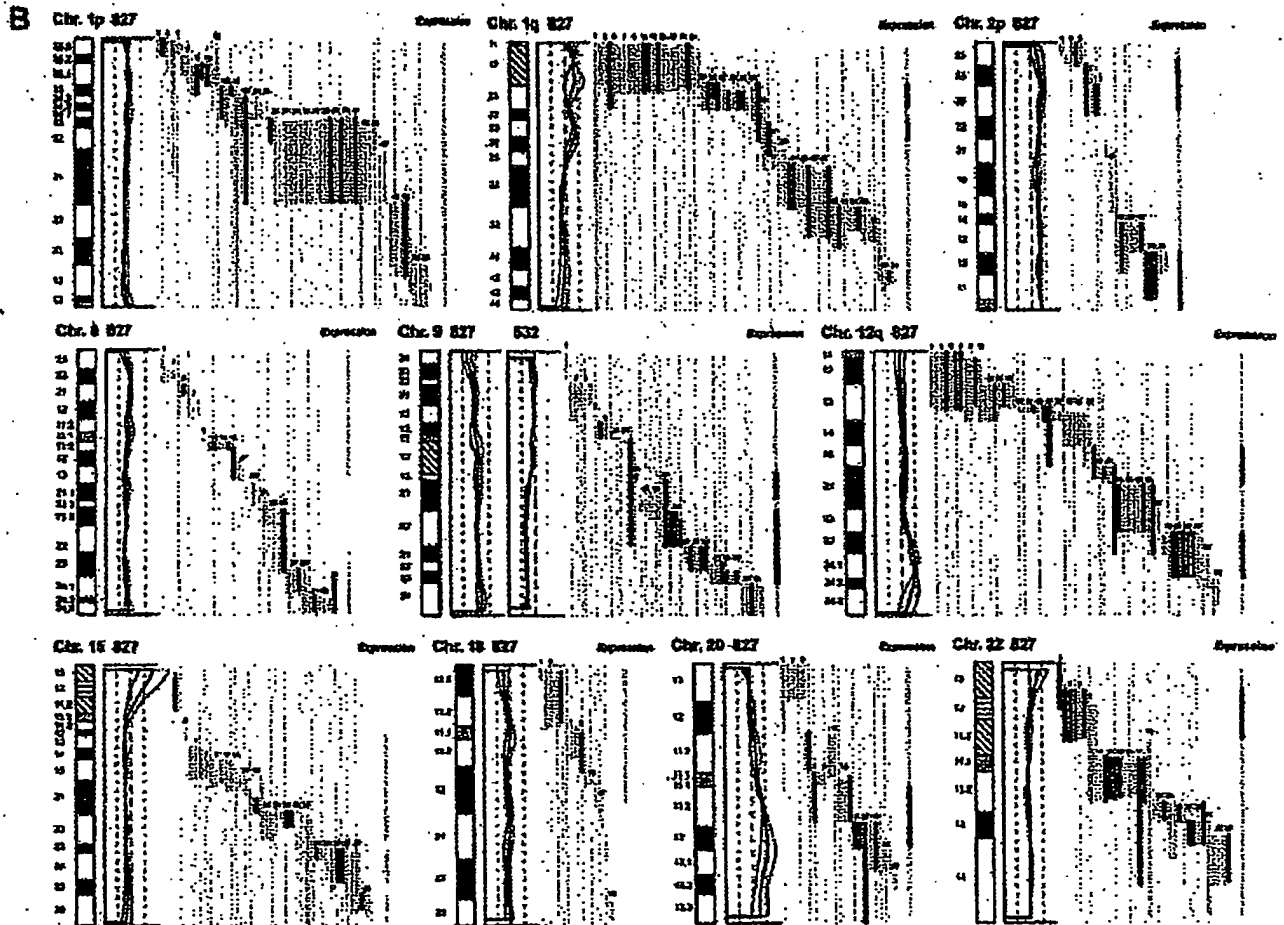


Fig. 1—continued

for 30 min at 25 °C followed by 10 washes in 6× SSPE-T at 25 °C. The probe arrays were scanned at 560 nm using a confocal laser scanning microscope (made for Affymetrix by Hewlett-Packard). The readings from the quantitative scanning were analyzed by Affymetrix gene expression analysis software.

Microsatellite Analysis—Microsatellite Analysis was performed as described previously (14). Microsatellites were selected by use of www.ncbi.nlm.nih.gov/genemap98, and primer sequences were obtained from the genome data base at www.gdb.org. DNA was extracted from tumor and blood and amplified by PCR in a volume of 20 μ l for 35 cycles. The amplicons were denatured and electrophoresed for 3 h in an ABI Prism 377. Data were collected in the Gene Scan program for fragment analysis. Loss of heterozygosity was defined as less than 33% of one allele detected in tumor amplicons compared with blood.

Proteomic Analysis—TCCs were minced into small pieces and homogenized in a small glass homogenizer in 0.5 ml of lysis solution. Samples were stored at -20 °C until use. The procedure for 2D gel electrophoresis has been described in detail elsewhere (15, 16). Gels were stained with silver nitrate and/or Coomassie Brilliant Blue. Proteins were identified by a combination of procedures that included microsequencing, mass spectrometry, two-dimensional gel Western immunoblotting, and comparison with the master two-dimensional gel image of human keratinocyte proteins; see biobase.dk/cgi-bin/cells.

CGH—Hybridization of differentially labeled tumor and normal DNA to normal metaphase chromosomes was performed as described previously (10). Fluorescein-labeled tumor DNA (200 ng), Texas Red-

labeled reference DNA (200 ng), and human Cot-1 DNA (20 μ g) were denatured at 37 °C for 5 min and applied to denatured normal metaphase slides. Hybridization was at 37 °C for 2 days. After washing, the slides were counterstained with 0.15 μ g/ml 4,6-diamidino-2-phenylindole in an anti-fade solution. A second hybridization was performed for all tumor samples using fluorescein-labeled reference DNA and Texas Red-labeled tumor DNA (inverse labeling) to confirm the aberrations detected during the initial hybridization. Each CGH experiment also included a normal control hybridization using fluorescein- and Texas Red-labeled normal DNA. Digital image analysis was used to identify chromosomal regions with abnormal fluorescence ratios, indicating regions of DNA gains and losses. The average green:red fluorescence intensity ratio profiles were calculated using four images of each chromosome (eight chromosomes total) with normalization of the green:red fluorescence intensity ratio for the entire metaphase and background correction. Chromosome identification was performed based on 4,6-diamidino-2-phenylindole banding patterns. Only images showing uniform high intensity fluorescence with minimal background staining were analyzed. All centromeres, p arms of acrocentric chromosomes, and heterochromatic regions were excluded from the analysis.

RESULTS

Comparative Genomic Hybridization—The CGH analysis identified a number of chromosomal gains and losses in the

Gene Copy Numbers, Transcripts, and Protein Levels

TABLE I
Correlation between alterations detected by CGH and by expression monitoring

Top, CGH used as independent variable (if CGH alteration – what expression ratio was found); bottom, altered expression used as independent variable (if expression alteration – what CGH deviation was found).

CGH alterations	Tumor 733 vs. 335		Concordance	CGH alterations	Tumor 827 vs. 532		Concordance
	Expression change clusters				Expression change clusters		
13 Gain	10 Up-regulation		77%	10 Gain	8 Up-regulation		80%
	0 Down-regulation				0 Down-regulation		
	3 No change				2 No change		
10 Loss	1 Up-regulation		50%	12 Loss	3 Up-regulation		17%
	6 Down-regulation				2 Down regulation		
	4 No change				7 No change		
Expression change clusters	Tumor 733 vs. 335		Concordance	Expression change clusters	Tumor 827 vs. 532		Concordance
	CGH alterations				CGH alterations		
16 Up-regulation	11 Gain		69%	17 Up-regulation	10 Gain		59%
	2 Loss				5 Loss		
	3 No change				2 No change		
21 Down-regulation	1 Gain		38%	9 Down-regulation	0 Gain		33%
	8 Loss				3 Loss		
	12 No change				6 No change		
15 No change	3 Gain		60%	21 No change	1 Gain		81%
	3 Loss				3 Loss		
	9 No change				17 No change		

two invasive tumors (stage pT1, TCCs 733 and 827), whereas the two non-invasive papillomas (stage pTa, TCCs 335 and 532) showed only 9p–, 9q22–q33–, and X–, and 7+, 9q–, and Y–, respectively. Both invasive tumors showed changes (1q22–24+, 2q14.1–qter–, 3q12–q13.3–, 6q12–q22–, 9q34+, 11q12–q13+, 17+, and 20q11.2–q12+) that are typical for their disease stage, as well as additional alterations, some of which are shown in Fig. 1. Areas with gains and losses deviated from the normal copy number to some extent, and the average numerical deviation from normal was 0.4-fold in the case of TCC 733 and 0.3-fold for TCC 827. The largest changes, amounting to at least a doubling of chromosomal content, were observed at 1q23 in TCC 733 (Fig. 1A) and 20q12 in TCC 827 (Fig. 1B).

mRNA Expression in Relation to DNA Copy Number—The mRNA levels from the two invasive tumors (TCCs 827 and 733) were compared with the two non-invasive counterparts (TCCs 532 and 335). This was done in two separate experiments in which we compared TCCs 733 to 335 and 827 to 532, respectively, using two different scaling settings for the arrays to rule out scaling as a confounding parameter. Approximately 1,800 genes that yielded a signal on the arrays were searched in the Unigene and Genemap data bases for chromosomal location, and those with a known location (1096) were plotted as bars covering their purported locus. In that way it was possible to construct a graphic presentation of DNA copy number and relative mRNA levels along the individual chromosomes (Fig. 1).

For each mRNA a ratio was calculated between the level in the invasive versus the non-invasive counterpart. Bars, which represent chromosomal location of a gene, were color-coded according to the expression ratio, and only differences larger

than 2-fold were regarded as informative (Fig. 1). The density of genes along the chromosomes varied, and areas containing only one gene were excluded from the calculations. The resolution of the CGH method is very low, and some of the outlier data may be because of the fact that the boundaries of the chromosomal aberrations are not known at high resolution.

Two sets of calculations were made from the data. For the first set we used CGH alterations as the independent variable and estimated the frequency of expression alterations in these chromosomal areas. In general, areas with a strong gain of chromosomal material contained a cluster of genes having increased mRNA expression. For example, both chromosomes 1q21–q25, 2p and 9q, showed a relative gain of more than 100% in DNA copy number that was accompanied by increased mRNA expression levels in the two tumor pairs (Fig. 1). In most cases, chromosomal gains detected by CGH were accompanied by an increased level of transcripts in both TCCs 733 (77%) and 827 (80%) (Table I, top). Chromosomal losses, on the other hand, were not accompanied by decreased expression in several cases, and were often registered as having unaltered RNA levels (Table I, top). The inability to detect RNA expression changes in these cases was not because of fewer genes mapping to the lost regions (data not shown).

In the second set of calculations we selected expression alterations above 2-fold as the independent variable and estimated the frequency of CGH alterations in these areas. As above, we found that increased transcript expression correlated with gain of chromosomal material (TCC 733, 69% and TCC 827, 59%), whereas reduced expression was often detected in areas with unaltered CGH ratios (Table I, bottom). Furthermore, as a control we looked at areas with no alter-

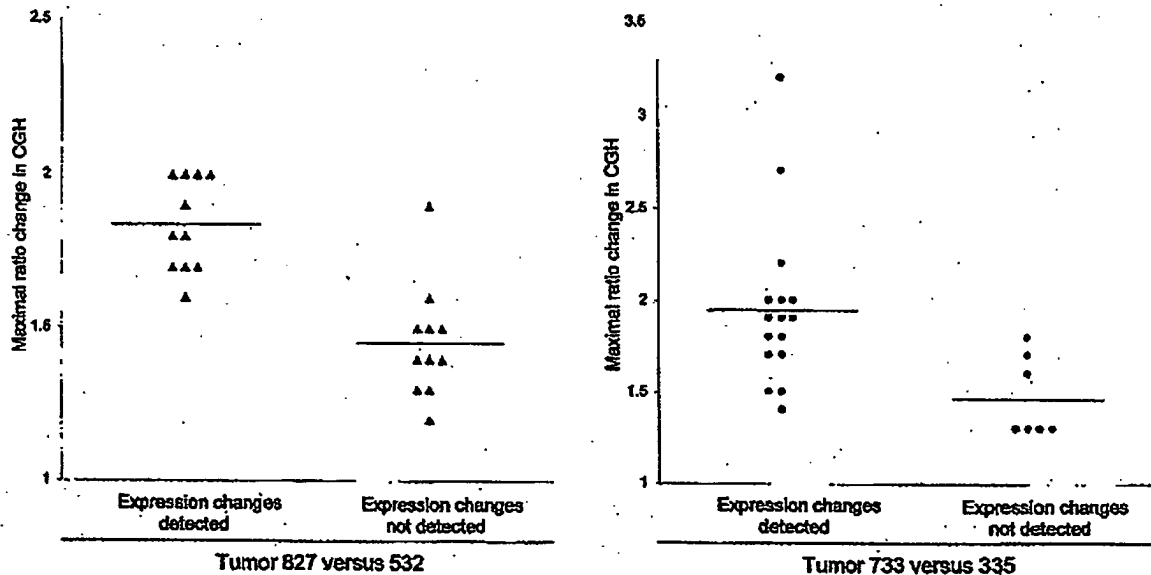


FIG. 2. Correlation between maximum CGH aberration and the ability to detect expression change by oligonucleotide array monitoring. The aberration is shown as a numerical -fold change in ratio between invasive tumors 827 (▲) and 733 (◆) and their non-invasive counterparts 532 and 335. The expression change was taken from the *Expression* line to the right in Fig. 1, which depicts the resulting expression change for a given chromosomal region. At least half of the mRNAs from a given region have to be either up- or down-regulated to be scored as an expression change. All chromosomal arms in which the CGH ratio plus or minus one standard deviation was outside the ratio value of one were included.

ation in expression. No alteration was detected by CGH in most of these areas (TCC 733, 60% and TCC 827, 81%; see Table I, bottom). Because the ability to observe reduced or increased mRNA expression clustering to a certain chromosomal area clearly reflected the extent of copy number changes, we plotted the maximum CGH aberrations in the regions showing CGH changes against the ability to detect a change in mRNA expression as monitored by the oligonucleotide arrays (Fig. 2). For both tumors TCC 733 ($p < 0.015$) and TCC 827 ($p < 0.00003$) a highly significant correlation was observed between the level of CGH ratio change (reflecting the DNA copy number) and alterations detected by the array based technology (Fig. 2). Similar data were obtained when areas with altered expression were used as independent variables. These areas correlated best with CGH when the CGH ratio deviated 1.6- to 2.0-fold (Table I, bottom) but mostly did not at lower CGH deviations. These data probably reflect that loss of an allele may only lead to a 50% reduction in expression level, which is at the cut-off point for detection of expression alterations. Gain of chromosomal material can occur to a much larger extent.

Microsatellite-based Detection of Minor Areas of Losses—In TCC 733, several chromosomal areas exhibiting DNA amplification were preceded or followed by areas with a normal CGH but reduced mRNA expression (see Fig. 1, TCC 733 chromosome 1q32, 2p21, and 7q21 and q32, 9q34, and 10q22). To determine whether these results were because of undetected loss of chromosomal material in these regions or

because of other non-structural mechanisms regulating transcription, we examined two microsatellites positioned at chromosome 1q25-32 and two at chromosome 2p22. Loss of heterozygosity (LOH) was found at both 1q25 and at 2p22 indicating that minor deleted areas were not detected with the resolution of CGH (Fig. 3). Additionally, chromosome 2p in TCC 733 showed a CGH pattern of gain/no change/gain of DNA that correlated with transcript increase/decrease/increase. Thus, for the areas showing increased expression there was a correlation with the DNA copy number alterations (Fig. 1A). As indicated above, the mRNA decrease observed in the middle of the chromosomal gain was because of LOH, implying that one of the mechanisms for mRNA down-regulation may be regions that have undergone smaller losses of chromosomal material. However, this cannot be detected with the resolution of the CGH method.

In both TCC 733 and TCC 827, the telomeric end of chromosome 11p showed a normal ratio in the CGH analysis; however, clusters of five and three genes, respectively, lost their expression. Two microsatellites (D11S1760, D11S922) positioned close to MUC2, IGF2, and cathepsin D indicated LOH as the most likely mechanism behind the loss of expression (data not shown).

A reduced expression of mRNA observed in TCC 733 at chromosomes 3q24, 11p11, 12p12.2, 12q21.1, and 16q24 and in TCC 827 at chromosome 11p15.5, 12p11, 15q11.2, and 18q12 was also examined for chromosomal losses using microsatellites positioned as close as possible to the gene loci

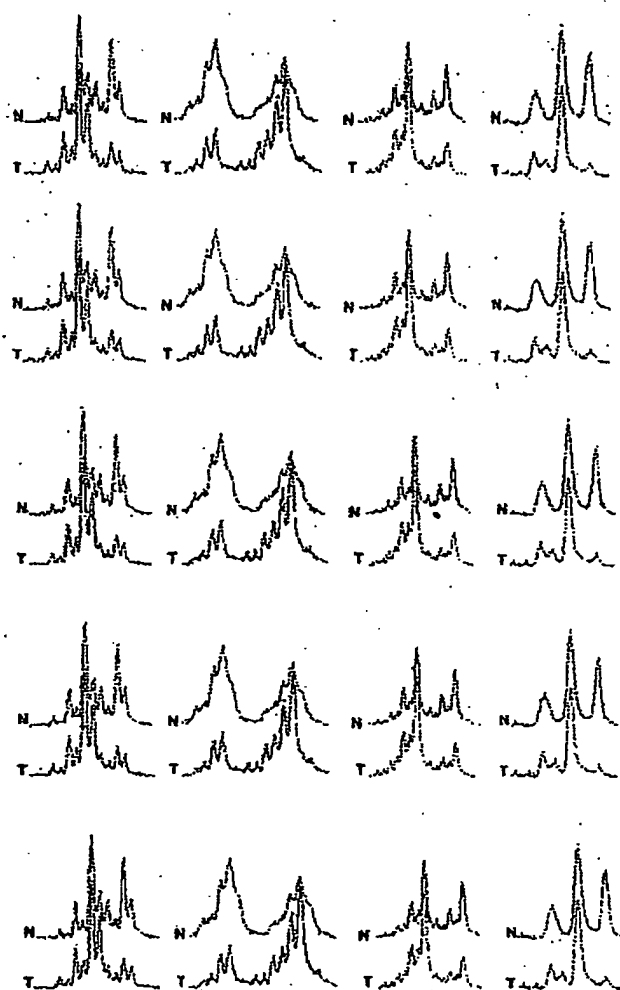


Fig. 3. Microsatellite analysis of loss of heterozygosity. Tumor 733 showing loss of heterozygosity at chromosome 1q25, detected (a) by D1S215 close to Hu class I histocompatibility antigen (gene number 38 in Fig. 1), (b) by D1S2735 close to cathepsin E (gene number 41 in Fig. 1), and (c) at chromosome 2p23 by D2S2251 close to general β -spectrin (gene number 11 on Fig. 1) and of (d) tumor 827 showing loss of heterozygosity at chromosome 18q12 by S18S1118 close to mitochondrial 3-oxoacyl-coenzyme A thiolase (gene number 12 in Fig. 1). The upper curves show the electropherogram obtained from normal DNA from leukocytes (N), and the lower curves show the electropherogram from tumor DNA (T). In all cases one allele is partially lost in the tumor amplicon.

showing reduced mRNA transcripts. Only the microsatellite positioned at 18q12 showed LOH (Fig. 3), suggesting that transcriptional down-regulation of genes in the other regions may be controlled by other mechanisms.

Relation between Changes in mRNA and Protein Levels—2D-PAGE analysis, in combination with Coomassie Brilliant Blue and/or silver staining, was carried out on all four tumors using fresh biopsy material. 40 well resolved abundant known proteins migrating in areas away from the edges of the pH

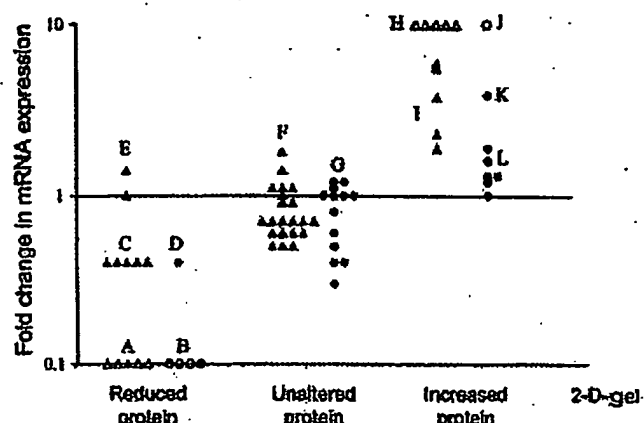


Fig. 4. Correlation between protein levels as judged by 2D-PAGE and transcript ratio. For comparison proteins were divided in three groups, unaltered in level or up- or down-regulated (horizontal axis). The mRNA ratio as determined by oligonucleotide arrays was plotted for each gene (vertical axis). Δ , mRNAs that were scored as present in both tumors used for the ratio calculation; \triangle , mRNAs that were scored as absent in the invasive tumors (along horizontal axis) or as absent in non-invasive reference (top of figure). Two different scalings were used to exclude scaling as a confounder, TCCs 827 and 532 ($\Delta\Delta$) were scaled with background suppression, and TCCs 733 and 335 ($\bullet\bullet$) were scaled without suppression. Both comparisons showed highly significant ($p < 0.005$) differences in mRNA ratios between the groups. Proteins shown were as follows: Group A (from left), phosphoglucomutase 1, glutathione transferase class μ number 4, fatty acid-binding protein homologue, cytochrome 15, and cytochrome 13; B (from left), fatty acid-binding protein homologue, 28-kDa heat shock protein, cytochrome 13, and calnexin; C (from left), α -enolase, hnRNP B1, 28-kDa heat shock protein, 14-3-3- ϵ , and pre-mRNA splicing factor; D, mesothelial keratin K7 (type II); E (from top), glutathione S-transferase- π and mesothelial keratin K7 (type II); F (from top and left), adenyl cyclase-associated protein, E-cadherin, keratin 19, calnexin, phosphoglycerate mutase, annexin IV, cytoskeletal γ -actin, hnRNP A1, integral membrane protein calnexin (IP90), hnRNP H, brain-type clathrin light chain-a, hnRNP F, 70-kDa heat shock protein, heterogeneous nuclear ribonucleoprotein A/B, translationally controlled tumor protein, liver glyceraldehyde-3-phosphate dehydrogenase, keratin 8, aldehyde reductase, and Na,K-ATPase β -1 subunit; G, (from top and left), TCP20, calnexin, 70-kDa heat shock protein, calnexin, hnRNP H, cytochrome 15, ATP synthase, keratin 19, triosephosphate isomerase, hnRNP F, liver glyceraldehyde-3-phosphate dehydrogenase, glutathione S-transferase- π , and keratin 8; H (from left), plasma gelosin, autoantigen calreticulin, thioredoxin, and NAD+-dependent 15 hydroxyprostaglandin dehydrogenase; I (from top), prolyl 4-hydroxylase β -subunit, cytochrome 20, cytochrome 17, prolyl 4-hydroxylase β -subunit, and fructose 1,6-bisphosphatase; J annexin II; K, annexin IV; L (from top and left), 90-kDa heat shock protein, prolyl 4-hydroxylase β -subunit, α -enolase, GRP 78, cyclophilin, and cofilin.

gradient, and having a known chromosomal location, were selected for analysis in the TCC pair 827/532. Proteins were identified by a combination of methods (see "Experimental Procedures"). In general there was a highly significant correlation ($p < 0.005$) between mRNA and protein alterations (Fig. 4). Only one gene showed disagreement between transcript alteration and protein alteration. Except for a group of cyto-

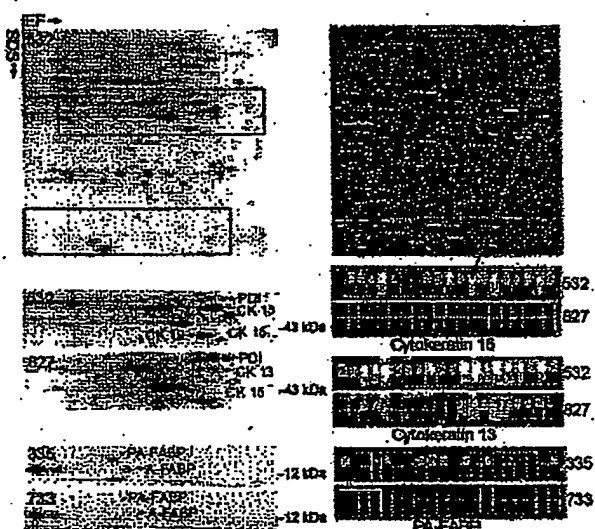


Fig. 5. Comparison of protein and transcript levels in invasive and non-invasive TCCs. The upper part of the figure shows a 2D gel (left) and the oligonucleotide array (right) of TCC 532. The red rectangles on the upper gel highlight the areas that are compared below. Identical areas of 2D gels of TCCs 532 and 827 are shown below. Clearly, cytokeratins 13 and 15 are strongly down-regulated in TCC 827 (red annotation). The tile on the array containing probes for cytokeratin 15 is enlarged below the array (red arrow) from TCC 532 and is compared with TCC 827. The upper row of squares in each tile corresponds to perfect match probes; the lower row corresponds to mismatch probes containing a mutation (used for correction for unspecific binding). Absence of signal is depicted as black, and the higher the signal the lighter the color. A high transcript level was detected in TCC 532 (6161 units) whereas a much lower level was detected in TCC 827 (absence of signals). For cytokeratin 13, a high transcript level was also present in TCC 532 (15659 units), and a much lower level was present in TCC 827 (623 units). The 2D gels at the bottom of the figure (left) show levels of PA-FABP and adipocyte-FABP in TCCs 335 and 733 (invasive), respectively. Both proteins are down-regulated in the invasive tumor. To the right we show the array tiles for the PA-FABP transcript. A medium transcript level was detected in the case of TCC 335 (1277 units) whereas very low levels were detected in TCC 733 (166 units). *IEF*, Isoelectric focusing.

keratins encoded by genes on chromosome 17 (Fig. 5) the analyzed proteins did not belong to a particular family. 26 well focused proteins whose genes had a known chromosomal location were detected in TCCs 733 and 335, and of these 19 correlated ($p < 0.005$) with the mRNA changes detected using the arrays (Fig. 4). For example, PA-FABP was highly expressed in the non-invasive TCC 335 but lost in the invasive counterpart (TCC 733; see Fig. 5). The smaller number of proteins detected in both 733 and 335 was because of the smaller size of the biopsies that were available.

11 chromosomal regions where CGH showed aberrations that corresponded to the changes in transcript levels also showed corresponding changes in the protein level (Table II). These regions included genes that encode proteins that are found to be frequently altered in bladder cancer, namely cytokeratins 17 and 20, annexins II and IV, and the fatty acid-binding proteins PA-FABP and FABP1. Four of these proteins were encoded by genes in chromosome 17q, a frequently amplified chromosomal area in invasive bladder cancers.

DISCUSSION

Most human cancers have abnormal DNA content, having lost some chromosomal parts and gained others. The present study provides some evidence as to the effect of these gains and losses on gene expression in two pairs of non-invasive and invasive TCCs using high throughput expression arrays and proteomics, in combination with CGH. In general, the results showed that there is a clear individual regulation of the mRNA expression of single genes, which in some cases was superimposed by a DNA copy number effect. In most cases, genes located in chromosomal areas with gains often exhibited increased mRNA expression, whereas areas showing losses showed either no change or a reduced mRNA expression. The latter might be because of the fact that losses most often are restricted to loss of one allele, and the cut-off point for detection of expression alterations was a 2-fold change, thus being at the border of detection. In several cases, how-

TABLE II
Proteins whose expression level correlates with both mRNA and gene dose changes

Protein	Chromosomal location	Tumor TCC	CGH alteration	Transcript alteration ^a	Protein alteration
Annexin II	1q21	733	Gain	Abs to Pres ^a	Increase
Annexin IV	2p13	733	Gain	3.9-Fold up	Increase
Cytokeratin 17	17q12-q21	827	Gain	3.8-Fold up	Increase
Cytokeratin 20	17q21.1	827	Gain	5.6-Fold up	Increase
(PA-)FABP	8q21.2	827	Loss	10-Fold down	Decrease
FABP1	9q22	827	Gain	2.3-Fold up	Increase
Plasma gelsolin	9q31	827	Gain	Abs to Pres	Increase
Heat shock protein 28	15q12-q13	827	Loss	2.5-Fold up	Decrease
Prohibitin	17q21	827/733	Gain	3.7-/2.5-Fold up ^b	Increase
Prolyl-4-hydroxyl	17q25	827/733	Gain	6.7-/1.6-Fold up	Increase
hnRNPB1	7p15	827	Loss	2.5-Fold down	Decrease

^a Abs, absent; Pres, present.

^b In cases where the corresponding alterations were found in both TCCs 827 and 733 these are shown as 827/733.

ever, an increase or decrease in DNA copy number was associated with *de novo* occurrence or complete loss of transcript, respectively. Some of these transcripts could not be detected in the non-invasive tumor but were present at relatively high levels in areas with DNA amplifications in the invasive tumors (e.g. In TCC 733 transcript from cellular ligand of annexin II gene (chromosome 1q21) from absent to 2670 arbitrary units; In TCC 827 transcript from small proline-rich protein 1 gene (chromosome 1q12-q21.1) from absent to 1326 arbitrary units). It may be anticipated from these data that significant clustering of genes with an increased expression to a certain chromosomal area indicates an increased likelihood of gain of chromosomal material in this area.

Considering the many possible regulatory mechanisms acting at the level of transcription, it seems striking that the gene dose effects were so clearly detectable in gained areas. One hypothetical explanation may lie in the loss of controlled methylation in tumor cells (17-19). Thus, it may be possible that in chromosomes with increased DNA copy numbers two or more alleles could be demethylated simultaneously leading to a higher transcription level, whereas in chromosomes with losses the remaining allele could be partly methylated, turning off the process (20, 21). A recent report has documented a ploidy regulation of gene expression in yeast, but in this case all the genes were present in the same ratio (22), a situation that is not analogous to that of cancer cells, which show marked chromosomal aberrations, as well as gene dosage effects.

Several CGH studies of bladder cancer have shown that some chromosomal aberrations are common at certain stages of disease progression, often occurring in more than 1 of 3 tumors. In pTa tumors, these include 9p-, 9q-, 1q+, Y- (2, 6), and in pT1 tumors, 2q-, 11p-, 11q-, 1q+, 5p+, 8q+, 17q+, and 20q+ (2-4, 6, 7). The pTa tumors studied here showed similar aberrations such as 9p- and 9q22-q33- and 9q- and Y-, respectively. Likewise, the two minimal invasive pT1 tumors showed aberrations that are commonly seen at that stage, and TCC 827 had a remarkable resemblance to the commonly seen pattern of losses and gains, such as 1q22-24 amplification (seen in both tumors), 11q14-q22 loss, the latter often linked to 17q+ (both tumors), and 1q+ and 9p-, often linked to 20q+ and 11q13+ (both tumors) (7-9). These observations indicate that the pairs of tumors used in this study exhibit chromosomal changes observed in many tumors, and therefore the findings could be of general importance for bladder cancer.

Considering that the mapping resolution of CGH is of about 20 megabases it is only possible to get a crude picture of chromosomal instability using this technique. Occasionally, we observed reduced transcript levels close to or inside regions with increased copy numbers. Analysis of these regions by positioning heterozygous microsatellites as close as possible to the locus showing reduced gene expression revealed loss of heterozygosity in several cases. It seems likely that multiple and different events occur along each chromosomal

arm and that the use of cDNA microarrays for analysis of DNA copy number changes will reach a resolution that can resolve these changes, as has recently been proposed (2). The outlier data were not more frequent at the boundaries of the CGH aberrations. At present we do not know the mechanism behind chromosomal aneuploidy and cannot predict whether chromosomal gains will be transcribed to a larger extent than the two native alleles. A mechanism as genetic imprinting has an impact on the expression level in normal cells and is often reduced in tumors. However, the relation between imprinting and gain of chromosomal material is not known.

We regard it as a strength of this investigation that we were able to compare invasive tumors to benign tumors rather than to normal urothelium, as the tumors studied were biologically very close and probably may represent successive steps in the progression of bladder cancer. Despite the limited amount of fresh tissue available it was possible to apply three different state of the art methods. The observed correlation between DNA copy number and mRNA expression is remarkable when one considers that different pieces of the tumor biopsies were used for the different sets of experiments. This indicates that bladder tumors are relatively homogenous, a notion recently supported by CGH and LOH data that showed a remarkable similarity even between tumors and distant metastasis (10, 23).

In the few cases analyzed, mRNA and protein levels showed a striking correspondence although in some cases we found discrepancies that may be attributed to translational regulation, post-translational processing, protein degradation, or a combination of these. Some transcripts belong to undertranslated mRNA pools, which are associated with few translationally inactive ribosomes; these pools, however, seem to be rare (24). Protein degradation, for example, may be very important in the case of polypeptides with a short half-life (e.g. signaling proteins). A poor correlation between mRNA and protein levels was found in liver cells as determined by arrays and 2D-PAGE (25), and a moderate correlation was recently reported by Ideker *et al.* (26) in yeast.

Interestingly, our study revealed a much better correlation between gained chromosomal areas and increased mRNA levels than between loss of chromosomal areas and reduced mRNA levels. In general, the level of CGH change determined the ability to detect a change in transcript. One possible explanation could be that by losing one allele the change in mRNA level is not so dramatic as compared with gain of material, which can be rather unlimited and may lead to a severalfold increase in gene copy number resulting in a much higher impact on transcript level. The latter would be much easier to detect on the expression arrays as the cut-off point was placed at a 2-fold level so as not to be biased by noise on the array. Construction of arrays with a better signal to noise ratio may in the future allow detection of lesser than 2-fold alterations in transcript levels, a feature that may facilitate the analysis of the effect of loss of chromosomal areas on transcript levels.

In eleven cases we found a significant correlation between DNA copy number, mRNA expression, and protein level. Four of these proteins were encoded by genes located at a frequently amplified area in chromosome 17q. Whether DNA copy number is one of the mechanisms behind alteration of these eleven proteins is at present unknown and will have to be proved by other methods using a larger number of samples. One factor making such studies complicated is the large extent of protein modification that occurs after translation, requiring immunoidentification and/or mass spectrometry to correctly identify the proteins in the gels.

In conclusion, the results presented in this study exemplify the large body of knowledge that may be possible to gather in the future by combining state of the art techniques that follow the pathway from DNA to protein (26). Here, we used a traditional chromosomal CGH method, but in the future high resolution CGH based on microarrays with many thousand radiation hybrid-mapped genes will increase the resolution and information derived from these types of experiments (2). Combined with expression arrays analyzing transcripts derived from genes with known locations, and 2D gel analysis to obtain information at the post-translational level, a clearer and more developed understanding of the tumor genome will be forthcoming.

Acknowledgments—We thank Mie Madsen, Hanne Steen, Inge Lis Thorsen, Hans Lund, Nikolaj Ørntoft, and Lynn Bjerke for technical help and Thomas Gingeras, Christine Harrington, and Morten Østergaard for valuable discussions.

* This work was supported by grants from The Danish Cancer Society, the University of Aarhus, Aarhus County, Novo Nordisk, the Danish Biotechnology Program, the Frenkels Foundation, the John and Birthe Meyer Foundation, and NCI, National Institutes of Health Grant CA47537. The costs of publication of this article were defrayed in part by the payment of page charges. This article must therefore be hereby marked "advertisement" in accordance with 18 U.S.C. Section 1734 solely to indicate this fact.

§ To whom correspondence should be addressed: Dept. of Clinical Biochemistry, Molecular Diagnostic Laboratory, Aarhus University Hospital, Skejby, DK-8200 Aarhus N, Denmark. Tel.: 45-89495100/45-86156201 (private); Fax: 45-89496018; E-mail: orntoft@kba.sks.au.dk.

REFERENCES

- Lengauer, C., Kinzler, K. W., and Vogelstein, B. (1998) Genetic instabilities in human cancers. *Nature* 396, 643–649.
- Pollack, J. R., Perou, C. M., Alizadeh, A. A., Eisen, M. B., Pergamenschikov, A., Williams, C. F., Jeffrey, S. S., Botstein, D., and Brown, P. O. (1999) Genome-wide analysis of DNA copy-number changes using cDNA microarrays. *Nat. Genet.* 23, 41–46.
- de Cremoux, P., Martin, E. C., Vincent-Salomon, A., Dieras, V., Barbaroux, C., Liva, S., Pouliart, P., Sastre-Garau, X., and Magdelenat, H. (1999) Quantitative PCR analysis of c-erb B-2 (HER2/neu) gene amplification and comparison with p185(HER2/neu) protein expression in breast cancer drill biopsies. *Int. J. Cancer* 83, 157–161.
- Brugler, P. P., Tamimi, Y., Shuuring, E., and Schalken, J. (1996) Expression of cyclin D1 and EMS1 in bladder tumors: relationship with chromosome 11q13 amplifications. *Oncogene* 12, 1747–1753.
- Slavc, I., Ellenbogen, R., Jung, W. H., Vawter, G. F., Kretschmar, C., Grier, H., and Korf, B. R. (1990) *myc* gene amplification and expression in primary human neuroblastoma. *Cancer Res.* 50, 1459–1463.
- Sauter, G., Carroll, P., Moch, H., Kallioniemi, A., Kerschmann, R., Narayan, P., Mihatsch, M. J., and Waldman, F. M. (1995) *c-myc* copy number gains in bladder cancer detected by fluorescence *in situ* hybridization. *Am. J. Pathol.* 148, 1131–1139.
- Richter, J., Jiang, F., Gorog, J. P., Sartorius, G., Egenter, C., Gasser, T. C., Moch, H., Mihatsch, M. J., and Sauter, G. (1997) Marked genetic differences between stage pTa and stage pT1 papillary bladder cancer detected by comparative genomic hybridization. *Cancer Res.* 57, 2860–2864.
- Richter, J., Biffa, L., Wagner, U., Schraml, P., Gasser, T. C., Moch, H., Mihatsch, M. J., and Sauter, G. (1998) Patterns of chromosomal imbalances in advanced urinary bladder cancer detected by comparative genomic hybridization. *Am. J. Pathol.* 153, 1615–1621.
- Bruch, J., Wöhr, G., Hautmann, R., Mattfeldt, T., Bruderlein, S., Moller, P., Sauter, S., Hamelster, H., Vogel, W., and Peiss, T. (1998) Chromosomal changes during progression of transitional cell carcinoma of the bladder and delineation of the amplified interval on chromosome arm 8q. *Genes Chromosomes Cancer* 23, 167–174.
- Hovey, R. M., Chu, L., Balazs, M., De Vries, S., Moore, D., Sauter, G., Carroll, P. R., and Waldman, F. M. (1998) Genetic alterations in primary bladder cancers and their metastases. *Cancer Res.* 58, 3555–3560.
- Simon, R., Burger, H., Brinkschmidt, C., Bocker, W., Hertle, L., and Terpe, H. J. (1998) Chromosomal aberrations associated with invasion in papillary superficial bladder cancer. *J. Pathol.* 185, 345–351.
- Koo, S. H., Kwon, K. C., Ihm, C. H., Jeon, Y. M., Park, J. W., and Sul, C. K. (1999) Detection of genetic alterations in bladder tumors by comparative genomic hybridization and cytogenetic analysis. *Cancer Genet. Cytogenet.* 110, 87–93.
- Wodicka, L., Dong, H., Mittmann, M., Ho, M. H., and Lockhart, D. J. (1997) Genome-wide expression monitoring in *Saccharomyces cerevisiae*. *Nat. Biotechnol.* 15, 1359–1367.
- Christensen, M., Sunde, L., Bolund, L., and Orntoft, T. F. (1999) Comparison of three methods of microsatellite detection. *Scand. J. Clin. Lab. Invest.* 59, 167–177.
- Celis, J. E., Østergaard, M., Basse, B., Celis, A., Lauridsen, J. B., Ratz, G. P., Andersen, L., Hein, B., Wolf, H., Orntoft, T. F., and Rasmussen, H. H. (1996) Loss of adipocyte-type fatty acid binding protein and other protein biomarkers is associated with progression of human bladder transitional cell carcinomas. *Cancer Res.* 56, 4782–4790.
- Celis, J. E., Ratz, G., Basse, B., Lauridsen, J. B., and Celis, A. (1994) In *Cell Biology: A Laboratory Handbook* (Celis, J. E., ed) Vol. 3, pp. 222–230, Academic Press, Orlando, FL.
- Ohlsson, R., Tycko, B., and Sapiezka, C. (1998) Monoallelic expression: 'there can only be one'. *Trends Genet.* 14, 435–438.
- Hollander, G. A., Zuklys, S., Morel, C., Mizoguchi, E., Mobisson, K., Simpson, S., Terhorst, C., Wishart, W., Golan, D. E., Bhan, A. K., and Burakoff, S. J. (1998) Monoallelic expression of the interleukin-2 locus. *Science* 279, 2118–2121.
- Brannan, C. L., and Bartolomei, M. S. (1999) Mechanisms of genomic imprinting. *Curr. Opin. Genet. Dev.* 9, 164–170.
- Ohlsson, R., Cui, H., He, L., Pfeifer, S., Malmikumpu, H., Jiang, S., Feinberg, A. P., and Hedborg, F. (1999) Mosaic allelic insulin-like growth factor 2 expression patterns reveal a link between Wilms' tumorigenesis and epigenetic heterogeneity. *Cancer Res.* 59, 3888–3892.
- Cui, H., Hedborg, F., He, L., Nordenskjöld, A., Sandstedt, B., Pfeifer, Ohlsson, S., and Ohlsson, R. (1997) Inactivation of H19, an imprinted and putative tumor repressor gene, is a preneoplastic event during Wilms' tumorigenesis. *Cancer Res.* 57, 4469–4473.
- Gafitisk, T., Saldanha, A. J., Styles, C. A., Lander, E. S., and Fink, G. R. (1999) Placental regulation of gene expression. *Science* 285, 251–254.
- Tsao, J., Yatabe, Y., Mark, I. D., Haiyan, K., Jones, P. A., and Shibata, D. (2000) Bladder cancer genotype stability during clinical progression. *Genes Chromosomes Cancer* 29, 28–32.
- Zong, Q., Schummer, M., Hood, L., and Morris, D. R. (1999) Messenger RNA translation state: the second dimension of high-throughput expression screening. *Proc. Natl. Acad. Sci. U. S. A.* 96, 10632–10636.
- Anderson, L., and Selinger, J. (1997) Comparison of selected mRNA and protein abundances in human liver. *Electrophoresis* 18, 533–537.
- Idker, T., Thorsson, V., Ranish, J. A., Christmas, P., Buhler, J., Eng, J. K., Bumgarner, R., Goodlett, D. R., Aebersold, R., and Hood, L. (2001) Integrated genomic and proteomic analyses of a systematically perturbed metabolic network. *Science* 292, 828–834.



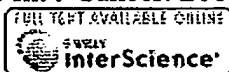
Expression of cadherins and catenins in paired tumor and non-neoplastic primary prostate cultures and corresponding prostatectomy specimens.

Wang J, Krill D, Torbenson M, Wang Q, Bisceglia M, Stoner J, Thomas A, DeFlavia P, Dhir R, Becich MJ.

Department of Pathology, University of Pittsburgh Medical Center, PA, USA.

Cadherins are a family of transmembrane proteins that play a crucial role in cell differentiation, cell migration, and intercellular adhesion. Cadherins are associated with catenins through their highly conserved cytoplasmic domain. Down-regulation of E-cadherin protein has been shown in various human cancers. This study examined the expression of cadherins and associated catenins at the mRNA level. Paired tumor and nonneoplastic primary prostate cultures were obtained from surgical specimens. Quantitative multiplex fluorescence reverse transcriptase-polymerase chain reaction (QMF RT-PCR) and quantitative analysis were performed and correlated with immunostain results. Six of seven cases of neoplastic cultures showed moderately-to-markedly decreased levels of E-cadherin and P-cadherin mRNA. Similar losses of alpha-catenin and beta-catenin mRNA were also observed. The results of QMF RT-PCR showed good correlation with the results of immunohistochemical studies based on corresponding formalin-fixed sections. In conclusion, this paper presents a coordinated down-regulation in the expression of E-cadherin and associated catenins at the mRNA and protein level in most of the cases studied. This down-regulation may play an important role in the pathogenesis of prostate cancer.

PMID: 11127708 [PubMed - indexed for MEDLINE]



Vascular endothelial growth factor expression correlates with matrix metalloproteinases MT1-MMP, MMP-2 and MMP-9 in human glioblastomas.

Munaut C, Noel A, Hougrand O, Foidart JM, Boniver J, Deprez M.

Laboratory of Tumour and Development Biology, University of Liege, Liege, Belgium.

Vascular endothelial growth factor (VEGF) is the major endothelial mitogen in central nervous system neoplasms and it is expressed in 64-95% of glioblastomas (GBMs). Tumour cells are the main source of VEGF in GBMs whereas VEGF receptors (VEGFR-1, its soluble form sVEGFR-1, VEGFR-2 and neuropilin-1) are expressed predominantly by endothelial cells. Infiltrating tumour cells and newly-formed capillaries progress through the extracellular matrix by local proteolysis involving matrix metalloproteinases (MMPs). Recent studies have shown that VEGF expression and bioavailability can be modulated by MMPs. We reported previously that the expression of MT1-MMP in human breast cancer cells was associated with an enhanced VEGF expression. We used quantitative RT-PCR, Western blot, gelatin zymography and immunohistochemistry to study the expression of VEGF, VEGFR-1, VEGFR-2, sVEGFR-1, neuropilin-1, MT1-MMP, MMP-2, MMP-9 and TIMP-2 in 20 human GBMs and 5 normal brains. The expression of these MMPs was markedly increased in most GBMs with excellent correlation between mRNA and protein levels; activated forms of MMP-2 and MMP-9 were present in 8/18 and 7/18 of GBMs. A majority of GBMs (17/20) also expressed high levels of VEGF, as previously reported, with strong correlation between VEGF and MT1-MMP gene expression levels, and double immunostaining showed that VEGF and MT1-MMP peptides co-localize in tumour and endothelial cells. Our results suggest that the interplay between metalloproteinases and VEGF previously described in experimental tumours may also be operative in human GBMs. Because of its dual ability to activate MMP-2 and to up-regulate VEGF, MT1-MMP might be of central importance in the growth of GBMs and represent an interesting target for anti-cancer treatments. Copyright 2003 Wiley-Liss, Inc.

PMID: 12918061 [PubMed - indexed for MEDLINE]

Real-time quantitative RT-PCR of cyclin D1 mRNA in mantle cell lymphoma: comparison with FISH and immunohistochemistry.

Hui P, Howe JG, Crouch J, Nimmakayalu M, Qumsiyeh MB, Tallini G, Flynn SD, Smith BR.

Department of Laboratory Medicine, Yale University School of Medicine, 333 Cedar Street, P.O. Box 208035, New Haven, CT 06520-8035, USA.

Presence of the balanced translocation t(11;14)(q13;q32) and the consequent overexpression of cyclin D1 found in mantle cell lymphoma (MCL) has been shown to be of important diagnostic value. Although many molecular and immunohistochemical approaches have been applied to analyze cyclin D1 status, correlative studies to compare different methods for the diagnosis of MCL are lacking. In this study, we examined 39 archived paraffin specimens from patients diagnosed with a variety of lymphoproliferative diseases including nine cases meeting morphologic and immunophenotypic criteria for MCL by: (1) real-time quantitative RT-PCR to evaluate cyclin D1 mRNA expression; (2) dual fluorescence in situ hybridization (FISH) to evaluate the t(11;14) translocation in interphase nuclei; and (3) tissue array immunohistochemistry to evaluate the cyclin D1 protein level. Among the nine cases of possible MCL, seven cases showed overexpression of cyclin D1 mRNA (cyclin D1 positive MCL) and two cases showed no cyclin D1 mRNA increase (cyclin D1 negative "MCL-like"). In six of seven cyclin D1 positive cases, the t(11;14) translocation was demonstrated by FISH analysis; in one case FISH was unsuccessful. Six of the seven cyclin D1 mRNA overexpressing cases showed increased cyclin D1 protein on tissue array immunohistochemistry; one was technically suboptimal. Among the two cyclin D1 negative MCL-like cases, FISH confirmed the absence of the t(11;14) translocation in both cases. All other lymphoproliferative diseases studied were found to have low or no cyclin D1 mRNA expression and were easily distinguishable from the cyclin D1 overexpressing MCLs by all three techniques. In addition, to confirming the need to assess cyclin D1 status, as well as, morphology and immunophenotyping to establish the diagnosis of MCL, this study demonstrates good correlation and comparability between measure of cyclin D1 mRNA, the 11;14 translocation and cyclin D1 protein.

Publication Types:

- Evaluation Studies

PMID: 12952233 [PubMed - indexed for MEDLINE]



Increased expression of proteasome subunits in skeletal muscle of cancer patients with weight loss.

Khal J, Hine AV, Fearon KC, Dejong CH, Tisdale MJ.

Pharmaceutical Sciences Research Institute, Aston University, Birmingham B4 7ET, UK.

Atrophy of skeletal muscle is common in patients with cancer and results in increased morbidity and mortality. In order to design effective therapy the mechanism by which this occurs needs to be elucidated. Most studies suggest that the ubiquitin-proteasome proteolytic pathway is most important in intracellular proteolysis, although there have been no reports on the activity of this pathway in patients with different extents of weight loss. In this report the expression of the ubiquitin-proteasome pathway in rectus abdominis muscle has been determined in cancer patients with weight loss of 0-34% using a competitive reverse transcriptase polymerase chain reaction to measure expression of mRNA for proteasome subunits C2 and C5, while protein expression has been determined by western blotting. Overall, both C2 and C5 gene expression was increased by about three-fold in skeletal muscle of cachectic cancer patients (average weight loss 14.5+/-2.5%), compared with that in patients without weight loss, with or without cancer. The level of gene expression was dependent on the amount of weight loss, increasing maximally for both proteasome subunits in patients with weight loss of 12-19%. Further increases in weight loss reduced expression of mRNA for both proteasome subunits, although it was still elevated in comparison with patients with no weight loss. There was no evidence for an increase in expression at weight losses less than 10%. There was a good correlation between expression of proteasome 20Salpha subunits, detected by western blotting, and C2 and C5 mRNA, showing that increased gene expression resulted in increased protein synthesis. Expression of the ubiquitin conjugating enzyme, E2(14k), with weight loss followed a similar pattern to that of proteasome subunits. These results suggest variations in the expression of key components of the ubiquitin-proteasome pathway with weight loss of cancer patients, and suggest that another mechanism of protein degradation must be operative for patients with weight loss less than 10%.

PMID: 16125116 [PubMed - in process]



Id-1 and Id-2 are overexpressed in pancreatic cancer and in dysplastic lesions in chronic pancreatitis.

Maruyama H, Kleeff J, Wildi S, Friess H, Buchler MW, Israel MA, Korc M.

Division of Endocrinology, Department of Medicine, University of California, Irvine, USA.

Id proteins antagonize basic helix-loop-helix proteins, inhibit differentiation, and enhance cell proliferation. In this study we compared the expression of Id-1, Id-2, and Id-3 in the normal pancreas, in pancreatic cancer, and in chronic pancreatitis (CP). Northern blot analysis demonstrated that all three Id mRNA species were expressed at high levels in pancreatic cancer samples by comparison with normal or CP samples. Pancreatic cancer cell lines frequently coexpressed all three Ids, exhibiting a good correlation between Id mRNA and protein levels, as determined by immunoblotting with highly specific anti-Id antibodies. Immunohistochemistry using these antibodies demonstrated the presence of faint Id-1 and Id-2 immunostaining in pancreatic ductal cells in the normal pancreas, whereas Id-3 immunoreactivity ranged from weak to strong. In the cancer tissues, many of the cancer cells exhibited abundant Id-1, Id-2, and Id-3 immunoreactivity. Scoring on the basis of percentage of positive cells and intensity of immunostaining indicated that Id-1 and Id-2 were increased significantly in the cancer cells by comparison with the respective controls. Mild to moderate Id immunoreactivity was also seen in the ductal cells in the CP-like areas adjacent to these cells and in the ductal cells of small and interlobular ducts in CP. In contrast, in dysplastic and atypical papillary ducts in CP, Id-1 and Id-2 immunoreactivity was as significantly elevated as in the cancer cells. These findings suggest that increased Id expression may be associated with enhanced proliferative potential of pancreatic cancer cells and of proliferating or dysplastic ductal cells in CP.

PMID: 10487839 [PubMed - indexed for MEDLINE]



Alterations in neuropeptide Y levels and Y1 binding sites in the Flinders Sensitive Line rats, a genetic animal model of depression.

Caberlotto L, Jimenez P, Overstreet DH, Hurd YL, Mathe AA, Fuxe K.

Department of Neuroscience, Karolinska Institute, Stockholm, Sweden.

Previously, we observed specific alterations of neuropeptide Y (NPY) and Y1 receptor mRNA expression in discrete regions of the Flinders Sensitive Line rats (FSL), an animal model of depression. In order to clarify the correlation between mRNA expression and protein content, radioimmunoassay and receptor autoradiography were currently performed. In the FSL rats, NPY-like immunoreactivity (NPY-LI) was decreased in the hippocampal CA region, while Y1 binding sites were increased; NPY-LI was increased in the arcuate nucleus. Fluoxetine treatment elevated NPY-LI in the arcuate and anterior cingulate cortex and increased Y1 binding sites in the medial amygdala and occipital cortex in both strains. No differences were found regarding the Y2 binding sites. The results demonstrate a good correlation between NPY peptide and mRNA expression, and sustain the possible involvement of NPY and Y1 receptors in depression.

PMID: 10327163 [PubMed - indexed for MEDLINE]

FREE full text article at
www.biolreprod.org

Follicle-stimulating hormone receptor and its messenger ribonucleic acid are present in the bovine cervix and can regulate cervical prostanoid synthesis.

Mizrachi D, Shemesh M.

Department of Hormone Research, Kimron Veterinary Institute, Bet Dagan, Israel 50250.

The hypothesis that FSH regulates the bovine cervical prostaglandin E(2) (PGE(2)) synthesis that is known to be associated with cervical relaxation and opening at the time of estrus was investigated. Cervical tissue from pre-estrous/estrous, luteal, and postovulatory cows were examined for 1) the presence of bovine (b) FSH receptor (R) and its corresponding mRNA and 2) the effect of FSH on the PGE(2) regulatory pathway in vitro. The presence of bFSHR mRNA in the cervix (maximal during pre-estrus/estrus) was demonstrated by the expression of a reverse transcription (RT) polymerase chain reaction (PCR) product (384 base pairs) specific for bFSHR mRNA and sequencing. Northern blotting revealed three transcripts (2.5, 3.3, and 3.8 kilobases [kb]) in cervix from pre-estrous/estrous cows. The level of FSHR (75 kDa) was significantly higher ($p < 0.01$) in Western blots of pre-estrous/estrous cervix than in other cervical tissues. There was a good correlation between the 75-kDa protein expression and its corresponding transcript of 2.55 kb throughout the estrous cycle as described by Northern blot analysis as well as RT-PCR. Incubation of FSH (10 ng/ml) with pre-estrous/estrous cervix resulted in a 3-fold increase in the expression of FSHR and a 2-fold increase in both G protein ($\alpha(s)$) and cyclooxygenase II. FSH (5-20 ng/ml) significantly increased ($p < 0.01$) cAMP, inositol phosphate ($p < 0.01$), and PGE(2) ($p < 0.01$) production by pre-estrous/estrous cervix but not by cervix at the other stages. We conclude that bovine cervix at the time of the peripheral plasma FSH peak (pre-estrus/estrus) contains high levels of FSHR and responds to FSH by increasing the PGE(2) production responsible for cervical relaxation at estrus.

PMID: 10456856 [PubMed - indexed for MEDLINE]



The decompensated detrusor III: impact of bladder outlet obstruction on sarcoplasmic endoplasmic reticulum protein and gene expression.

Stein R, Gong C, Hutcheson JC, Canning DA, Zderic SA.

Division of Urology, Children's Hospital of Philadelphia, Philadelphia, Pennsylvania, USA.

PURPOSE: Regulation of calcium ion homeostasis has a significant role in smooth muscle contractility. The sarcoplasmic endoplasmic reticulum, calcium, magnesium, adenosine triphosphatase (SERCA) is a regulatory ion pump that may have a role in the functional outcome after outlet obstruction. We investigate what correlation if any existed between SERCA protein and gene expression, and the contractile properties in the same bladder. **MATERIALS AND METHODS:** Standardized partial bladder outlet obstructions were created in adult New Zealand white rabbits, which were divided into control, sham operated and obstructed groups. Muscle strip studies subcategorized the obstructed group into compensated (force greater than 50% of control) and decompensated (force less than 50% of control). Microsomal membrane and total RNA fractions were prepared from the same bladder tissue. Membrane proteins were used for Western blot analysis using a SERCA specific monoclonal antibody, and total RNA was assessed with Northern blot analysis. **RESULTS:** The relative intensities of signals for the Western and Northern blots demonstrated a strong correlation between protein and gene expression. Furthermore there was a strong association between the loss of SERCA messenger RNA and protein expression and loss of bladder function. **CONCLUSIONS:** Bladder contractility after outlet obstruction is influenced in part by smooth muscle cell ability to maintain calcium homeostasis via SERCA. The loss of SERCA protein expression is mediated by down-regulation in gene expression in the same bladder. These data suggest that smooth muscle ion pump gene expression is in part mechanically (pressure work) regulated.

PMID: 10958733 [PubMed - indexed for MEDLINE]

[The pathogenic role of macrophage migration inhibitory factor in acute respiratory distress syndrome]

[Article in Chinese]

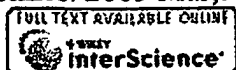
Guo Y, Xie C.

Department of Respiratory Medicine, First Affiliated Hospital of Zhongshan University, Guangzhou 510080 China.

OBJECTIVE To investigate the expression and pathogenic role of macrophage migration inhibitory factor(MIF) in human acute respiratory distress syndrome(ARDS)

METHODS The serum level of MIF in ARDS patients and normal persons were measured by ELISA method. Peripheral blood mononuclear cell (PBMC) MIF expression was determined by flow- cytometry. The expression of MIF mRNA and protein in the lung tissues were detected by using double immuno histochemistry labeling and in situ hybridization. **RESULTS** The serum level of MIF increased significantly in ARDS patients as compared with normal persons ($P < 0.01$). The percentage of PBMC MIF expression was higher in ARDS patients than in normal controls ($P < 0.01$). In situ hybridization and immunohistochemistry showed undetectable or weak MIF mRNA and protein expression in normal lungs. In contrast, there was marked upregulation of MIF mRNA and protein expression in the ARDS lungs. In ARDS macro phages infiltrated the alveolar space and interstitium, most of which also expressed MIF. Infiltrating macrophages were almost restricted to the areas of severe tissue damage. The MIF expression level showed a strong correlation with the number of infiltrating macrophages. **CONCLUSIONS** The serum level of MIF and PBMC MIF expression increased in ARDS patients with enhanced pulmonary MIF expression and macrophage infiltration, which suggests that MIF plays a pivotal role in the pathogenesis of ARDS.

PMID: 12126556 [PubMed - indexed for MEDLINE]



A transcriptomic and proteomic analysis of the effect of CpG-ODN on human THP-1 monocytic leukemia cells.

Kuo CC, Kuo CW, Liang CM, Liang SM.

Institute of BioAgricultural Sciences, Academia Sinica, Taipei, Taiwan.

The CpG motif of bacterial DNA (CpG-DNA) is a potent immunostimulating agent whose mechanism of action is not yet clear. Here, we used both DNA microarray and proteomic approaches to investigate the effects of oligodeoxynucleotides containing the CpG motif (CpG-ODN) on gene transcription and protein expression profiles of CpG-ODN responsive THP-1 cells. Microarray analysis revealed that 2 h stimulation with CpG-ODN up-regulated 50 genes and down-regulated five genes. These genes were identified as being associated with inflammation, antimicrobial defense, transcriptional regulation, signal transduction, tumor progression, cell differentiation, proteolysis and metabolism. Longer stimulation (8 h) with CpG-ODN enhanced transcriptional expression of 58 genes. Among these 58 genes, none except one, namely WNT1 inducible signaling pathway protein 2, was the same as those induced after 2 h stimulation. Proteomic analysis by two-dimensional gel electrophoresis, followed by mass spectrometry identified several proteins up-regulated by CpG-ODN. These proteins included heat shock proteins, modulators of inflammation, metabolic proteins and energy pathway proteins. Comparison of microarray and proteomic expression profiles showed poor correlation. Use of more reliable and sensitive analyses, such as reverse transcriptase polymerase chain reaction, Western blotting and functional assays, on several genes and proteins, nonetheless, confirmed that there is indeed good correlation between mRNA and protein expression after CpG-ODN treatment. This study also revealed that several anti-apoptotic and neuroprotective related proteins, not previously reported, are activated by CpG-DNA. These findings have extended our knowledge on the activation of cells by CpG-DNA and may contribute to further understanding of mechanisms that link innate immunity with acquired immune response(s).

PMID: 15693060 [PubMed - indexed for MEDLINE]

Expression of human telomerase reverse transcriptase gene and protein, and of estrogen and progesterone receptors, in breast tumors: Preliminary data from neo-adjuvant chemotherapy.

Kammori M, Izumiyama N, Hashimoto M, Nakamura K, Okano T, Kurabayashi R, Naoki H, Honma N, Ogawa T, Kaminishi M, Takubo K.

Division of Breast and Endocrine Surgery, Department of Surgery, Graduate School of Medicine, The University of Tokyo, Bunkyo-ku, Tokyo 113-8655, Japan. kanmori-dis@umin.ac.jp.

Human telomerase reverse transcriptase (hTERT), the catalytic subunit of telomerase, is very closely associated with telomerase activity. Telomerase has been implicated in cellular immortalization and carcinogenesis. In situ detection of hTERT will aid in determining the localization of telomerase-positive cells. The aim of this study was to detect expression of hTERT mRNA, hTERT protein, estrogen receptor (ER) and progesterone receptor (PR) in paraffin-embedded breast tissue samples and to investigate the relationship between hTERT expression and various clinicopathological parameters in breast tumorigenesis. We used in situ hybridization (ISH) to examine hTERT gene expression, and immunohistochemistry (IHC) to examine expression of hTERT protein, ER and PR, in breast tissues including 64 adenocarcinomas, 2 phyllode tumors and their adjacent normal breast tissues. hTERT gene expression was detected by ISH in 56 (88%) carcinomas, but in neither of the 2 phyllode tumors. hTERT protein expression was detected by IHC in 52 (81%) carcinomas, but in neither of the 2 phyllode tumors. Moreover, ER and PR were expressed in 42 (66%) and 42 (66%) carcinomas, respectively, and in neither of the 2 phyllode tumors. In 4 cases of breast carcinoma that strongly expressed hTERT gene and protein before treatment, neo-adjuvant chemotherapy led to disappearance of gene and protein expression in all cases. There was a strong correlation between detection of hTERT gene expression by ISH and of hTERT protein by ICH in tissue specimens from breast tumors. These results suggest that detection of hTERT protein by ICH can be used to distinguish breast cancers as a potential diagnostic and therapeutic marker.

PMID: 16211220 [PubMed - in process]

Expression of the ubiquitin-proteasome pathway and muscle loss in experimental cancer cachexia.

Khal J, Wyke SM, Russell ST, Hine AV, Tisdale MJ.

Pharmaceutical Sciences Research Institute, Aston University, Birmingham, UK.

Muscle protein degradation is thought to play a major role in muscle atrophy in cancer cachexia. To investigate the importance of the ubiquitin-proteasome pathway, which has been suggested to be the main degradative pathway mediating progressive protein loss in cachexia, the expression of mRNA for proteasome subunits C2 and C5 as well as the ubiquitin-conjugating enzyme, E2(14k), has been determined in gastrocnemius and pectoral muscles of mice bearing the MAC16 adenocarcinoma, using competitive quantitative reverse transcriptase polymerase chain reaction. Protein levels of proteasome subunits and E2(14k) were determined by immunoblotting, to ensure changes in mRNA were reflected in changes in protein expression. Muscle weights correlated linearly with weight loss during the course of the study. There was a good correlation between expression of C2 and E2(14k) mRNA and protein levels in gastrocnemius muscle with increases of 6-8-fold for C2 and two-fold for E2(14k) between 12 and 20% weight loss, followed by a decrease in expression at weight losses of 25-27%, although loss of muscle protein continued. In contrast, expression of C5 mRNA only increased two-fold and was elevated similarly at all weight losses between 7.5 and 27%. Both proteasome functional activity, and proteasome-specific tyrosine release as a measure of total protein degradation was also maximal at 18-20% weight loss and decreased at higher weight loss. Proteasome expression in pectoral muscle followed a different pattern with increases in C2 and C5 and E2(14k) mRNA only being seen at weight losses above 17%, although muscle loss increased progressively with increasing weight loss. These results suggest that activation of the ubiquitin-proteasome pathway plays a major role in protein loss in gastrocnemius muscle, up to 20% weight loss, but that other factors such as depression in protein synthesis may play a more important role at higher weight loss.

PMID: 16160695 [PubMed - in process]



Selective apoptosis of natural killer-cell tumours by l-asparaginase.

Ando M, Sugimoto K, Kitoh T, Sasaki M, Mukai K, Ando J, Egashira M, Schuster SM, Oshimi K.

Department of Haematology, Juntendo University School of Medicine, Tokyo, Japan.

We examined the effectiveness of various anti-tumour agents to natural killer (NK)-cell tumour cell lines and samples, which are generally resistant to chemotherapy, using flow cytometric terminal deoxynucleotidyl transferase-mediated dUTP-biotin nick end-labelling (TUNEL) assay. Although NK-YS and NK-92 were highly resistant to various anti-tumour agents, l-asparaginase induced apoptosis in these two NK-cell lines. NK-cell leukaemia/lymphoma and acute lymphoblastic leukaemia (ALL) samples were selectively sensitive to l-asparaginase and to doxorubicin (DXR) respectively. Samples of chronic NK lymphocytosis, an NK-cell disorder with an indolent clinical course, were resistant to both drugs. Our study clearly separated two major categories of NK-cell disorders and ALL according to the sensitivity to DXR and l-asparaginase. We examined asparagine synthetase levels by real-time quantitative polymerase chain reaction (RQ-PCR) and immunostaining in these samples. At least in nasal-type NK-cell lymphoma, there was a good correlation among asparagine synthetase expression, in vitro sensitivity and clinical response to l-asparaginase. In aggressive NK-cell leukaemia, although asparagine synthetase expression was high at both mRNA and protein levels, l-asparaginase induced considerable apoptosis. Furthermore, samples of each disease entity occupied a distinct area in two-dimensional plotting with asparagine synthetase mRNA level (RQ-PCR) and in vitro l-asparaginase sensitivity (TUNEL assay). We confirmed rather specific anti-tumour activity of l-asparaginase against NK-cell tumours in vitro, which provides an experimental background to the clinical use of l-asparaginase for NK-cell tumours.

PMID: 16156856 [PubMed - in process]

Full text article at
clincancerres.aacrjournals.org

P-cadherin overexpression is an indicator of clinical outcome in invasive breast carcinomas and is associated with CDH3 promoter hypomethylation.

Paredes J, Albergaria A, Oliveira JT, Jeronimo C, Milanezi F, Schmitt FC.

Institute of Pathology and Molecular Immunology of Porto University (IPATIMUP),
Braga, Portugal. jparedes@ipatimup.pt

PURPOSE: P-cadherin overexpression has been reported in breast carcinomas, where it was associated with proliferative high-grade histological tumors. This study aimed to analyze P-cadherin expression in invasive breast cancer and to correlate it with tumor markers, pathologic features, and patient survival. Another purpose was to evaluate the P-cadherin promoter methylation pattern as the molecular mechanism underlying this gene regulation. **EXPERIMENTAL DESIGN:** Using a series of invasive breast carcinomas, P-cadherin expression was evaluated and correlated with histologic grade, estrogen receptor, MIB-1, and p53 and c-erbB-2 expression. In order to assess whether P-cadherin expression was associated with changes in CDH3 promoter methylation, we studied the methylation status of a gene 5'-flanking region in these same carcinomas. This analysis was also done for normal tissue and for a breast cancer cell line treated with a demethylating agent. **RESULTS:** P-cadherin expression showed a strong correlation with high histologic grade, increased proliferation, c-erbB-2 and p53 expression, lack of estrogen receptor, and poor patient survival. This overexpression can be regulated by gene promoter methylation because the 5-Aza-2'-deoxycytidine treatment of MCF-7/AZ cells increased P-cadherin mRNA and protein levels. Additionally, we found that 71% of P-cadherin-negative cases showed promoter methylation, whereas 65% of positive ones were unmethylated ($P = 0.005$). The normal P-cadherin-negative breast epithelial cells showed consistent CDH3 promoter methylation. **CONCLUSIONS:** P-cadherin expression was strongly associated with tumor aggressiveness, being a good indicator of clinical outcome. Moreover, the aberrant expression of P-cadherin in breast cancer might be regulated by gene promoter hypomethylation.

PMID: 16115928 [PubMed - in process]

[Expression of human telomerase reverse transcriptase in cervix cancer and its significance]

[Article in Chinese]

Xi L, Zhu T, Wu P, Xu Q, Huang L, Li KZ, Lu YP, Ma D.

Department of Obstetrics and Gynecology, Tongji Hospital, Tongji Medical College, Huazhong University of Science and Technology, Wuhan 430030, China.

OBJECTIVE: To investigate the expression of human telomerase reverse transcriptase (hTERT) mRNA and protein in cervix cancer, cervical intraepithelial neoplasia (CIN) and normal cervix. **METHODS:** Expression of hTERT mRNA and the other two subunits of telomerase, human telomerase RNA component (hTR), human telomerase-associated protein (hTP1) was determined by RT-PCR in 3 cervix cancer cell lines, 2 diploid cell lines, 38 cases of cervix cancer, 16 cases of CIN and 20 cases of normal cervix.

Telomerase activity was also examined by telomeric repeat amplification protocol enzyme-linked immunosorbent assay (TRAP-ELISA). Expression of hTERT protein was detected in all the cell lines and 101 cases of paraffinized cervix tissue sections.

RESULTS: hTERT mRNA expression was detected in all of the three cervix cancer cell lines, 81.6% of cervix cancer, 37.5% of CIN, 5.0% of normal cervix, while in neither of the two diploid cell lines. The other two subunits of telomerase were prevalently expressed in all of the cell lines and most cervix tissues. There was a strong correlation between hTERT mRNA expression and telomerase activity. Immunostaining also revealed that hTERT protein was expressed in all three cervix cancer cell lines, 65.5% of cervix cancer, 28.0% of CIN and 4.8% of normal cervix. **CONCLUSION:** Up-regulation of hTERT may play an important role in the development of CIN and cervix cancer, hTERT could be used as an early diagnostic biomarker for cervix cancer.

PMID: 16008894 [PubMed - in process]

Multidrug resistance phosphoglycoprotein (ABCB1) in the mouse placenta: fetal protection.

Kalabis GM, Kostaki A, Andrews MH, Petropoulos S, Gibb W, Matthews SG.

Department of Physiology, University of Toronto, Ontario, Canada.

The multidrug resistance phosphoglycoprotein ATP-binding cassette subfamily B (ABCB1) actively extrudes a range of structurally and functionally diverse xenobiotics as well as glucocorticoids. ABCB1 is present in many cancer cell types as well as in normal tissues. Although it has been localized within the mouse placenta, virtually nothing is known about its regulation. In the mouse, two genes, *Abcb1a* and *Abcb1b*, encode ABCB1. We hypothesized that there are changes in placental *Abcb1a* and *Abcb1b* gene expression and ABCB1 protein levels during pregnancy. Using in situ hybridization, we demonstrated that *Abcb1b* mRNA is the predominant placental isoform and that there are profound gestational changes in the expression of both *Abcb1a* and *Abcb1b* mRNA. Placentas from pregnant mice were analyzed between Embryonic Days (E) 9.5 and 19 (term approximately 19.5d). *Abcb1b* mRNA was detected in invading trophoblast cells by E9.5, peaked within the placental labyrinth at E12.5, and then progressively decreased toward term ($P < 0.0001$). *Abcb1a* mRNA, although lower than that of *Abcb1b* at midgestation, paralleled changes in *Abcb1b* mRNA. Changes in *Abcb1* mRNA were reflected by a significant decrease in ABCB1 protein ($P < 0.05$). A strong correlation existed between placental *Abcb1b* mRNA and maternal progesterone concentrations, indicating a potential role of progesterone in regulation of placental *Abcb1b* mRNA. In conclusion, there are dramatic decreases in *Abcb1a* and *Abcb1b* mRNA and in ABCB1 at the maternal-fetal interface over the second half of gestation, suggesting that the fetus may become increasingly susceptible to the influences of xenobiotics and natural steroids in the maternal circulation.

PMID: 15917342 [PubMed - in process]



Restored expression and activity of organic ion transporters rOAT1, rOAT3 and rOCT2 after hyperuricemia in the rat kidney.

Habu Y, Yano I, Okuda M, Fukatsu A, Inui K.

Department of Pharmacy, Kyoto University Hospital, Faculty of Medicine, Kyoto University, Sakyo-ku, Kyoto 606-8507, Japan.

We previously reported that in hyperuricemic rats, renal impairment occurred and organic ion transport activity decreased, accompanied with a specific decrease in the expression of rat organic anion transporters, rOAT1 and rOAT3, and organic cation transporter, rOCT2. In the present study, we investigated the reversibility of the organic ion transport activity and expression of organic ion transporters (slc22a) during recovery from hyperuricemia. Hyperuricemia was induced by the administration of a chow containing uric acid and oxonic acid, an inhibitor of uric acid metabolism. Four days after discontinuance of the chow, the plasma uric acid concentration returned to the normal level, and renal functions such as creatinine clearance and BUN levels were restored, although the recovery of tubulointerstitial injury was varied in sites of the kidney. Basolateral uptake of p-aminohippurate (PAH) and tetraethylammonium (TEA), and both protein and mRNA levels of rOAT1, rOAT3 and rOCT2 in the kidney gradually improved during 14 days of recovery from hyperuricemia. Basolateral PAH transport showed a higher correlation with the protein level of rOAT1 ($r(2)=0.80$) than rOAT3 ($r(2)=0.34$), whereas basolateral TEA transport showed a strong correlation with rOCT2 protein ($r(2)=0.91$). The plasma testosterone concentration, which is a dominant factor in the regulation of rOCT2, was gradually restored during the recovery from hyperuricemia, but the correlation between the plasma testosterone level and rOCT2 protein expression in the kidney was not significant. These results suggest that the regulation of organic ion transporters, rOAT1, rOAT3 and rOCT2, by hyperuricemia is reversible, and the organic ion transport activity restores according to the expression levels of these transporters.

PMID: 15748710 [PubMed - indexed for MEDLINE]



Silencing of the thrombomodulin gene in human malignant melanoma.

Furuta J, Kaneda A, Umebayashi Y, Otsuka F, Sugimura T, Ushijima T.

Carcinogenesis Division, National Cancer Center Research Institute, Tokyo, Japan.

The loss of thrombomodulin (TM) expression is associated with tumour growth, infiltration and lymph node metastasis in human tumours. In melanoma cell lines, TM is reported to mediate cell adhesion, and its introduction into TM-negative melanoma cell lines suppresses their growth. In this study, we analysed TM expression in surgical melanoma specimens and the role of its promoter methylation in the loss of its expression. In 15 (75%) of the 20 specimens (five from a primary site and 15 from metastatic sites), melanoma cells lacked TM immunoreactivity. Methylation of the TM promoter region was detected in 10 (67%) of the 15 TM-negative specimens by methylation-specific polymerase chain reaction, whereas methylation was detected in two (40%) of the five TM-positive specimens. In cell lines, complete methylation of the TM promoter CpG island was detected in six (46%) of 13 melanoma cell lines, whereas no methylation was detected in two cultured normal melanocytes. There was a good correlation between the methylated status of the CpG island and the loss of TM messenger RNA (mRNA) expression. Treatment of melanoma cell lines with a demethylating agent, 5-aza-2'-deoxycytidine, induced demethylation of the promoter CpG island and the restoration of mRNA and protein expression. These findings suggest that most human melanomas lack TM expression, and that methylation of the promoter CpG island is one of the mechanisms responsible.

PMID: 15714116 [PubMed - indexed for MEDLINE]



Enhanced expressions of arachidonic acid-sensitive tandem-pore domain potassium channels in rat experimental acute cerebral ischemia.

Li ZB, Zhang HX, Li LL, Wang XL.

Institute of Materia Medica, Chinese Academy of Medical Sciences and Peking Union Medical College, Beijing 100050, China.

To further explore the pathophysiological significance of arachidonic acid-sensitive potassium channels, RT-PCR and Western blot analysis were used to investigate the expression changes of TREK channels in cortex and hippocampus in rat experimental acute cerebral ischemia in this study. Results showed that TREK-1 and TRAAK mRNA in cortex, TREK-1 and TREK-2 mRNA in hippocampus showed significant increases 2 h after middle cerebral artery occlusion (MCAO). While the mRNA expression levels of the all three channel subtypes increased significantly 24 h after MCAO in cortex and hippocampus. At the same time, the protein expressions of all the three channel proteins showed significant increase 24 h after MCAO in cortex and hippocampus, but only TREK-1 showed increased expression 2 h after MCAO in cortex and hippocampus. Immunohistochemical experiments verified that all the three channel proteins had higher expression levels in cortical and hippocampal neurons 24 h after MCAO. These results suggested a strong correlation between TREK channels and acute cerebral ischemia. TREK channels might provide a neuroprotective mechanism in the pathological process.

PMID: 15652517 [PubMed - indexed for MEDLINE]



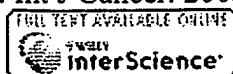
Alteration of frizzled expression in renal cell carcinoma.

Janssens N, Andries L, Janicot M, Perera T, Bakker A.

Department of Biochemistry, University of Antwerp, Wilrijk, Belgium.
njansse9@prdbe.jnj.com

To evaluate the involvement of frizzled receptors (Fzds) in oncogenesis, we investigated mRNA expression levels of several human Fzds in more than 30 different human tumor samples and their corresponding (matched) normal tissue samples, using real-time quantitative PCR. We observed that the mRNA level of Fzd5 was markedly increased in 8 of 11 renal carcinoma samples whilst Fzd8 mRNA was increased in 7 of 11 renal carcinoma samples. Western blot analysis of crude membrane fractions revealed that Fzd5 protein expression in the matched tumor/normal kidney samples correlated with the observed mRNA level. Wnt/beta-catenin signaling pathway activation was confirmed by the increased expression of a set of target genes. Using a kidney tumor tissue array, Fzd5 protein expression was investigated in a broader panel of kidney tumor samples. Fzd5 membrane staining was detected in 30% of clear cell carcinomas, and there was a strong correlation with nuclear cyclin D1 staining in the samples. Our data suggested that altered expression of certain members of the Fzd family, and their downstream targets, could provide alternative mechanisms leading to activation of the Wnt signaling pathway in renal carcinogenesis. Fzd family members may have a role as a biomarker.

PMID: 15557753 [PubMed - indexed for MEDLINE]



Localization of tissue inhibitor of metalloproteinases 1 (TIMP-1) in human colorectal adenoma and adenocarcinoma.

Holten-Andersen MN, Hansen U, Brunner N, Nielsen HJ, Illemann M, Nielsen BS.

The Finsen Laboratory, Rigshospitalet, Denmark.

Tissue inhibitor of matrix metalloproteinases 1 (TIMP-1) inhibits the proteolytic activity of matrix metalloproteinases and hereby prevents cancer invasion. However, TIMP-1 also possesses other functions such as inhibition of apoptosis, induction of malignant transformation and stimulation of cell-growth. We have previously demonstrated that TIMP-1 is elevated in blood from colorectal cancer patients and that high TIMP-1 levels predict poor prognosis. To clarify the role of TIMP-1 in colorectal tumorigenesis, the expression pattern of TIMP-1 in benign and malignant colorectal tumors was studied. In all of 24 cases of colorectal adenocarcinoma TIMP-1 mRNA was detected by in situ hybridization. In all cases TIMP-1 expression was found in fibroblast-like cells located at the invasive front but was seen only sporadically in normal mucosa. No TIMP-1 mRNA was seen in any of the cases in benign or malignant epithelial cells, in vascular cells or smooth muscle cells. Comparison of sections processed for TIMP-1 in situ hybridization with sections immunohistochemically stained with antibodies against TIMP-1 showed good correlation between TIMP-1 mRNA and immunoreactivity. Combining TIMP-1 in situ hybridization with immunohistochemical staining for alpha-smooth muscle actin or CD68 showed TIMP-1 mRNA in myofibroblasts but not in macrophages. TIMP-1 mRNA was detected in 2 of 7 adenomatous polyps in the adenoma area: in both cases associated with focal stromal inflammation at the epithelial-stromal interface. In conclusion, TIMP-1 expression is a rare event in benign human colon tissue but is highly expressed by myofibroblasts in association with invading colon cancer cells.

PMID: 15386409 [PubMed - indexed for MEDLINE]



FREE full text article at
www.jbc.org

Cell type-specific occurrence of caveolin-1alpha and -1beta in the lung caused by expression of distinct mRNAs.

Kogo H, Aiba T, Fujimoto T.

Department of Anatomy and Molecular Cell Biology, Nagoya University Graduate School of Medicine, Showa-ku, Nagoya 466-8550, Japan. hkogo@fujita-hu.ac.jp

Two isoforms of caveolin-1, alpha and beta, had been thought to be generated by alternative translation initiation of an mRNA (FL mRNA), but we showed previously that a variant mRNA (5'V mRNA) encodes the beta isoform specifically. In the present study, we demonstrated strong correlation between the expression of the caveolin-1 protein isoforms and mRNA variants in culture cells and the developing mouse lung. The alpha isoform protein and FL mRNA were expressed constantly during the lung development, whereas expression of the beta isoform protein and 5'V mRNA was negligible in the fetal lung before 17.5 days post coitum, and markedly increased simultaneously at 18.5 days post coitum, when the alveolar type I cells started to differentiate. Immunohistochemical analysis revealed the cell type-specific expression of the two isoforms; the alveolar type I cell expresses the beta isoform predominantly, while the endothelium harbors the alpha isoform chiefly. The mutually exclusive expression of caveolin-1 isoforms was verified by Western blotting of the selective plasma membrane preparation obtained from the endothelial and alveolar epithelial cells. The present result indicates that the two caveolin-1 isoforms are generated from distinct mRNAs in vivo and that their production is regulated independently at the transcriptional level. The result also suggests that the alpha and beta isoforms of caveolin-1 may have unique physiological functions.

PMID: 15067006 [PubMed - indexed for MEDLINE]

Society for Endocrinology
FREE FULL TEXT

Tightly regulated and inducible expression of a yoked hormone-receptor complex in HEK 293 cells.

Meehan TP, Puett D, Narayan P.

Department of Biochemistry and Molecular Biology, University of Georgia, Athens, Georgia 30602, USA.

We have previously reported the construction of a constitutively active luteinizing hormone receptor by covalently linking a fused heterodimeric hormone to the extracellular domain of the G protein-coupled receptor. This yoked hormone-receptor complex (YHR) was found to produce high levels of cAMP in the absence of exogenous hormone. Stable lines expressing YHR were generated in HEK 293 cells to obtain lines with different expression levels; however, in a relatively short time of continued passage, it was found that YHR expression was greatly reduced. Herein, we describe the development of clonal lines of HEK 293 cells in which the expression of YHR is under the control of a tetracycline-regulated system. Characterization of clonal lines revealed tight control of YHR expression both by dose and time of incubation with doxycycline. These experiments demonstrated a good correlation between expression levels of the receptor and basal cAMP production. Moreover, the reduction in receptor expression following doxycycline removal revealed that YHR mRNA and protein decayed at similar rates, again suggesting a strong linkage between mRNA and protein levels. The controlled expression of YHR in this cell system will allow for a more detailed analysis of the signaling properties associated with constitutive receptor activation and may prove to be advantageous in developmental studies with transgenic animals.

PMID: 14766006 [PubMed - indexed for MEDLINE]

An increased high-mobility group A2 expression level is associated with malignant phenotype in pancreatic exocrine tissue.

Abe N, Watanabe T, Suzuki Y, Matsumoto N, Masaki T, Mori T, Sugiyama M, Chiappetta G, Fusco A, Atomi Y.

First Department of Surgery, Kyorin University School of Medicine, 6-20-2, Shinkawa, Mitaka, Tokyo 181-8611, Japan. abenbtg@kyorin-u.ac.jp

The altered form of the high-mobility group A2 (HMGA2) gene is somehow related to the generation of human benign and malignant tumours of mesenchymal origin. However, only a few data on the expression of HMGA2 in malignant tumour originating from epithelial tissue are available. In this study, we examined the HMGA2 expression level in pancreatic carcinoma, and investigated whether alterations in the HMGA2 expression level are associated with a malignant phenotype in pancreatic tissue. High-mobility group A2 mRNA and protein expression was determined in eight surgically resected specimens of non-neoplastic tissue (six specimens of normal pancreatic tissue and two of chronic pancreatitis tissue) and 27 pancreatic carcinomas by highly sensitive reverse transcriptase-polymerase chain reaction (RT-PCR) techniques and immunohistochemical staining, respectively. Reverse transcriptase-polymerase chain reaction analysis revealed the expression of the HMGA2 gene in non-neoplastic pancreatic tissue, although its expression level was significantly lower than that in carcinoma. Immunohistochemical analysis indicated that the presence of the HMGA2 gene in non-neoplastic pancreatic tissue observed in RT-PCR reflects its abundant expression in islet cells, together with its focal expression in duct epithelial cells. Intense and multifocal or diffuse HMGA2 immunoreactivity was noted in all the pancreatic carcinoma examined. A strong correlation between HMGA2 overexpression and the diagnosis of carcinoma was statistically verified. Based on these findings, we propose that an increased expression level of the HMGA2 protein is closely associated with the malignant phenotype in the pancreatic exocrine system, and accordingly, HMGA2 could serve as a potential diagnostic molecular marker for distinguishing pancreatic malignant cells from non-neoplastic pancreatic exocrine cells.

PMID: 14647145 [PubMed - indexed for MEDLINE]



Butyrate-induced reversal of dexamethasone resistance in autonomous rat Nb2 lymphoma cells.

Buckley AR, Krumenacker JS, Buckley DJ, Leff MA, Magnuson NS, Reed JC, Miyashita T, de Jong G, Gout PW.

Department of Pharmacology and Toxicology, University of North Dakota School of Medicine and Health Sciences, Grand Forks 58202-9037, USA.
abuckley@mail.med.und.nodak.edu

The parental rat Nb2 lymphoma is a prolactin (PRL)-dependent T cell line. Exposure of a PRL-independent subline, Nb2-SFJCD1, to sodium butyrate (NaBT) causes transient reversal of their growth factor-independent proliferation in association with constitutive expression of protooncogenes pim-1 and c-myc. In the present study, we investigated the effect of NaBT treatment on the sensitivity of Nb2-SFJCD1 cells to dexamethasone (DEX)-induced apoptosis. Pretreatment with NaBT (2 mM, 72 h) partially reversed resistance to apoptosis in Nb2-SFJCD1 cells exposed to DEX (100 nM) for 12 h, assessed by flow cytometric analyses of DNA fragmentation. However, the cytolytic effect of DEX was abrogated by PRL in a time- and concentration-dependent manner. Evaluation of apoptosis-associated gene expression in NaBT-pre-treated cultures incubated with DEX or DEX+PRL indicated that the apoptosis resistance did not stem from altered bcl-2 or bax expression. However, there was a strong correlation between the resistance to DEX-activated apoptosis and their enhanced expression of pim-1 mRNA and protein. The results show that it is possible to reverse DEX-induced apoptosis of Nb2 pre-T cells and suggest the pim-1 gene product has an important role as a suppressor of this process, perhaps functioning as a mediator of PRL action.

PMID: 14646523 [PubMed]

MetaPress

GLUT1 messenger RNA and protein induction relates to the malignant transformation of cervical cancer.

Rudlowski C, Becker AJ, Schroder W, Rath W, Buttner R, Moser M.

Dept of Gynecology and Obstetrics, University Hospital Heidelberg, Vossstr 7-9, D-69115 Heidelberg, Germany.

We studied whether induction of glucose transporters (GLUTs) 1 to 4 correlates with human papillomavirus (HPV)-dependent malignant transformation of cervical epithelium. Tissue samples of cervical intraepithelial neoplasia (CIN; grades 1 to 3), invasive carcinomas, and lymph node metastasis were examined. HPV typing was performed. Tissue sections were immunostained with GLUT1 to GLUT4 antibodies. Messenger RNA (mRNA) in situ hybridization confirmed GLUT1 protein expression. Weak expression of GLUT1 was found in nondysplastic HPV-positive and HPV-negative epithelium; significant expression was observed in preneoplastic lesions, correlating with the degree of dysplasia. In CIN 3 high-risk HPV lesions, cervical cancer, and metastasis, GLUT1 was expressed at highest levels with a strong correlation of GLUT1 mRNA and protein expression. Immunostains for GLUT2 to GLUT4 were negative. Cervical tumor cells respond to enhanced glucose utilization by up-regulation of GLUT1. The strong induction of GLUT1 mRNA and protein in HPV-positive CIN 3 lesions suggests GLUT1 overexpression as an early event in cervical neoplasia. GLUT1 is potentially relevant as a diagnostic tool and glucose metabolism as a therapeutic target in cervical cancer.

PMID: 14608894 [PubMed - indexed for MEDLINE]

FREE full text article at
ajplung.physiology.org

Downregulation of ENaC activity and expression by TNF-alpha in alveolar epithelial cells.

Dagenais A, Frechette R, Yamagata Y, Yamagata T, Carmel JF, Clermont ME, Brochiero E, Masse C, Berthiaume Y.

Centre de recherche, CHUM-Hotel-Dieu, 3850 St-Urbain, Montreal, Quebec, Canada H2W 1T7. andre.dagenais.chum@ssss.gouv.qc.ca

Sodium absorption by an amiloride-sensitive channel is the main driving force of lung liquid clearance at birth and lung edema clearance in adulthood. In this study, we tested whether tumor necrosis factor-alpha (TNF-alpha), a proinflammatory cytokine involved in several lung pathologies, could modulate sodium absorption in cultured alveolar epithelial cells. We found that TNF-alpha decreased the expression of the alpha-, beta-, and gamma-subunits of epithelial sodium channel (ENaC) mRNA to 36, 43, and 16% of the controls after 24-h treatment and reduced to 50% the amount of alpha-ENaC protein in these cells. There was no impact, however, on alpha(1) and beta(1) Na(+)-K(+)-ATPase mRNA expression. Amiloride-sensitive current and ouabain-sensitive Rb(+) uptake were reduced, respectively, to 28 and 39% of the controls. A strong correlation was found at different TNF-alpha concentrations between the decrease of amiloride-sensitive current and alpha-ENaC mRNA expression. All these data show that TNF-alpha, a proinflammatory cytokine present during lung infection, has a profound influence on the capacity of alveolar epithelial cells to transport sodium.

PMID: 14514522 [PubMed - indexed for MEDLINE]

FREE full text article at
www.jbc.org

Adiposity elevates plasma MCP-1 levels leading to the increased CD11b-positive monocytes in mice.

Takahashi K, Mizuarai S, Araki H, Mashiko S, Ishihara A, Kanatani A, Itadani H, Kotani H.

Banyu Tsukuba Research Institute in collaboration with Merck Research Laboratories, Tsukuba, Ibaraki 300-2611, Japan.

Obesity is currently considered as an epidemic in the western world, and it represents a major risk factor for life-threatening diseases such as heart attack, stroke, diabetes, and cancer. Taking advantage of DNA microarray technology, we tried to identify the molecules explaining the relationship between obesity and vascular disorders, comparing mRNA expression of about 12,000 genes in white adipose tissue between normal, high fat diet-induced obesity (DIO) and d-Trp34 neuropeptide Y-induced obesity in mice. Expression of monocyte chemoattractant protein-1 (MCP-1) mRNA displayed a 7.2-fold increase in obese mice as compared with normal mice, leading to substantially elevated MCP-1 protein levels in adipocytes. MCP-1 levels in plasma were also increased in DIO mice, and a strong correlation between plasma MCP-1 levels and body weight was identified. We also showed that elevated MCP-1 protein levels in plasma increased the CD11b-positive monocyte/macrophage population in DIO mice. Furthermore, infusion of MCP-1 into lean mice increased the CD11b-positive monocyte population without inducing changes in body weight. Given the importance of MCP-1 in activation of monocytes and subsequent atherosclerotic development, these results suggest a novel role of adiposity in the development of vascular disorders.

PMID: 13129912 [PubMed - indexed for MEDLINE]



Relationship between cyclin D1 and p21(Waf1/Cip1) during differentiation of human myeloid leukemia cell lines.

Ullmannova V, Stockbauer P, Hradcova M, Soucek J, Haskovec C.

Department of Molecular Genetics, Institute of Hematology and Blood Transfusion, U Nemocnice 1, 128 20 Prague 2, Czech Republic. ullman@uhkt.cz

Expression of cell cycle-regulating genes was studied in human myeloid leukemia cell lines ML-1, ML-2 and ML-3 during induction of differentiation in vitro. Myelomonocytic differentiation was induced by phorbol ester (12-o-Tetradecanoyl-phorbol-13-acetate, TPA), tumor necrosis factor alpha (TNFalpha) or interferon gamma (INFgamma), or their combination. Differentiation (with the exception of TNFalpha alone) was accompanied by inhibition of DNA synthesis and cell cycle arrest. Inhibition of proliferation was associated with a decrease in the expression of cdc25A and cdc25B, cdk6 and Ki-67 genes, and with increased p21(Waf1/Cip1) gene expression, as measured by comparative RT-PCR. Expression of the following genes was not changed after induction of differentiation: cyclin A1, cyclin D3, cyclin E1 and p27(Kip1). Surprisingly, cyclin D1 expression was upregulated after induction by TPA, TNFalpha with IFNgamma or BA. Cyclin D2 was upregulated only after induction by BA. The results of the expression of the tested genes obtained by comparative RT-PCR were confirmed by quantitative real-time (RQ) RT-PCR and Western blotting. Quantitative RT-PCR showed as much as a 288-fold increase of cyclin D1 specific mRNA after a 24h induction by TPA. The upregulation of cyclin D1 in differentiating cells seems to be compensated by the upregulation of p21(Waf1/Cip1). These results, besides others, point to a strong correlation between the expression of cyclin D1 and p21(Waf1/Cip1) on the one hand and differentiation on the other hand in human myeloid leukemic cells and reflect a rather complicated network regulating proliferation and differentiation of leukemic cells.

PMID: 12921950 [PubMed - indexed for MEDLINE]

Comment in:

- [Hum Pathol. 2003 Jul;34\(7\):635-8.](#)

Human Pathology

Molecular and immunohistochemical analysis of HER2/neu oncogene in synovial sarcoma.

Nuciforo PG, Pellegrini C, Fasani R, Maggioni M, Coggi G, Parafioriti A, Bosari S.

Department of Medicine, Surgery and Dental Sciences, University of Milan, A.O.S. Paolo and IRCCS Ospedale Maggiore, Italy.

Amplification and/or overexpression of HER2/neu have been documented in many types of epithelial tumor and recently has been reported in sarcomas, particularly in osteosarcomas. But the role of HER2/neu alterations in soft tissue tumors remains poorly understood. Thus the present study investigates the expression of HER2/neu in 13 patients with synovial sarcoma (SS). In this study, HER2/neu mRNA levels were measured in frozen tissue samples using a real-time reverse transcription-polymerase chain reaction assay; protein expression was assessed by immunohistochemistry using an anti-HER2/neu polyclonal antibody. Six normal skeletal muscle specimens were used to establish basal levels of HER2/neu mRNA. HER2/neu transcripts were detected in all normal tissues and SSs. Four of 13 sarcomas (31%) demonstrated HER2/neu mRNA levels above the mean value, whereas 3 tumors (23%) displayed HER2/neu protein overexpression. Both membranous and cytoplasmic patterns of immunostaining were observed, and a strong correlation was found between protein expression and mRNA level ($P = 0.01$). Increased HER2/neu mRNA levels were significantly associated with a lower risk of developing recurrences ($P = 0.02$). Moreover, none of the patients with HER2/neu overexpression developed metastasis. Our data demonstrate that HER2/neu is expressed in SSs and that both membrane and cytoplasmic HER2/neu expression correlate with mRNA levels. Our results show that the presence of increased levels of HER2/neu in SSs is associated with a more favorable clinical course. Further studies are needed to assess the role of this oncogene in SSs and to evaluate the application of inhibitory humanized monoclonal antibodies in the treatment regimens for this malignancy.

PMID: 12874758 [PubMed - indexed for MEDLINE]



Tissue plasminogen activator induced by dengue virus infection of human endothelial cells.

Huang YH, Lei HY, Liu HS, Lin YS, Chen SH, Liu CC, Yeh TM.

Department of Microbiology and Immunology, College of Medicine, National Cheng Kung University, Tainan, Taiwan, ROC.

Dengue hemorrhagic fever and dengue shock syndrome (DHF/DSS) are severe complications of dengue virus (DV) infection. However, the pathogenesis of hemorrhage induced by dengue virus infection is poorly understood. Since endothelial cells play a pivotal role in the regulation of hemostasis, we studied the effect of DV infection on the production of tissue plasminogen activator (tPA) and plasminogen activator inhibitor 1 (PAI-1) in vitro using both primary isolated endothelial cells, human umbilical cord veins cells, and a human microvascular endothelial cell line. DV infection significantly induced the secretion of tPA but not PAI-1 of human endothelial cells. In addition, tPA mRNA of endothelial cells was induced by DV as demonstrated by RT-PCR. Antibody against IL-6 but not control antibody inhibited DV-induced tPA production of endothelial cells. Furthermore, a good correlation between sera levels of IL-6 and tPA was found in DHF but not DF patients. These results suggest that IL-6 can regulate DV-induced tPA production of endothelial cells, which may play important roles in the pathogenic development of DHF/DSS. Copyright 2003 Wiley-Liss, Inc.

PMID: 12794725 [PubMed - indexed for MEDLINE]

Decreased uncoupling protein expression and intramyocytic triglyceride depletion in formerly obese subjects.

Mingrone G, Rosa G, Greco AV, Manco M, Vega N, Hesselink MK, Castagneto M, Schrauwen P, Vidal H.

Istituto di Clinica Medica and. Clinica Chirurgica and Centro CNR Fisiopatologia Shock, Universita Cattolica S Cuore, Rome, Italy. gmingrone@rm.unicatt.it

OBJECTIVE: To examine the muscular uncoupling protein expression 2 (UCP2) and UCP3 gene expression in morbid obese subjects before and after bariatric surgery [bilio-pancreatic diversion (BPD)]. **RESEARCH METHODS AND PROCEDURES:** Eleven obese subjects (BMI = 49 ± 2 kg/m²) were studied before BPD and 24 months after BPD. Skeletal muscle UCP2 and UCP3 mRNA was measured using reverse transcriptase-competitive polymerase chain reaction and UCP3 protein by Western blotting. Intramyocytic triglycerides were quantified by high-performance liquid chromatography. Twenty-four-hour energy expenditure and respiratory quotient (RQ) were measured in a respiratory chamber. **RESULTS:** After BPD, the average weight loss was approximately 38%. Nonprotein RQ was increased in the postobese subjects (0.73 ± 0.00 vs. 0.83 ± 0.02 , $p < 0.001$). The intramyocytic triglyceride level dropped (3.66 ± 0.16 to 1.60 ± 0.29 mg/100 mg of fresh tissue, $p < 0.0001$) after BPD. Expression of UCP2 and UCP3 mRNA was significantly reduced (from $35.9 \pm 6.1\%$ to $18.6 \pm 4.5\%$ of cyclophilin, $p = 0.02$; from $60.2 \pm 14.0\%$ to $33.4 \pm 8.5\%$, $p = 0.03$; respectively). UCP3 protein content was also significantly reduced (272.19 ± 84.13 vs. 175.78 ± 60.31 , AU, $p = 0.04$). A multiple regression analysis ($R^2 = 0.90$) showed that IMTG levels ($p = 0.007$) represented the most powerful independent variable for predicting UCP3 variation. **DISCUSSION:** The strong correlation of UCP expression and decrease in IMTG levels suggests that triglyceride content plays an even more important role in the regulation of UCP gene expression than the circulating levels of free fatty acids or the achieved degree of weight loss.

PMID: 12740453 [PubMed - indexed for MEDLINE]

Society for Endocrinology
FREE FULL TEXT

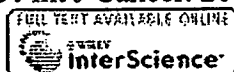
Modulation of gap junction mediated intercellular communication in TM3 Leydig cells.

Goldenberg RC, Fortes FS, Cristancho JM, Morales MM, Franci CR, Varanda WA, Campos de Carvalho AC.

Institute of Biophysics Carlos Chagas Filho, UFRJ, Brazil.

Long-term modulation of intercellular communication via gap junctions was investigated in TM3 Leydig cells, under low and high confluence states, and upon treatment of the cells for different times with activators of protein kinase A (PKA) and protein kinase C (PKC). Cells in low confluence were readily coupled, as determined by transfer of the dye Lucifer Yellow; on reaching confluence, the cells uncoupled. Western blots and RT-PCR revealed that connexin 43 (Cx43) was abundantly expressed in TM3 Leydig cells and its expression was decreased after the cells achieved confluence. Stimulation of PKA or PKC induced a decrease in cell-cell communication. Staurosporin, an inhibitor of protein kinases, increased coupling and was able to prevent and reverse the uncoupling actions of dibutyryl cAMP and 12-O-tetradecanoyl-phorbol-13-acetate (TPA). Under modulation by confluence, Cx43 was localized to the appositional membranes when cells were coupled and was mainly in the cytoplasm when they were uncoupled. In addition, cAMP and TPA reduced the surface membrane labeling for Cx43, whereas staurosporin increased it. These data show a strong correlation between functional coupling and the membrane distribution of Cx43, implying that this connexin has an important role in intercellular communication between TM3 cells. Furthermore, increased testosterone secretion in response to luteinizing hormone was accompanied by a decrease in intercellular communication, suggesting that gap junction mediated coupling may be a modulator of hormone secretion in TM3 cells.

PMID: 12740021 [PubMed - indexed for MEDLINE]



Urokinase-mediated posttranscriptional regulation of urokinase-receptor expression in non small cell lung carcinoma.

Montuori N, Mattiello A, Mancini A, Taglialatela P, Caputi M, Rossi G, Ragno P.

Istituto di Endocrinologia ed Oncologia Sperimentale, Consiglio Nazionale delle Ricerche, Naples, Italy.

The urokinase-type plasminogen activator (uPA) and its cellular receptor (uPAR) are involved in the proteolytic cascade required for tumor cell dissemination and metastasis, and are highly expressed in many human tumors. We have recently reported that uPA, independently of its enzymatic activity, is able to increase the expression of its own receptor in uPAR-transfected kidney cells at a posttranscriptional level. In fact, uPA, upon binding uPAR, modulates the activity and/or the level of a mRNA-stabilizing factor that binds the coding region of uPAR-mRNA. We now investigate the relevance of uPA-mediated posttranscriptional regulation of uPAR expression in non small cell lung carcinoma (NSCLC), in which the up-regulation of uPAR expression is a prognostic marker. We show that uPA is able to increase uPAR expression, both at protein and mRNA levels, in primary cell cultures obtained from tumor and adjacent normal lung tissues of patients affected by NSCLC, thus suggesting that the enzyme can exert its effect in lung cells. We investigated the relationship among the levels of uPA, uPAR and uPAR-mRNA binding protein(s) in NSCLC. Lung tissue analysis of 35 NSCLC patients shows an increase of both uPA and uPAR in tumor tissues, as compared to adjacent normal tissues, in 27 patients (77%); 19 of these 27 patients also show a parallel increase of the level and/or binding activity of a cellular protein capable of binding the coding region of uPAR-mRNA. Therefore, in tumor tissues, a strong correlation is observed among these 3 parameters, uPA, uPAR and the level and/or the activity of a uPAR-mRNA binding protein. We then suggest that uPA regulates uPAR expression in NSCLC at a posttranscriptional level by increasing uPAR-stability through a cellular factor that binds the coding region of uPAR-mRNA. Copyright 2003 Wiley-Liss, Inc.

PMID: 12704669 [PubMed - indexed for MEDLINE]

Retinal preconditioning and the induction of heat-shock protein 27.

Li Y, Roth S, Laser M, Ma JX, Crosson CE.

Department of Ophthalmology, Medical University of South Carolina, Charleston, South Carolina 29425, USA.

PURPOSE: Brief periods of ischemia have been shown to protect the retina from potentially damaging periods of ischemia. This phenomenon has been termed ischemic preconditioning or ischemic tolerance. In the present study the cellular changes in levels of heat shock protein (Hsp)27, -70, and -90 mRNA and expression of Hsp in the rat retina associated with ischemic preconditioning were evaluated. **METHODS:** Unilateral retinal ischemia was created in Long-Evans and Sprague-Dawley rats for 5 minutes. Rats were then left for 1 hour to 7 days, to allow the retina to reperfuse. Retinas were dissected, the mRNA and protein isolated, and Northern and Western blot analyses conducted to detect changes in expression of Hsp27, -70, and -90. Immunohistochemical studies were used to identify retinal regions where Hsp changes occurred. Selected animals were subjected to a second ischemic event, 60 minutes in duration, to correlate the changes in expression of Hsp with functional protection of the retina from ischemic injury. **RESULTS:** In control and sham-treated animals retinal Hsp27, -70, and -90 mRNAs were detectable. Five hours after retinal preconditioning, levels of Hsp27 mRNA were elevated above control levels, and 24 hours later, mRNA levels increased 200% over basal levels. Hsp27 expression remained elevated for up to 72 hours and then began to return to control levels. Hsp27 protein levels were increased by 200% over basal levels 24 hours after retinal preconditioning, remained at this level for 72 hours, and then returned to control levels. In contrast, no consistent change in Hsp70 or -90 mRNA or protein levels was observed during the course of the study. Immunohistochemical studies demonstrated that the increase in expression of Hsp27 was localized to neuronal and non-neuronal cells in the inner layers of the retina. Electoretinography studies demonstrated a strong correlation between the protection of retinal function from ischemic injury and the expression of Hsp27. **CONCLUSIONS:** These results provide evidence that the induction of Hsp27 is a gene-specific event associated with ischemic preconditioning in the retina. This increase in expression of Hsp27 occurs in both neuronal and non-neuronal retinal cells, and appears to be one component of the neuroprotective events induced by ischemic preconditioning in the retina.

PMID: 12601062 [PubMed - indexed for MEDLINE]



The role of the epidermal growth factor receptor in sustaining neutrophil inflammation in severe asthma.

Hamilton LM, Torres-Lozano C, Puddicombe SM, Richter A, Kimber I, Dearman RJ, Vrugt B, Aalbers R, Holgate ST, Djukanovic R, Wilson SJ, Davies DE.

Division of Infection, Inflammation & Repair, School of Medicine, University of Southampton, UK.

BACKGROUND: The extent of epithelial injury in asthma is reflected by expression of the epidermal growth factor receptor (EGFR), which is increased in proportion to disease severity and is corticosteroid refractory. Although the EGFR is involved in epithelial growth and differentiation, it is unknown whether it also contributes to the inflammatory response in asthma. **OBJECTIVES:** Because severe asthma is characterized by neutrophilic inflammation, we investigated the relationship between EGFR activation and production of IL-8 and macrophage inhibitory protein-1 alpha (MIP-1alpha) using in vitro culture models and examined the association between epithelial expression of IL-8 and EGFR in bronchial biopsies from asthmatic subjects. **METHODS:** H292 or primary bronchial epithelial cells were exposed to EGF or H2O2 to achieve ligand-dependent and ligand-independent EGFR activation; IL-8 mRNA was measured by real-time PCR and IL-8 and MIP-1alpha protein measured by enzyme-linked immunosorbent assay (ELISA). Epithelial IL-8 and EGFR expression in bronchial biopsies from asthmatic subjects was examined by immunohistochemistry and quantified by image analysis. **RESULTS:** Using H292 cells, EGF and H2O2 increased IL-8 gene expression and release and this was completely suppressed by the EGFR-selective tyrosine kinase inhibitor, AG1478, but only partially by dexamethasone. MIP-1alpha release was not stimulated by EGF, whereas H2O2 caused a 1.8-fold increase and this was insensitive to AG1478. EGF also significantly stimulated IL-8 release from asthmatic or normal primary epithelial cell cultures established from bronchial brushings. In bronchial biopsies, epithelial IL-8, MIP-1alpha, EGFR and submucosal neutrophils were all significantly increased in severe compared to mild disease and there was a strong correlation between EGFR and IL-8 expression ($r = 0.70$, $P < 0.001$). **CONCLUSIONS:** These results suggest that in severe asthma, epithelial damage has the potential to contribute to neutrophilic inflammation through enhanced production of IL-8 via EGFR-dependent mechanisms.

PMID: 12580917 [PubMed - indexed for MEDLINE]

**Specific inhibition of AQP1 water channels in isolated rat intrahepatic bile duct units by small interfering RNAs.****Splinter PL, Masyuk AI, LaRusso NF.**

Center for Basic Research in Digestive Diseases, Division of Gastroenterology and Hepatology, Mayo Medical School, Clinic, and Foundation, Rochester, Minnesota 55905, USA.

Cholangiocytes express water channels (i.e. aquaporins (AQPs)), proteins that are increasingly recognized as important in water transport by biliary epithelia. However, direct functional studies demonstrating AQP-mediated water transport in cholangiocytes are limited, in part because of the lack of specific AQP inhibitors. To address this issue, we designed, synthesized, and utilized small interfering RNAs (siRNAs) selective for AQP1 and investigated their effectiveness in altering AQP1-mediated water transport in intrahepatic bile duct units (IBDUs) isolated from rat liver. Twenty-four hours after transfection of IBDUs with siRNAs targeting two different regions of the AQP1 transcript, both AQP1 mRNA and protein expression were inhibited by 76.6-92.0 and 57.9-79.4%, respectively. siRNAs containing the same percent of base pairs as the AQP1-siRNAs but in random sequence (i.e. scrambled siRNAs) had no effect. Suppression of AQP1 expression in cholangiocytes resulted in a decrease in water transport by IBDUs in response to both an inward osmotic gradient (200 mosm) or a secretory agonist (forskolin), the osmotic water permeability coefficient ($P(f)$) decreasing up to 58.8% and net water secretion ($J(v)$) decreasing up to 87%. A strong correlation between AQP1 protein expression and water transport in IBDUs transfected with AQP1-siRNAs was consistent with the decrease in water transport by IBDUs resulting from AQP1 gene silencing by AQP1-siRNAs. This study is the first to demonstrate the feasibility of utilizing siRNAs to specifically reduce the expression of AQPs in epithelial cells and provides direct evidence of the contribution of AQP1 to water transport by biliary epithelia.

PMID: 12468529 [PubMed - indexed for MEDLINE]



Quantification of CK20 gene and protein expression in colorectal cancer by RT-PCR and immunohistochemistry reveals inter- and intratumour heterogeneity.

Lassmann S, Bauer M, Soong R, Schreglmann J, Tabiti K, Nahrig J, Ruger R, Hofler H, Werner M.

Pathologisches Institut, Universitätsklinikum Freiburg, Albertstrasse 19, 79104 Freiburg, Germany. lassmann@ukl.uni-freiburg.de

Cytokeratin 20 (CK20) is an epithelial protein expressed almost exclusively in the gastrointestinal (GI) tract and is widely used as immunohistochemical marker for routine diagnosis. In contrast, CK20 gene expression is not an established marker for the classification of tumours and the detection of disseminated cancer cells in colorectal cancer. Recently, real-time reverse transcriptase polymerase chain reaction (RT-PCR) has provided the means for reproducible and quantitative investigation of molecular markers. This report directly compares CK20 mRNA and protein expression in serial sections of archival, formalin-fixed, paraffin-embedded (FFPE) colorectal adenocarcinomas. CK20 expression was detected by immunohistochemistry (IHC) in 60/63 (95.2%) cases, by conventional RT-PCR in 58/60 (96.7%) and by quantitative RT-PCR using the LightCycler (LightCycler is a trademark of a Member of the Roche Group) System in 29/32 (90.6%) microdissected cases, one case yielding variable results. Despite the high detection rate of all three techniques, marked heterogeneity of CK20 expression was seen between different cases and also within individual cases. CK20 expression profiles were not related to particular histopathological features of the tumours. A good correlation ($r = 0.8964$) was found between CK20 mRNA and protein expression by comparing quantitative RT-PCR with IHC in 32 cases. This was also true for selected heterogeneous tumour cells within individual cases. Both RT-PCR and IHC are therefore valuable tools for CK20 detection in colorectal adenocarcinoma, with real-time RT-PCR providing supplementary quantitative information. This suggests a promising supportive role for quantitative RT-PCR in molecular pathology. Copyright 2002 John Wiley & Sons, Ltd.

Publication Types:

- Evaluation Studies

PMID: 12237879 [PubMed - indexed for MEDLINE]

Effect of duration of fixation on quantitative reverse transcription polymerase chain reaction analyses.

Macabeo-Ong M, Ginzinger DG, Dekker N, McMillan A, Regezi JA, Wong DT, Jordan RC.

Oral Pathology, Department of Stomatology, University of California San Francisco, California 94143-0424, USA.

Increasingly, there is the need to analyze gene expression in tumor tissues and correlate these findings with clinical outcome. Because there are few tissue banks containing enough frozen material suitable for large-scale genetic analyses, methods to isolate and quantify messenger RNA (mRNA) from formalin-fixed, paraffin-embedded tissue sections are needed. Recovery of RNA from routinely processed biopsies and quantification by the polymerase chain reaction (PCR) has been reported; however, the effects of formalin fixation have not been well studied. We used a proteinase K-salt precipitation RNA isolation protocol followed by TaqMan quantitative PCR to compare the effect of formalin fixation for 24, 48, and 72 hours and for 1 week in normal (2), oral epithelial dysplasia (3), and oral squamous cell carcinoma (4) specimens yielding 9 fresh and 36 formalin-fixed samples. We also compared mRNA and protein expression levels using immunohistochemistry for epidermal growth factor receptor (EGFR), matrix metalloproteinase (MMP)-1, p21, and vascular endothelial growth factor (VEGF) in 15 randomly selected and routinely processed oral carcinomas. We were able to extract RNA suitable for quantitative reverse transcription (RT) from all fresh (9/9) and formalin-fixed (36/36) specimens fixed for differing lengths of time and from all (15/15) randomly selected oral squamous cell carcinoma. We found that prolonged formalin fixation (>48 h) had a detrimental effect on quantitative RT polymerase chain reaction results that was most marked for MMP-1 and VEGF but less evident for p21 and EGFR. Comparisons of quantitative RT polymerase chain reaction and immunohistochemistry showed that for all markers, except p21, there was good correlation between mRNA and protein levels. p21 mRNA was overexpressed in only one case, but protein levels were elevated in all but one tumor, consistent with the established translational regulation of p21. These results show that RNA can be reliably isolated from formalin-fixed, paraffin-embedded tissue sections and can produce reliable quantitative RT-PCR data. However, results for some markers are adversely affected by prolonged formalin fixation times.

PMID: 12218216 [PubMed - indexed for MEDLINE]



The p21(Cip1) protein, a cyclin inhibitor, regulates the levels and the intracellular localization of CDC25A in mice regenerating livers.

Jaime M, Pujol MJ, Serratosa J, Pantoja C, Canela N, Casanovas O, Serrano M, Agell N, Bachs O.

Department of Cell Biology and Pathology, Faculty of Medicine, Institut d'Investigacions Biomediques August Pi Sunyer (IDIBAPS), University of Barcelona, Barcelona, Spain.

Liver cells from p21(Cip1^{-/-}) mice subjected to partial hepatectomy (PH) progress into DNA synthesis faster than those from wild-type mice. These cells also show a premature induction of cyclin E/cyclin-dependent kinase (CDK) 2 activity. We studied the mechanisms whereby cells lacking p21(Cip1) showed a premature induction of this activity. Whereas the levels of CDK2, cyclin E, and p27(Kip1) were similar in both wild-type and p21(Cip1^{-/-}) mice, those of the activator CDC25A were much higher in p21(Cip1^{-/-}) quiescent and regenerating livers than in wild-type animals. Moreover, p21(Cip1^{-/-}) cells also showed a premature translocation of CDC25A from cytoplasm into the nucleus. The ectopic expression of p21(Cip1) into mice embryo fibroblasts from p21(Cip1^{-/-}) mice decreased the levels of CDC25A and delayed its nuclear translocation. The levels of CDC25A messenger RNA in p21(Cip1^{-/-}) cells were higher than in wild-type cells, suggesting that this increase might be responsible, at least in part, for the high levels of CDC25A protein in these cells. Thus, the results reported here indicate that p21(Cip1) regulates the levels and the intracellular localization of CDC25A. We also found a good correlation between CDC25A nuclear translocation and cyclin E/CDK2 activation. In conclusion, premature translocation of CDC25A to the nucleus might be involved in the advanced induction of cyclin E/CDK2 activity and DNA replication in cells from animals lacking p21(Cip1).

PMID: 11981756 [PubMed - indexed for MEDLINE]



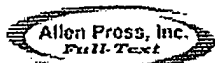
Matrilin-3 in human articular cartilage: increased expression in osteoarthritis.

Pullig O, Weseloh G, Klatt AR, Wagener R, Swoboda B.

Division of Orthopaedic Rheumatology, Department of Orthopaedics, University of Erlangen-Nuremberg, Rathsberger Str. 57, D-91054 Erlangen, Germany.
oliver.pullig@med.uni-erlangen.de

OBJECTIVE: Matrilin-3 is a member of the recently described matrilin family of extracellular matrix proteins containing von Willebrand factor A-like domains. The matrilin-3 subunit can form homo-tetramers as well as hetero-oligomers together with subunits of matrilin-1 (cartilage matrix protein). It has a restricted tissue distribution and is strongly expressed in growing skeletal tissues. Detailed information on expression and distribution of extracellular matrix proteins is important to understand cartilage function in health and in disease like osteoarthritis (OA). **METHODS:** Normal and osteoarthritic cartilage were systematically analysed for matrilin-3 expression, using immunohistochemistry, Western blot analysis, in situ hybridization, and quantitative PCR. **RESULTS:** Our results indicate that matrilin-3 is a mandatory component of mature articular cartilage with its expression being restricted to chondrocytes from the tangential zone and the upper middle cartilage zone. Osteoarthritic cartilage samples with only moderate morphological osteoarthritic degenerations have elevated levels of matrilin-3 mRNA. In parallel, we found an increased deposition of matrilin-3 protein in the cartilage matrix. Matrilin-3 staining was diffusely distributed in the cartilage matrix, with no cellular staining being detectable. In cartilage samples with minor osteoarthritic lesions, matrilin-3 deposition was restricted to the middle zone and to the upper deep zone. A strong correlation was found between enhanced matrilin-3 gene and protein expression and the extent of tissue damage. Sections with severe osteoarthritic degeneration showed the highest amount of matrilin-3 mRNA, strong signals in in situ hybridization, and prominent protein deposition in the middle and deep cartilage zone. **CONCLUSION:** We conclude that matrilin-3 is an integral component of human articular cartilage matrix and that the enhanced expression of matrilin-3 in OA may be a cellular response to the modified microenvironment in the disease. Copyright 2002 OsteoArthritis Research Society International.

PMID: 11950247 [PubMed - indexed for MEDLINE]



UVA irradiation-induced activation of activator protein-1 is correlated with induced expression of AP-1 family members in the human keratinocyte cell line HaCaT.

Silvers AL, Bowden GT.

Department of Radiation Oncology, Arizona Cancer Center, The University of Arizona, Tucson 85724, USA.

To determine whether the transcription factor activator protein-1 (AP-1) could be modulated by ultraviolet A (UVA) exposure, we examined AP-1 DNA-binding activity and transactivation after exposure to UVA in the human immortalized keratinocyte cell line HaCaT. Maximal AP-1 transactivation was observed with 250 kJ/m² UVA between 3 and 4 h after irradiation. DNA binding of AP-1 to the target 12-O-tetradecanoylphorbol-13-acetate response element sequence was maximally induced 1-3 h after irradiation. Both de novo transcription and translation contributed to the UVA-induced AP-1 DNA binding. c-Fos was implicated as a primary component of the AP-1 DNA-binding complex. Other components of the complex included Fra-2, c-Jun, JunB and JunD. UVA irradiation induced protein expression of c-Fos, c-Jun, Fra-1 and Fra-2. Phosphorylated forms of these induced proteins were determined at specific time points. A strong correlation existed between UVA-induced AP-1 activity and accumulation of c-Fos, c-Jun and Fra-1 proteins. UVA irradiation also induced c-fos and c-jun mRNA expression and transcriptional activation of the c-fos gene promoter. These results demonstrate that UVA irradiation activates AP-1 and that c-fos induction may play a critical role in the response of these human keratinocytes to UVA irradiation.

PMID: 11950097 [PubMed - indexed for MEDLINE]

FREE full text article at
www.jimmunol.org

Suppressors of cytokine signaling proteins are differentially expressed in Th1 and Th2 cells: implications for Th cell lineage commitment and maintenance.

Egwuagu CE, Yu CR, Zhang M, Mahdi RM, Kim SJ, Gery I.

Laboratory of Immunology, National Eye Institute, National Institutes of Health, Bethesda, MD 20892, USA. emeka@helix.nih.gov

Positive regulatory factors induced by IL-12/STAT4 and IL-4/STAT6 signaling during T cell development contribute to polarized patterns of cytokine expression manifested by differentiated Th cells. These two critical and antagonistic signaling pathways are under negative feedback regulation by a multimember family of intracellular proteins called suppressor of cytokine signaling (SOCS). However, it is not known whether these negative regulatory factors also modulate Th1/Th2 lineage commitment and maintenance. We show here that CD4(+) naive T cells constitutively express low levels of SOCS1, SOCS2, and SOCS3 mRNAs. These mRNAs and their proteins increase significantly in nonpolarized Th cells after activation by TCR signaling. We further show that differentiation into Th1 or Th2 phenotype is accompanied by preferential expression of distinct SOCS mRNA transcripts and proteins. SOCS1 expression is 5-fold higher in Th1 than in Th2 cells, whereas Th2 cells contain 23-fold higher levels of SOCS3. We also demonstrate that IL-12-induced STAT4 activation is inhibited in Th2 cells that express high levels of SOCS3 whereas IL-4/STAT6 signaling is constitutively activated in Th2 cells, but not Th1 cells, with high SOCS1 expression. These results suggest that mutually exclusive use of STAT4 and STAT6 signaling pathways by differentiated Th cells may derive in part, from SOCS3- or SOCS1-mediated repression of IL-12/STAT4- or IL-4/STAT6 signaling in Th2 and Th1 cells, respectively. Given the strong correlation between distinct patterns of SOCS expression and differentiation into the Th1 or Th2 phenotype, SOCS1 and SOCS3 proteins are therefore Th lineage markers that can serve as therapeutic targets for immune modulation therapy.

PMID: 11907070 [PubMed - indexed for MEDLINE]



Characterization of cyclin D2 expression in human endometrium.

Choi D, Yoon S, Lee E, Hwang S, Song S, Kim J, Yoon BK, Lee JH.

Department of Obstetrics and Gynecology, Samsung Medical Center, Sungkyunkwan University School of Medicine, Seoul, South Korea. dschoi@smc.samsung.co.kr

OBJECTIVE: This study was undertaken to investigate cyclin D2 mRNA and protein expression in human endometrium during the menstrual cycle. **METHODS:** Endometrial samples were obtained from 15 premenopausal nonpregnant women who had hysterectomies for benign gynecologic reasons. They were divided into the following five groups according to histologic dating: early proliferative (n = 3), mid to late proliferative (n = 3), early secretory (n = 3), mid secretory (n = 3), and late secretory (n = 3). Cyclin D2 mRNA and protein expression were analyzed using reverse transcriptase-polymerase chain reaction, Western blotting, and immunohistochemistry. **RESULTS:** Cyclin D2 mRNA and protein were expressed in human endometrial tissue throughout the menstrual cycle. Cyclin D2 mRNA and protein expression of proliferative phase endometrium were significantly higher than those of secretory phase endometrium ($P < .05$). The staining intensity of cyclin D2 in proliferative phase endometrium was higher than that in secretory phase ($P < .05$). Cyclin D2 mRNA level showed good correlation with cyclin D2 protein level ($R = 0.579$, $P < .03$), and cyclin D2 protein also showed good correlation with immunohistochemical staining intensity ($R = 0.562$, $P < .03$). **CONCLUSION:** Cyclin D2 was expressed in human endometrium throughout the menstrual cycle. Cyclin D2 mRNA and protein were expressed at high levels in proliferative phase endometrium, especially in the early proliferative phase, and then decreased in the secretory phase.

PMID: 11839508 [PubMed - indexed for MEDLINE]

FREE full text article at
circ.ahajournals.org

Augmented expression of neuronal nitric oxide synthase in the atria parasympathetically decreases heart rate during acute myocardial infarction in rats.

Takimoto Y, Aoyama T, Tanaka K, Keyamura R, Yui Y, Sasayama S.

Department of Cardiovascular Medicine, Graduate School of Medicine, Kyoto University, Kyoto, Japan.

BACKGROUND: Nitric oxide (NO) synthesized within sinoatrial cells recently has been shown to participate in the autonomic control of heart rate. We hypothesized that NO in the neuronal cells in the heart was increased and parasympathetically regulated heart rate after myocardial infarction (MI). **METHODS AND RESULTS:** We examined heart rate dynamics and neuronal NO synthase (nNOS) expression and activities in the atria of rats with MI 1, 3, 7, and 14 days after MI (n=7 to 22 for each group). Both the mRNA levels of nNOS in the atria determined by competitive reverse transcriptase-polymerase chain reaction and the protein levels determined by Western blotting were significantly increased compared with controls 1, 3, and 7 days after MI. nNOS activity in the atria 1 day after infarction was also increased in MI rats. nNOS immunoreactivity was observed in nerve fibers in the atria. After infusion of a specific inhibitor of nNOS and iNOS, 1-(2-trifluoromethylphenyl) imidazole (TRIM) (50 mg/kg IV), heart rate was significantly ($P<0.01$) increased in MI rats compared with controls 1, 3, and 7 days after MI. The iNOS-specific inhibitor, 1400W (10 mg/kg SC), did not significantly affect the heart rate in rats with MI. The effect of TRIM was abolished by pretreatment with L-arginine (25 mg/kg IV) or by parasympathetic blockade with atropine but not by propranolol. There was a strong correlation ($r=0.837$, $P<0.0001$) between the nNOS protein expression and heart rate change after TRIM infusion. **CONCLUSIONS:** These results indicate that increased nNOS parasympathetically decreased heart rate via the production of NO in rats with acute MI.

PMID: 11815433 [PubMed - indexed for MEDLINE]

FREE full text article at
www.iovs.org

Expression of membrane-type matrix metalloproteinases 4, 5, and 6 in mouse corneas infected with *P. aeruginosa*.

Dong Z, Katar M, Alousi S, Berk RS.

Department of Immunology and Microbiology, Wayne State University School of Medicine, 540 E. Canfield, Detroit, MI 48201, USA.

PURPOSE: To investigate the expression and regulation of membrane-type matrix metalloproteinases (MT-MMPs) 4, 5, and 6 in the mouse corneas infected with *Pseudomonas aeruginosa*. **METHODS:** C57BL/6J mice were intracorneally infected with *P. aeruginosa*. The expression of MT4-, MT5-, and MT6-MMP was detected at both the mRNA and protein levels by RT-PCR and immunoblot analysis. Immunohistochemical staining was performed to localize the expression of MT4- and MT5-MMP in the mouse corneas. **RESULTS:** Expression of MT4- and MT5-MMP was detected in the normal (uninfected) cornea by RT-PCR and immunoblot analysis. When infected with *P. aeruginosa*, the corneas showed significant induction of each MT-MMP. Localization of MT4- and MT5-MMP revealed that the expression of MT5-MMP was restricted to the epithelial tissue in the normal cornea, whereas the induced expression of MT4- and MT5-MMP was predominantly in the substantia propria, which contained most of the infiltrating cells. MT6-MMP expression was not detected in the uninfected cornea but was upregulated in the infected corneas. **CONCLUSIONS:** Expression of MT4-, MT5-, and MT6-MMP was induced in corneas infected with *P. aeruginosa*. Immunohistochemistry showed predominant immunoreactivity of MT4- and MT5-MMP in the substantia propria. Previous histologic studies have revealed different patterns of inflammatory cell infiltration with an increased number of polymorphonuclear neutrophils (PMNs) during the early stage of inflammation and increased macrophages during the late stage. These results indicate a good correlation between the overexpression of the MT-MMPs in the infected corneas and the inflammatory response—that is, leukocyte infiltration—indicating that inflammatory cells such as macrophages and PMNs may play a role in the upregulation of MT-MMPs during corneal infection, which in turn can cause the destruction of corneal tissue.

PMID: 11726626 [PubMed - indexed for MEDLINE]

FREE full text article at
carcin.oupjournals.org

DNA hypermethylation is a mechanism for loss of expression of the HLA class I genes in human esophageal squamous cell carcinomas.

Nie Y, Yang G, Song Y, Zhao X, So C, Liao J, Wang LD, Yang CS.

Laboratory for Cancer Research, College of Pharmacy, Rutgers-The State University of New Jersey, 164 Frelinghuysen Road, Piscataway, NJ 08854-8020, USA.

The three human leukocyte antigen (HLA) class I antigens, HLA-A, HLA-B and HLA-C, play important roles in the elimination of transformed cells by cytotoxic T cells. Frequent loss of expression of these antigens at the cell surface has been observed in many human cancers. Various mechanisms for post-transcriptional regulation have been proposed and tested but the molecular mechanisms for transcriptional regulation are not clear. We show by immunohistochemistry that the HLA class I antigens are absent in 26 of 29 (89%) samples of human esophageal squamous cell carcinomas (ESCC). Eleven of the 26 ESCC samples lost mRNA expression for at least one of the HLA genes, as shown by RT-PCR. DNA from the 29 pairs of ESCC and neighboring normal epithelium were examined for CpG island hypermethylation, homozygous deletion, microsatellite instability (MSI) and loss of heterozygosity (LOH). DNA from normal epithelial tissues had no detectable methylation of the CpG islands of any of these gene loci. Thirteen of 29 ESCC samples (45%) exhibited methylation of one or more of the three HLA loci and six samples (21%) exhibited methylation of all three loci. The HLA-B gene locus was most frequently methylated (38%). HLA-B mRNA expression in an ESCC cell line, where HLA-B was hypermethylated and did not express mRNA, was activated after treatment with 5-aza-2'-deoxycytidine. Homozygous deletion of these three gene loci was not observed. Relatively low rates of LOH and MSI were observed for the microsatellite markers D6S306, D6S258, D6S273 and D6S1666, close to the HLA-A, -B and -C loci, although a high ratio of LOH was observed at a nearby locus (represented by the markers D6S1051 and D6S1560), where the tumor suppressor gene p21(Waf1) resides. A strong correlation between genetic alterations and mRNA inactivation was observed in the ESCC samples. Our results indicate that HLA class I gene expression was frequently down-regulated in ESCC at both the protein and mRNA levels and that hypermethylation of the promoter regions of the HLA-A, -B and -C genes is a major mechanism of transcriptional inactivation.

PMID: 11577000 [PubMed - indexed for MEDLINE]

Comment in:

- [Cancer Res. 2002 Jan 15;62\(2\):618-9.](#)

FREE full text article at
concerres.aacrjournals.org

BMI-1 gene amplification and overexpression in hematological malignancies occur mainly in mantle cell lymphomas.

Bea S, Tort F, Pinyol M, Puig X, Hernandez L, Hernandez S, Fernandez PL, van Lohuizen M, Colomer D, Campo E.

The Hematopathology Section, Laboratory of Anatomic Pathology, Hospital Clinic, Institut d'Investigacions Biomediques August Pi i Sunyer (IDIBAPS), University of Barcelona, Spain.

The BMI-1 gene is a putative oncogene belonging to the Polycomb group family that cooperates with c-myc in the generation of mouse lymphomas and seems to participate in cell cycle regulation and senescence by acting as a transcriptional repressor of the INK4a/ARF locus. The BMI-1 gene has been located on chromosome 10p13, a region involved in chromosomal translocations in infant leukemias, and amplified in occasional non-Hodgkin's lymphomas (NHLs) and solid tumors. To determine the possible alterations of this gene in human malignancies, we have examined 160 lymphoproliferative disorders, 13 myeloid leukemias, and 89 carcinomas by Southern blot analysis and detected BMI-1 gene amplification (3- to 7-fold) in 4 of 36 (11%) mantle cell lymphomas (MCLs) with no alterations in the INK4a/ARF locus. BMI-1 and p16INK4a mRNA and protein expression were also studied by real-time quantitative reverse transcription-PCR and Western blot, respectively, in a subset of NHLs. BMI-1 expression was significantly higher in chronic lymphocytic leukemia and MCL than in follicular lymphoma and large B cell lymphoma. The four tumors with gene amplification showed significantly higher mRNA levels than other MCLs and NHLs with the BMI-1 gene in germline configuration. Five additional MCLs also showed very high mRNA levels without gene amplification. A good correlation between BMI-1 mRNA levels and protein expression was observed in all types of lymphomas. No relationship was detected between BMI-1 and p16INK4a mRNA levels. These findings suggest that BMI-1 gene alterations in human neoplasms are uncommon, but they may contribute to the pathogenesis in a subset of malignant lymphomas, particularly of mantle cell type.

PMID: 11289106 [PubMed - indexed for MEDLINE]



Expression of bcr-abl mRNA in individual chronic myelogenous leukaemia cells as determined by in situ amplification.

Pachmann K, Zhao S, Schenk T, Kantarjian H, El-Naggar AK, Siciliano MJ, Guo JQ, Arlinghaus RB, Andreeff M.

The University of Texas M.D. Anderson Cancer Center, Department of Molecular Haematology and Therapy, 1515 Holcombe Boulevard, Houston, TX 77030, USA.

We present the results of a novel method developed for evaluation of in situ amplification, a molecular genetic method at the cellular level. Reverse transcription polymerase chain reaction (RT-PCR) was used to study bcr-abl transcript levels in individual cells from patients with chronic myelogenous leukaemia (CML). After hybridizing a fluorochrome-labelled probe to the cell-bound RT-PCR product, bcr-abl mRNA-positive cells were determined using image analysis. A dilution series of bcr-abl-positive BV173 into normal cells showed a good correlation between expected and actual values. In 25 CML samples, the percentage of in situ PCR-positive cells showed an excellent correlation with cytogenetic results ($r = 0.94$, $P < 0.0001$), interphase fluorescence in situ hybridization (FISH) ($r = 0.95$, $P = 0.001$) and hypermetaphase FISH ($r = 0.81$, $P < 0.001$). The fluorescence intensity was higher in residual CML cells after interferon (IFN) treatment than in newly diagnosed patients ($P = 0.004$), and was highest in late-stage CML resistant to IFN therapy and lowest in CML blast crisis ($P = 0.001$). Mean fluorescence values correlated with bcr-abl protein levels, as determined by Western blot analysis ($r = 0.62$). Laser scanning cytometry allowing automated analysis of large numbers of cells confirmed the results. Thus, fluorescence in situ PCR provides a novel and quantitative approach for monitoring tumour load and bcr-abl transcript levels in CML.

PMID: 11260080 [PubMed - indexed for MEDLINE]



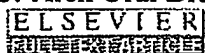
Differential upregulation of cellular adhesion molecules at the sites of oxidative stress in experimental acute pancreatitis.

Telek G, Ducroc R, Scoazec JY, Pasquier C, Feldmann G, Roze C.

INSERM U 410, Universite Paris 7 Denis Diderot, 75870 Paris, France.

BACKGROUND: Severe acute pancreatitis (AP)(2) is associated with exaggerated leukocyte adherence and activation. Endothelial cellular adhesion molecules (CAMs) can be induced by cytokines, but also directly by oxygen free radicals (OFRs), mediated by nuclear factor kappa-B (NF-kappa B). We investigated the behavior of inducible CAMs in relation to pancreatic oxidative stress. Our novel modification of cerium capture histochemistry (reaction of OFRs with cerium produces laser reflective Ce perhydroxide precipitates) combined with reflectance confocal laser scanning microscopy (CLSM) allows the histological codemonstration of in vivo OFR production and immunolabeled CAMs, or NF-kappa B. **METHODS:** Taurocholate AP was induced in rats; sham operated and normal animals served as controls. To achieve in situ, in vivo reaction of cerium with OFRs, animals were perfused with CeCl(3) solution at different time points (1, 2, 8, 24 h) and then sacrificed. E-selectin, P-selectin, ICAM-1, VCAM, and NF-kappa B p65 were labeled by immunofluorescence (IF) on frozen sections of cerium perfused pancreata. IF and Ce perhydroxide reflectance were simultaneously detected by CLSM. Pancreatic gene expression of the same CAMs was quantified by competitive RT-PCR (MIMIC internal control). **RESULTS:** Control pancreata showed negligible reflectance and minimal CAM expression. Early (1, 2 h) AP samples were characterized by intense, heterogeneous acinar OFR production, strong P-selectin, and increasing ICAM expression, with nuclear translocation of p65, histologically all colocalizing with the areas of acinar oxidative stress. Adherent polymorphonuclear leukocytes (PMNs) displayed weak OFR formation. Later (8, 24 h), a slowly declining P-selectin, but persisting ICAM-1 expression, was paralleled by widespread adherence of PMNs producing surprisingly large amounts of OFRs. VCAM and E-selectin showed a mild increase at 24 h. CAM gene activation was in good correlation with the protein expression. **CONCLUSIONS:** The early acinar oxidative stress is colocalized with NF-kappa B activation, preferential P-selectin, and ICAM upregulation in this AP model. Subsequently, adherent, activated PMNs become the major source of OFRs, thereby contributing to tissue damage. Copyright 2001 Academic Press.

PMID: 11180997 [PubMed - indexed for MEDLINE]



Increasing expression of tissue plasminogen activator and plasminogen activator inhibitor type 2 in dog gingival tissues with progressive inflammation.

Lindberg P, Kinnby B, Lecander I, Lang NP, Matsson L.

Center for Oral Health Sciences, Malmo University, S-214 21 Malmo, Sweden.
pia.lindberg@od.mah.se

Urokinase and tissue-type plasminogen activators (u--PA and t--PA) are serine proteases that convert plasminogen into plasmin, which degrades matrix proteins and activates metalloproteinases. The PAs are balanced by specific inhibitors (PAI--1 and PAI--2). Local production of t--PA and PAI--2 was recently demonstrated in human gingival tissues. The aim now was to investigate the production and localization of t--PA and PAI--2 in gingival tissues from dogs in three well-defined periodontal conditions; clinically healthy gingiva, chronic gingivitis and an initial stage of ligature-induced loss of attachment. At the start of the experiment the gingiva showed clear signs of inflammation. Clinically healthy gingiva were obtained after 21 days period of intense oral hygiene. Attachment loss was induced by placing rubber ligatures around the neck of some teeth. Biopsies were taken from areas representing the different conditions and prepared for in situ hybridization and immunohistochemistry. In clinically healthy gingiva both t--PA mRNA and antigen were expressed in a thin outer layer of the sulcular and junctional epithelia. No t--PA signals or staining were seen in connective tissue. Both mRNA signaling and immunostaining for t--PA were stronger in chronic gingivitis. In areas with loss of attachment, t--PA mRNA as well as antigen were found in the sulcular and junctional epithelia to a similar degree as in gingivitis. Occasionally the connective tissue was involved, especially in connection with vessels. PAI--2 mRNA was seen in a thin outer layer of the sulcular and junctional epithelia in clinically healthy gingiva, but no signals were seen in connective tissue. PAI--2 antigen was found primarily in the outer layer of the sulcular and junctional epithelia. Some cells in the connective tissue were stained. In gingivitis, PAI--2 signals were mainly found in the same locations, but more intense and extending towards the connective tissue. Immunostaining was seen in the outer half of the sulcular and junctional epithelia as well as in the upper part of the connective tissue, close to the sulcular epithelium. In sites with loss of attachment, PAI--2 mRNA was found throughout the sulcular and junctional epithelia, as was the antigen, which stained intensely. No PAI--2 mRNA was seen in connective tissue; the antigen was found scattered, especially near vessels. This study shows that the expression of both t--PA and PAI--2 increases with experimental gingival inflammation in the dog, and furthermore, the two techniques demonstrate a strong correlation between the topographical distribution of the site of protein synthesis and the tissue location of the antigens for both t--PA and PAI--2. The distribution correlates well with previous findings in humans.



Rapid quantitation of proinflammatory and chemoattractant cytokine expression in small tissue samples and monocyte-derived dendritic cells: validation of a new real-time RT-PCR technology.

Blaschke V, Reich K, Blaschke S, Zipprich S, Neumann C.

Department of Dermatology, von-Siebold-Str. 3, D-37075, Goettingen, Germany.
vblasch@gwdg.de

The analysis of cytokine profiles plays a central part in the characterization of disease-related inflammatory pathways and the identification of functional properties of immune cell subpopulations. Because tissue biopsy samples are too small to allow the detection of cytokine protein, the detection of mRNA by RT-PCR analysis is often used to investigate the cytokine milieu in inflammatory lesions. RT-PCR itself is a qualitative method, indicating the presence or absence of specific transcripts. With the use of internal or external standards it may also serve as a quantitative method. The most widely accepted method is quantitative competitive RT-PCR, based on internal shortened standards. Recently, online real-time PCR has been introduced (LightCycler), which allows quantitation in less than 30 min. Here, we have tested its use for the analysis of cytokine gene expression in different experimental in vitro and ex vivo settings. First, we compared quantitative competitive RT-PCR with real-time RT-PCR in the quantitation of transcription levels of the CD4(+) cell-specific chemoattractant Interleukin-16 during the maturation of monocyte-derived dendritic cells, and found a good correlation between both methods. Second, differences in the amounts of IL-16 mRNA in synovial tissue from patients with rheumatoid arthritis and osteoarthritis as assessed by real-time RT-PCR paralleled differences in the level of IL-16 protein in the synovial fluid. Finally, we employed real-time RT-PCR to study the cutaneous expression of several cytokines during experimental immunomodulatory therapy of psoriasis by Interleukin-10, and demonstrate that the technique is suitable for pharmacogenomic monitoring. In summary, real-time RT-PCR is a sensitive and rapid tool for quantifying mRNA expression even with small quantities of tissue. The results obtained do not differ from those generated by quantitative competitive RT-PCR.

Publication Types:

- Evaluation Studies

PMID: 11121549 [PubMed - indexed for MEDLINE]



Up-regulation of mitochondrial peripheral benzodiazepine receptor expression by tumor necrosis factor alpha in testicular leydig cells. Possible involvement in cell survival.

Rey C, Mauduit C, Naureils O, Benahmed M, Louisot P, Gasnier F.

INSERM U. 189, Faculte de Medecine Lyon-Sud, BP12, 69921 cedex, Oullins, France.

Porcine Leydig cells in primary cultures are resistant to tumor necrosis factor alpha (TNFalpha) cytotoxicity. Here we report that these cells can be rendered sensitive to TNFalpha killing by treatment with the translational inhibitor cycloheximide, suggesting the existence of proteins that can suppress the death stimulus induced by the cytokine. In search of these cytoprotective proteins, we focused on the constituents of the mitochondrial permeability transition pore (PT pore), whose opening has been shown to play a critical role in the TNFalpha-mediated death pathway. We found that TNFalpha up-regulated mRNA and protein expression of the mitochondrial peripheral benzodiazepine receptor (PBR), an outer membrane-derived constituent of the pore. A strong correlation was established between the resistance of the cells to TNFalpha killing and the density of PBR-binding sites. Concomitantly, TNFalpha down-regulated Bcl-2 mRNA and protein expression. As Bcl-2 has been shown to be an endogenous inhibitor of the PT pore, we hypothesize that the TNFalpha-induced up-regulation of PBR expression may compensate for the decrease in Bcl-2 levels to prevent the opening of the PT pore.

PMID: 11077046 [PubMed - indexed for MEDLINE]

FREE full text article of
www.jimmunol.org

Cyclooxygenase-2 expression in macrophages: modulation by protein kinase C-alpha.

Giroux M, Descoteaux A.

Institut National de la Recherche Scientifique-Institut Armand-Frappier, Universite du Quebec, Laval, Canada.

Cyclooxygenase-2 (COX-2) is an inducible enzyme responsible for high levels of PG production during inflammation and immune responses. Previous studies with pharmacological inhibitors suggested a role for protein kinase C (PKC) in PG production possibly by regulating COX-2 expression. In this study, we addressed the role of PKC-alpha in the modulation of COX-2 expression and PGE2 synthesis by the overexpressing of a dominant-negative (DN) mutant of this isoenzyme in the mouse macrophage cell line RAW 264.7. We investigated the effect of various stimuli on COX-2 expression, namely, LPS, IFN-gamma, and the intracellular parasite *Leishmania donovani*. Whereas LPS-induced COX-2 mRNA and protein expression were down-regulated in DN PKC-alpha-overexpressing clones, IFN-gamma-induced COX-2 expression was up-regulated in DN PKC-alpha-overexpressing clones with respect to normal RAW 264.7 cells. Measurements of PGE2 levels revealed a strong correlation between PGE2 secretion and IFN-gamma-induced COX-2 mRNA and protein levels in DN PKC-alpha-overexpressing clones. Taken together, these results suggest a role for PKC-alpha in the modulation of LPS- and IFN-gamma-induced COX-2 expression, as well as in IFN-gamma-induced PGE2 secretion.

PMID: 11034408 [PubMed - indexed for MEDLINE]

FREE full text article at
molehr.oupjournals.org

Inhibin and activin production and subunit expression in human placental cells cultured in vitro.

Debieve F, Pampfer S, Thomas K.

Department of Obstetrics and Gynecological Endocrinology, Universite Catholique de Louvain, 1200 Brussels, Belgium.

Inhibins and activins are dimeric proteins, with each subunit being one of three related protein subunits (alpha, betaA or betaB). The mRNA levels of these subunits were studied quantitatively during in-vitro differentiation of human cytotrophoblast cells into syncytium, using Northern blot analysis and semi-quantitative reverse transcription-polymerase chain reaction (RT-PCR) analysis. The corresponding protein concentrations were determined by specific enzyme-linked immunosorbent assays for inhibin A, B, pro alphaC and activin A in cellular protein extracts and culture medium (n = 5).

Immunofluorescence studies showed syncytium formation after 48 h. The alpha subunit was present before plating and increased at 48 h ($P < 0.001$) while the betaA subunit was weak before plating and increased at 24 h. The betaB subunit was not detected. With respect to corresponding protein synthesis, inhibin A (alpha + betaA) had risen after 48 h in cellular protein extract and after 72 h in culture medium, while activin A (betaA + betaB) was detected after 24 h, with no significant variations in culture medium. There was a good correlation between inhibin A and alpha subunit expression ($r = 0.736$, $P < 0.001$), as well as between activin A and betaA subunit expression ($r = 0.755$, $P < 0.001$). This study showed that mRNA expression parallels protein synthesis of inhibin and activin in trophoblast cells. Inhibin A synthesis appears to be dependent on alpha subunit mRNA expression, rather than on the betaA subunit which controls activin A synthesis. This study has also shown that isolated cytotrophoblast cells do not produce dimeric inhibin. However, during the transformation of cytotrophoblast cells into syncytium, betaA subunit mRNA expression may be an indicator of cell aggregation, while alpha subunit mRNA expression may be an indicator of cell fusion.

PMID: 10908285 [PubMed - indexed for MEDLINE]



Basic fibroblast growth factor expression is increased in human renal fibrogenesis and may mediate autocrine fibroblast proliferation.

Strutz F, Zeisberg M, Hemmerlein B, Sattler B, Hummel K, Becker V, Muller GA.

Department of Nephrology and Rheumatology, Georg-August-University Gottingen, Germany. fstrutz@gwdg.de

BACKGROUND: Interstitial fibroblasts play a critical role in renal fibrogenesis, and autocrine proliferation of these cells may account for continuous matrix synthesis. Basic fibroblast growth factor (FGF-2) is mitogenic for most cells and exerts intracrine, autocrine, and paracrine effects on epithelial and mesenchymal cells. The aims of the present studies were to localize and quantitate the expression of FGF-2 in normal and pathologic human kidneys and to study the in vitro effects of FGF-2 on proliferation, differentiation, and matrix production of isolated cortical kidney fibroblasts. **METHODS:** FGF-2 protein expression was localized by immunofluorescence double labelings in normal and fibrotic human kidneys. Subsequently, interstitial FGF-2 labeling was determined semiquantitatively in 8 normal kidneys and 39 kidneys with variable degrees of interstitial fibrosis and was correlated with the morphometrically determined interstitial cortical volume. In addition, FGF-2 expression was quantitated by immunoblot analysis in three normal and six fibrotic kidneys. FGF-2 mRNA was localized by in situ hybridizations. Seven primary cortical fibroblast lines were established, and expression of FGF-2 and FGF receptor-1 (FGFR-1) were examined. The effects of FGF-2 on cell proliferation were determined by bromodeoxyuridine incorporation and cell counts, those on differentiation into myofibroblasts by staining for alpha-smooth muscle actin, and those on matrix synthesis by enzyme-linked immunosorbent assay for collagen type I and fibronectin. Finally, proliferative activity in vivo was evaluated by expression of MIB-1 (Ki-67 antigen). **RESULTS:** In normal kidneys, FGF-2 expression was confined to glomerular, vascular, and a few tubular as well as interstitial fibroblast-like cells. The expression of FGF-2 protein was increased in human kidneys, with tubulointerstitial scarring correlating with the degree of interstitial fibrosis ($r = 0.84$, $P < 0.01$). Immunoblot analyses confirmed a significant increase in FGF-2 protein expression in kidneys with interstitial scarring. In situ hybridization studies demonstrated low-level detection of FGF-2 mRNA in normal kidneys. However, FGF-2 mRNA expression was robustly up-regulated in interstitial and tubular cells in end-stage kidneys, indicating that these cells are the source of excess FGF-2 protein. Primary cortical fibroblasts express FGF-2 and FGFR-1 in vitro. FGF-2 induced a robust growth response in these cells that could be blocked specifically by a neutralizing FGF-2 antibody. Interestingly, the addition of the neutralizing antibody alone did reduce basal proliferation up to 31.5%. In addition, FGF-2 induced expression of alpha-smooth muscle actin up to 1.6-fold, but no significant effect was observed on the synthesis of collagen type I and fibronectin. Finally, staining for MIB-1 revealed a good correlation of interstitial FGF-2 positivity

with interstitial and tubular proliferative activity ($r = 0.71$, $P < 0.01$ for interstitial proliferation, $N = 30$). CONCLUSIONS: Interstitial FGF-2 protein and mRNA expression correlate with interstitial scarring. FGF-2 is a strong mitogen for cortical kidney fibroblasts and may promote autocrine fibroblast growth. Expression of FGF-2 correlates with interstitial and tubular proliferation in vivo.

PMID: 10760088 [PubMed - indexed for MEDLINE]



Correlative immunohistochemical and reverse transcriptase polymerase chain reaction analysis of somatostatin receptor type 2 in neuroendocrine tumors of the lung.

Papotti M, Croce S, Macri L, Funaro A, Pecchioni C, Schindler M, Bussolati G.

Department of Biomedical Sciences and Oncology, University of Turin, Italy.

Somatostatin receptors type 2 (sst2) have been frequently detected in neuroendocrine tumors and bind somatostatin analogues, such as octreotide, with high affinity. Receptor autoradiography, specific mRNA detection and, more recently, antisst2 polyclonal antibodies are currently employed to reveal sst2. The aim of the present study was to investigate by three different techniques the presence of sst2 in a series of 26 neuroendocrine tumors of the lung in which fresh frozen tissue and paraffin sections were available. It was possible, therefore, to compare, in individual cases, RNA analysis studied by reverse transcriptase polymerase chain reaction (RT-PCR), in situ hybridization (ISH), and immunohistochemistry. A series of 20 nonneuroendocrine lung carcinoma samples served as controls. RT-PCR was positive for sst2 in 22 of 26 samples, including 15 of 15 typical carcinoids, 5 of 6 atypical carcinoids, and 2 of 5 small-cell carcinomas. The sst2 mRNA signal obtained by RT-PCR was strong in the majority (87%) of typical carcinoids and of variable intensity in atypical carcinoids and small-cell carcinomas. A weakly positive signal was observed in 5 of 20 control samples. In immunohistochemistry, two different antibodies (anti-sst2) were employed, including a monoclonal antibody, generated in the Department of Pathology, University of Turin. In the majority of samples a good correlation between sst2 mRNA (as detected by RT-PCR) and sst2 protein expression (as detected by immunohistochemistry) was observed. However, one atypical carcinoid and one small-cell carcinoma had focal immunostaining but no RT-PCR signal. ISH performed in selected samples paralleled the results obtained with the other techniques. A low sst2 expression was associated with high grade neuroendocrine tumors and with aggressive behavior. It is concluded that 1) neuroendocrine tumors of the lung express sst2, and there is a correlation between the mRNA amount and the degree of differentiation; 2) immunohistochemistry and ISH are reliable tools to demonstrate sst2 in these tumors; and 3) sst2 identification in tissue sections may provide information on the diagnostic or therapeutic usefulness of somatostatin analogues in individual patients with neuroendocrine tumors.

PMID: 10718213 [PubMed - indexed for MEDLINE]



Overexpression of chemokines, fibrogenic cytokines, and myofibroblasts in human membranous nephropathy.

Mezzano SA, Droguett MA, Burgos ME, Ardiles LG, Aros CA, Caorsi I, Egido J.

Division of Nephrology, School of Medicine, Universidad Austral, Valdivia, Chile.
smezzano@uach.cl

Overexpression of chemokines, fibrogenic cytokines, and myofibroblasts in human membranous nephropathy. **BACKGROUND:** Proteinuria plays a central role in the progression of glomerular disease, and there is growing evidence suggesting that it may determine tubular cell activation with release of chemokines and fibrogenic factors, leading to interstitial inflammatory reaction. However, most studies on this subject have been performed in experimental models, and the experience in human kidney biopsies has been scarce. We analyzed the tissue sections of patients with idiopathic membranous nephropathy (IMN), a noninflammatory glomerular disease that may follow a progressive disease with heavy persistent proteinuria, interstitial cell infiltration, and decline of renal function. **METHODS:** Paraffin-embedded biopsy specimens from 25 patients with IMN (13 progressive and 12 nonprogressive) were retrospectively studied by immunohistochemistry [monocyte chemoattractant protein-1 (MCP-1), regulated on activation normal T-cell expressed and secreted chemokine (RANTES), osteopontin (OPN), platelet-derived growth factor-BB (PD-GF-BB)] and in situ hybridization [MCP-1, RANTES, PDGF-BB, transforming growth factor-beta1 (TGF-beta1)]. Moreover, we studied the presence of myofibroblasts, which were identified by the expression of alpha-smooth muscle actin (alpha-SMA), the monocytes/macrophages (CD68-positive cells), and T-cell infiltration (CD4+ and CD8+ cells). All of the patients were nephrotic and without treatment at time of the biopsy. **RESULTS:** A strong up-regulation of MCP-1, RANTES, and OPN expression was observed, mainly in tubular epithelial cells, with a significant major intensity in the progressive IMN patients. A strong correlation between the mRNA expression and the corresponding protein was noted. The presence of these chemokines and OPN was associated with interstitial cell infiltration. TGF-beta and PDGF were also up-regulated, mainly in tubular epithelial cells, with a stronger expression in the progressive IMN, and an association with the presence of myofibroblasts was found. **CONCLUSIONS:** Patients with severe proteinuria and progressive IMN have an overexpression in tubular epithelial cells of the chemokines MCP-1, RANTES, and OPN and the profibrogenic cytokines PDGF-BB and TGF-beta. Because this up-regulation was associated with an interstitial accumulation of mononuclear cells and an increase in myofibroblastic activity, it is suggested that those mediators are potential predictors of progression in IMN. Finally, based on experimental data and the findings of this article, we speculate that severe proteinuria is the main factor responsible for the up-regulation of these factors in tubular epithelial cells.

FREE full text article at
www.jhc.org

Expression of embryonic fibronectin isoform EIIIA parallels alpha-smooth muscle actin in maturing and diseased kidney.

Barnes VL, Musa J, Mitchell RJ, Barnes JL.

Department of Medicine, Division of Nephrology, University of Texas Health Science Center, San Antonio, Texas, USA.

In this study we examined if an association exists between expression of an alternatively spliced "embryonic" fibronectin isoform EIIIA (Fn-EIIIA) and alpha-smooth muscle actin (alpha-SMA) in the maturing and adult rat kidney and in two unrelated models of glomerular disease, passive accelerated anti-glomerular basement membrane (GBM) nephritis and Habu venom (HV)-induced proliferative glomerulonephritis, using immunohistochemistry and in situ hybridization. Fn-EIIIA and alpha-SMA proteins were abundantly expressed in mesangium and in periglomerular and peritubular interstitium of 20-day embryonic and 7-day (D-7) postnatal kidneys in regions of tubule and glomerular development. Staining was markedly reduced in these structures in maturing juvenile (D-14) kidney and was largely lost in adult kidney. Expression of Fn-EIIIA and alpha-SMA was reinitiated in the mesangium and the periglomerular and peritubular interstitium in both models and was also observed in glomerular crescents in anti-GBM nephritis. Increased expression of Fn-EIIIA mRNA by in situ hybridization corresponded to the localization of protein staining. Dual labeling experiments verified co-localization of Fn-EIIIA and alpha-SMA, showing a strong correlation of staining between location and staining intensity during kidney development, maturation, and disease. Expression of EIIIA mRNA corresponded to protein expression in developing and diseased kidneys and was lost in adult kidney. These studies show a recapitulation of the co-expression of Fn-EIIIA and alpha-SMA in anti-GBM disease and suggest a functional link for these two proteins.

PMID: 10330455 [PubMed - indexed for MEDLINE]

Tumor necrosis factor-alpha upregulates the prostaglandin E2 EP1 receptor subtype and the cyclooxygenase-2 isoform in cultured amnion WISH cells.

Spaziani EP, Benoit RR, Tsibris JC, Gould SF, O'Brien WF.

University of South Florida Health Science Center, Department of Obstetrics & Gynecology, Tampa 33612, USA. espazian@com1.med.usf.edu

Recent studies have demonstrated a strong correlation between infection and preterm labor. Preterm delivery is also associated with high levels of cytokines and prostaglandins in amniotic fluid. The purpose of this study was to investigate the effect of tumor necrosis factor-alpha (TNF-alpha) on the levels of cyclooxygenase, prostaglandin E2 production (PGE2), and expression of the PGE2 receptor subtype EP1 in amnion WISH cell culture. Amnion WISH cell cultures were incubated in increasing concentrations of TNF-alpha (0-50 ng/ml). Changes in cyclooxygenase and EP1 receptor proteins were evaluated by Western blot analysis. Changes in EP1 mRNA were evaluated by Northern blot, and culture fluid concentrations of PGE2 were estimated by enzyme immunoassay (EIA). EP1 protein ($p<0.01$), EP1 mRNA ($p<0.05$), cyclooxygenase-2 (COX-2) protein ($p<0.001$), and PGE2 concentrations ($p<0.01$) all increased with increasing concentrations of TNF-alpha. Changes in COX-1 protein were not observed following TNF-alpha-incubation. The results suggest that TNF-alpha may play a role in infection-induced preterm labor by its pleiotropic ability to simultaneously stimulate COX-2 activity, PGE2 concentrations, and PGE2 EP1 receptor levels in human amnion.

PMID: 9877447 [PubMed - indexed for MEDLINE]

FREE full text article at
www.jhc.org

Intestinal carbamoyl phosphate synthase I in human and rat. Expression during development shows species differences and mosaic expression in duodenum of both species.

Van Beers EH, Rings EH, Posthuma G, Dingemanse MA, Taminiau JA, Heymans HS, Einerhand AW, Buller HA, Dekker J.

Pediatric Gastroenterology and Nutrition, Department Pediatrics, Emma Children's Hospital, Academic Medical Center, Amsterdam, The Netherlands.

The clinical importance of carbamoyl phosphate synthase I (CPSI) relates to its capacity to metabolize ammonia, because CPSI deficiencies cause lethal serum ammonia levels. Although some metabolic parameters concerning liver and intestinal CPSI have been reported, the extent to which enterocytes contribute to ammonia conversion remains unclear without a detailed description of its developmental and spatial expression patterns. Therefore, we determined the patterns of enterocytic CPSI mRNA and protein expression in human and rat intestine during embryonic and postnatal development, using in situ hybridization and immunohistochemistry. CPSI protein appeared during human embryogenesis in liver at 31-35 e. d. (embryonic days) before intestine (59 e.d.), whereas in rat CPSI detection in intestine (at 16 e.d.) preceded liver (20 e.d.). During all stages of development there was a good correlation between the expression of CPSI protein and mRNA in the intestinal epithelium. Strikingly, duodenal enterocytes in both species exhibited mosaic CPSI protein expression despite uniform CPSI mRNA expression in the epithelium and the presence of functional mitochondria in all epithelial cells. Unlike rat, CPSI in human embryos was expressed in liver before intestine. Although CPSI was primarily regulated at the transcriptional level, CPSI protein appeared mosaic in the duodenum of both species, possibly due to post-transcriptional regulation.

PMID: 9446830 [PubMed - indexed for MEDLINE]

Human thyroid carcinoma cell lines and normal thyrocytes: expression and regulation of matrix metalloproteinase-1 and tissue matrix metalloproteinase inhibitor-1 messenger-RNA and protein.

Aust G, Hofmann A, Laue S, Rost A, Kohler T, Scherbaum WA.

Institut of Anatomy, University of Leipzig, Germany.

Matrix metalloproteinase-1 (MMP-1) and tissue matrix metalloproteinase inhibitor 1 (TIMP-1) play an important role in remodeling the extracellular matrix in normal and pathological processes. The effect of phorbol-myristate acetate (PMA), interleukin-1 (IL-1), and tumor necrosis factor-alpha (TNF-alpha) on MMP-1 and TIMP-1 expression was studied on highly purified thyrocytes and undifferentiated 8505 C, C 643, HTh 74, SW 1736 thyroid carcinoma cells compared with thyroid-derived fibroblasts. Messenger RNA (mRNA) levels were monitored by competitive semiquantitative reverse transcriptase polymerase chain reaction (RT-PCR) after 24 hours. Culture supernatants were assayed for free and/or complexed MMP-1 and TIMP-1 after 48 hours using enzyme-linked immunosorbent assay (ELISA) systems (detection limit: <2 ng/mL). MMP-1 and TIMP-1 mRNA were present in all cell types, although thyrocytes showed MMP-1 mRNA levels near the detection limit. 8505 C expressed MMP-1 mRNA levels of up to 10(6) times those of the other cells analyzed. PMA and IL-1 increased MMP-1 mRNA in most cell types. TIMP-1 mRNA increased after treatment with PMA in all cells except 8505 C, whereas only slight effects were shown after IL-1 stimulation. MMP-1 protein was undetectable in normal thyrocyte cultures, but was secreted spontaneously by all cell lines ([ng/mL]; C 643: 15+/-7; HTh 74: 81+/-1; SW 1736: 13+/-2; 8505 C: 2097+/-320). There was a strong correlation between levels of MMP-1 mRNA and protein ($r = 0.99$, $p < .0001$). PMA and IL-1 increased MMP-1 secretion in all cell types after 48 hours. Fibroblasts ([ng/mL] 517+/-55) and the cell lines (C 643: 142+/-48; HTh 74: 115+/-13; SW 1736: 202+/-14; 8505C: 120+/-19) secreted TIMP-1 in unstimulated cultures, whereas only a trace amount was detected in thyrocyte cultures, even after PMA treatment. IL-1 upregulated TIMP-1 secretion after 48 hours in SW 1736, HTh 74, and C 643 cells. Our data suggest that in contrast to normal thyrocytes, dedifferentiated thyroid carcinoma cell lines are potential producers of MMP-1 as well as TIMP-1. High MMP-1 or MMP-1/TIMP-1 expression may play a role in tissue invasion of undifferentiated thyroid cancer cells.

PMID: 9349574 [PubMed - indexed for MEDLINE]

TNF-alpha and IL-8 are upregulated in the epidermis of normal human skin after UVB exposure: correlation with neutrophil accumulation and E-selectin expression.

Strickland I, Rhodes LE, Flanagan BF, Friedmann PS.

Department of Dermatology, University of Liverpool, United Kingdom.

The in vivo response to ultraviolet B (UVB) radiation in skin is characterized by the accumulation of both mononuclear and polymorphonuclear cells within the dermis and an induction of vascular endothelial adhesion molecules. Epidermal production of cytokines (IL-8 and TNF-alpha) has been strongly implicated in the development of UVB-induced inflammation. In the current study, we examined the time course of IL-8 and TNF-alpha mRNA and protein expression in the epidermis over a 24-h period after in vivo UVB irradiation. Also, the induction of adhesion molecule expression and the accumulation of neutrophils within the dermis were followed. We found constitutive expression of both cytokines (mRNA and protein) in the epidermis of unirradiated skin. IL-8 was rapidly upregulated after irradiation and mRNA and protein increased at 4 h, reaching a maximum between 8 and 24 h. TNF-alpha mRNA and protein was minimally increased by 8 h after UVB irradiation and reached a maximum by 24 h. No significant alteration in ICAM-1 or VCAM-1 expression was observed. E-selectin expression, which was absent from control samples, was increased from 4 h onward and also reached a maximum at 24 h, coinciding with peak neutrophil accumulation. A strong correlation ($r = 0.96$) was found between number of E-selectin-positive vessels and numbers of infiltrating neutrophils at this time. Moreover, because E-selectin expression was increased before any apparent increase in TNF-alpha protein (4 h), TNF-alpha does not appear to be involved in the early induction of the adhesion molecule, but cytokines such as TNF-alpha and IL-8 may act subsequently to augment the inflammatory response.

PMID: 9129230 [PubMed - indexed for MEDLINE]

Down-regulation of prostate-specific antigen expression by finasteride through inhibition of complex formation between androgen receptor and steroid receptor-binding consensus in the promoter of the PSA gene in LNCaP cells.

Wang LG, Liu XM, Kreis W, Budman DR.

Department of Medicine, New York University, Manhasset 11030, USA.

As a specific competitive inhibitor of 5alpha-reductase, an intracellular enzyme that converts testosterone to dihydrotestosterone, finasteride is being extensively used for the treatment of benign prostatic hyperplasia and in experimental settings for prostate cancer. In this study, we showed that finasteride markedly inhibited prostate-specific antigen (PSA) secretion and expression. The promoter of the PSA gene contains several well-known cis-regulatory elements. Among them, steroid receptor-binding consensus (SRBC) has been identified as a functional androgen-responsive element. Our previous study showed that PSA was not only present in conditioned medium of the PSA-positive LNCaP cells but was also detectable in small amounts in PSA-negative cell lines, PC-3 and DU-145 (L. G. Wang et al., *Oncol. Rep.*, 3: 911-917, 1996). A strong correlation between binding of nuclear factors to SRBC and the level of PSA present in the conditioned medium and cell extracts was found in these three cell lines, whereas no such correlation with binding was obtained using Sp1 oligonucleotide as a probe. Binding of LNCaP cell nuclear proteins to SRBC was diminished when the cells were exposed to 25 microM finasteride, at which concentration 50% of both PSA mRNA and protein were inhibited. As a major component of DNA-protein complexes, the level of androgen receptor was dramatically decreased in the cells treated with finasteride. Our data indicate that inhibition of complex formation between SRBC and nuclear proteins due to the remarkable decrease in the level of androgen receptor plays a key role in the down-regulation of PSA gene expression by finasteride in LNCaP cells.

PMID: 9044850 [PubMed - indexed for MEDLINE]

Altered levels of scavenging enzymes in embryos subjected to a diabetic environment.

Forsberg H, Borg LA, Cagliero E, Eriksson UJ.

Department of Medical Cell Biology, University of Uppsala, Sweden.

Maternal diabetes during pregnancy is associated with an increased rate of congenital malformations in the offspring. The exact molecular etiology of the disturbed embryogenesis is unknown, but an involvement of radical oxygen species in the teratological process has been suggested. Oxidative damage presupposes an imbalance between the activity of the free oxygen radicals and the antioxidant defence mechanisms on the cellular level. The aim of the present study was to investigate if maternal diabetes *in vivo*, or high glucose *in vitro* alters the expression of the free oxygen radical scavenging enzymes superoxide dismutase (CuZnSOD and MnSOD), catalase and glutathione peroxidase in rat embryos during late organogenesis. We studied offspring of normal and diabetic rats on gestational days 11 and 12, and also evaluated day-11 embryos after a 48 hour culture period in 10 mM or 50 mM glucose concentration. Both maternal diabetes and high glucose culture caused growth retardation and increased rate of congenital malformations in the embryos. The CuZnSOD and MnSOD enzymes were expressed on gestational day 11 and both CuZnSOD, MnSOD and catalase were expressed on day 12 with increased concentrations of MnSOD transcripts when challenged by a diabetic milieu. There was a good correlation between mRNA, protein, and activity levels, suggesting that the regulation of these enzymes occurs primarily at the pretranslational level. Maternal diabetes *in vivo* and high glucose concentration *in vitro* induced increased MnSOD expression, concomitant with increased total SOD activity, and a tentative decrease in catalase expression and activity in the embryos. These findings support the notion of enhanced oxidative stress in the embryo as an etiologic agent in diabetic teratogenesis.

PMID: 8804988 [PubMed - indexed for MEDLINE]

FREE full text article at
www.biolreprod.org

Oxytocin receptors in bovine cervix: distribution and gene expression during the estrous cycle.

Fuchs AR, Ivell R, Fields PA, Chang SM, Fields MJ.

Department of Obstetrics and Gynecology, Cornell University Medical College, New York, New York 10021, USA.

Oxytocin (OT) receptor (OTR) concentrations were determined in the cervix of nonpregnant cows on cycle Days 0, 3, 7-8, 17, and 19 (n = 3-4 cows each day); [3H]OT was used as the labeled ligand. Mucosal and muscle layers of the cervix were also analyzed separately for both ligand binding and expression of the OTR gene using a newly developed RNase protection assay (RAP). Cellular localization of OTR protein was determined by immunohistochemistry. All regions of cervix from cows at estrus had high concentrations of OTR; in the luteal phase, all were sharply down-regulated. At estrus the mucosal layer had about 30-fold higher concentrations than the muscle layer. OTR mRNA was readily detected by RAP in the mucosa from estrous cows, while much weaker signals were found in the muscle. On Days 7-17, the OTR mRNA signals in both mucosa and muscle were very faint or nondetectable. Thus, there was a good correlation between ligand binding and mRNA expression, which suggests that OTR concentrations are mainly regulated at the transcriptional level. The epithelial cells at the luminal surface of the mucosa were the principal site of immunoreactive OTR; muscle cells showed significantly weaker signals. Previously, OT was found to stimulate prostaglandin (PG) E2 output in vitro in bovine cervical tissues. Since PGE2 is capable of softening the cervix, our findings suggest that OT may have a novel physiological function to cause softening of the bovine cervix mediated by the release of PGE2.

PMID: 8835394 [PubMed - indexed for MEDLINE]

Involvement of the CCND1 gene in hairy cell leukemia.

de Boer CJ, Kluin-Nelemans JC, Dreef E, Kester MG, Kluin PM, Schuuring E, van Krieken JH.

Department of Pathology, University of Leiden, The Netherlands.

BACKGROUND: Previous results suggested increased mRNA expression of CCND1 in hairy cell leukemia (HCL). The CCND1 gene is involved in the t(11;14)(q13;q32) chromosomal rearrangement, a characteristic abnormality in mantle cell lymphoma (MCL). We and others reported that, in contrast to other B-cell lymphomas, almost all MCL have over-expression of the CCND1 gene with a good correlation between RNA and protein analysis. Recent studies showed that overexpression of the cyclin D1 protein can be easily detected by immunohistochemistry (IHC) on formalin-fixed, paraffin embedded tissues. **PATIENTS AND METHODS:** To investigate whether the CCND1 gene is involved in HCL, we performed IHC on a series of 22 cases using formalin-fixed paraffin embedded splenectomy specimens. For IHC the sections were boiled in citrate buffer. The presence of rearrangements within the BCL-1 locus and the CCND1 gene was analyzed in 13 of 22 cases by Southern blot analysis using all available break-point probes. Expression of CCND1 was analyzed at the mRNA level (Northern blot) and protein level (IHC). **RESULTS:** Overexpression of the cyclin D1 protein using IHC was observed in all cases, with strong expression in 5 cases. Pre-existing B- and T-cell areas of the spleen did not express significant levels of the cyclin D1 protein. Seven of 9 cases analyzed by both IHC and Northern blotting showed overexpression of the CCND1 gene with both methods. No genomic abnormalities were observed in any of the 13 cases studied by Southern blot analysis. Additionally, no 11q13 abnormalities were detected by banding analysis of 19 of 22 cases. **CONCLUSIONS:** The elevated levels of CCND1 mRNA and protein in conjunction with the absence of overt rearrangements within the BCL-1 locus distinguish HCL from MCL and other B-cell malignancies. This suggests that activation of the CCND1 gene in HCL is due to mechanisms other than chromosomal rearrangement.

PMID: 8740788 [PubMed - indexed for MEDLINE]

Malignant transformation of the human endometrium is associated with overexpression of lactoferrin messenger RNA and protein.

Walmer DK, Padin CJ, Wrona MA, Healy BE, Bentley RC, Tsao MS, Kohler MF, McLachlan JA, Gray KD.

Department of Obstetrics and Gynecology, Duke University Medical Center, Durham, North Carolina 27710.

In the mouse uterus, lactoferrin is a major estrogen-inducible uterine secretory protein, and its expression correlates directly with the period of peak epithelial cell proliferation. In this study, we examine the expression of lactoferrin mRNA and protein in human endometrium, endometrial hyperplasias, and adenocarcinomas using immunohistochemistry, Western immunoblotting, and Northern and in situ RNA hybridization techniques. Our results reveal that lactoferrin is expressed in normal cycling endometrium by a restricted number of glandular epithelial cells located deep in the zona basalis. Two thirds (8 of 12) of the endometrial adenocarcinomas examined overexpress lactoferrin. This tumor-associated increase in lactoferrin expression includes an elevation in the mRNA and protein of individual cells and an increase in the number of cells expressing the protein. In comparison, only 1 of the 10 endometrial hyperplasia specimens examined demonstrates an increase in lactoferrin. We also observe distinct cytoplasmic and nuclear immunostaining patterns under different fixation conditions in both normal and malignant epithelial cells, similar to those previously reported in the mouse reproductive tract. Serial sections of malignant specimens show a good correlation between the localization of lactoferrin mRNA and protein in individual epithelial cells by in situ RNA hybridization and immunohistochemistry. Although the degree of lactoferrin expression in the adenocarcinomas did not correlate with the tumor stage, grade, or depth of invasion in these 12 patients, there was a striking inverse correlation between the presence of progesterone receptors and lactoferrin in all 8 lactoferrin-positive adenocarcinomas. In summary, lactoferrin is expressed in a region of normal endometrium known as the zona basalis which is not shed with menstruation and is frequently overexpressed by progesterone receptor-negative cells in endometrial adenocarcinomas.

PMID: 7867003 [PubMed - indexed for MEDLINE]

Myotonic dystrophy: an unstable CTG repeat in a protein kinase gene.

Timchenko L, Monckton DG, Caskey CT.

Department of Molecular and Human Genetics, Baylor College of Medicine, Texas Medical Center, Houston 77030, USA.

Myotonic dystrophy (DM) is caused by the amplification of CTG repeats in the 3' untranslated region of a gene encoding a protein homologous to serine/threonine protein kinases. In DM patients the CTG repeats are extremely unstable, varying in length from patient to patient and generally increasing in length in successive generations. There is a strong correlation between the size of the repeats and the age of onset and severity of the disease. The molecular basis of the effect of the CTG expansion on the development of the DM phenotype continues to be investigated. The first working hypothesis of the molecular mechanism of DM was a reduction in steady-state myotonin-protein kinase (Mt-PK) mRNA and protein levels. However, although the consensus finding is that the Mt PK mRNA and protein levels are decreased in DM patients, it is still not clear if this reduction leads directly to the DM phenotype. In this short review we discuss the molecular aspects of CTG instability and the expression of the myotonin-protein kinase gene in normal and DM populations.

Publication Types:

- Review
- Review, Tutorial

PMID: 7620117 [PubMed - indexed for MEDLINE]



Regulation of cytochrome P4501A1 in teleosts: sustained induction of CYP1A1 mRNA, protein, and catalytic activity by 2,3,7,8-tetrachlorodibenzofuran in the marine fish *Stenotomus chrysops*.

Hahn ME, Stegeman JJ.

Biology Department, Woods Hole Oceanographic Institution, Massachusetts 02543.

Cytochrome P4501A1 (CYP1A1) is known to play important roles in the activation and detoxification of carcinogens and other toxicants in vertebrate animals, including fish. Although extensively studied in mammalian systems, the regulation of CYP1A forms in other vertebrates is less well understood. We examined the time course and dose-response relationships for induction of CYP1A1 mRNA, protein, and catalytic activity by 2,3,7,8-tetrachlorodibenzofuran (TCDF) in the marine fish *Stenotomus chrysops* (scup). The time course of CYP1A1 induction was determined following a single ip dose (10 nmol/kg) of 2,3,7,8-TCDF. Hepatic ethoxyresorufin O-deethylase activity was increased after 1 day, reached a maximum by 8 days, and was still elevated 14 days after treatment. The content of immunodetectable CYP1A1 protein in liver was elevated on Day 1 and continued to increase through 14 days. CYP1A1 protein content was also strongly induced in heart and gill beginning at 2 days after treatment and extending through Day 14. Hepatic CYP1A1 mRNA was strongly induced by 1 day after dosing and remained elevated through 14 days. The sustained induction of CYP1A1 mRNA by 2,3,7,8-TCDF contrasts with the transient induction seen previously in fish treated with nonhalogenated inducers and most likely reflects differences in persistence of the inducers. Dose-response studies indicated that induction of CYP1A1 mRNA, protein, and catalytic activity occurred following doses of 2,3,7,8-TCDF as low as 0.4 nmol/kg (120 ng/kg), within the range of whole-body contents of this congener measured in fish from contaminated environments. The estimated dose producing half-maximal CYP1A1 induction in scup was approximately 2-10 nmol/kg, suggesting that the sensitivity of these fish to induction may be as great as or greater than that of rats. In contrast to previous results obtained with 3,3',4,4'-tetrachlorobiphenyl (TCB) and beta-naphthoflavone, which appear to inhibit or inactivate CYP1A1 in fish and other vertebrates, there was a good correlation among levels of CYP1A1 mRNA, protein, and catalytic activity in individual fish following various doses of 2,3,7,8-TCDF. The difference in response to 2,3,7,8-TCDF versus 3,3',4,4'-TCB may reflect differences in the inducing potencies of the two compounds relative to their similar potencies as inhibitors of CYP1A1 catalytic activity. In additional studies to evaluate structure-activity relationships for CYP1A1 induction by chlorinated dibenzofurans in fish, scup were treated with 2,3,6,8-tetrachlorodibenzofuran (2,3,6,8-TCDF). At 10 or 50 nmol/kg, 2,3,6,8-TCDF was inactive as an inducer of CYP1A1 mRNA, protein, or catalytic activity.(ABSTRACT TRUNCATED AT 400 WORDS)

PMID: 8048062 [PubMed - indexed for MEDLINE]

Elevation of topoisomerase I messenger RNA, protein, and catalytic activity in human tumors: demonstration of tumor-type specificity and implications for cancer chemotherapy.

Husain I, Mohler JL, Seigler HF, Besterman JM.

Department of Cell Biology, Glaxo Inc. Research Institute, Research Triangle Park, North Carolina 27709.

Topoisomerase I has been identified as an intracellular target of camptothecin, a plant alkaloid with anticancer activity. Various lines of evidence suggest that the sensitivity of cells to this drug is directly related to the topoisomerase I content. In humans, the levels of topoisomerase I have been shown to be elevated in colorectal tumors, compared to normal colon mucosa. The aim of our study was to determine whether (a) topoisomerase I levels are elevated in other solid tumors, (b) the elevated enzyme is catalytically active in these tumors, and (c) the increase in topoisomerase I levels in colorectal tumors is a result of increased transcription or translation. Topoisomerase I levels were quantitated in crude extracts from colorectal, prostate, and kidney tumors and their matched normal counterparts by Western blotting and by direct determination of catalytic activity, and mRNA levels were determined by Northern blotting. By Western blotting, colorectal tumors showed 5-35-fold increases in topoisomerase I levels, compared to their normal colon mucosa. In the case of prostate tumors, the increase was 2-10-fold, compared with benign hyperplastic prostate tissue from the same patients. However, no difference was observed in topoisomerase I levels in kidney tumors, compared to their normal counterparts. The catalytic activity of topoisomerase I was determined by a quantitative ³²P-transfer assay in crude homogenates, without isolating nuclei. Colorectal and prostate tumors exhibited 11-40- and 4-26-fold increases, respectively, in catalytic activity. However, kidney tumors did not show any alteration in catalytic activity, compared to their normal matched samples. Thus, for all three tumor types there was a good correlation between enzyme levels and catalytic activity. Finally, colorectal tumors were analyzed for steady state mRNA levels. A 2-33-fold increase in mRNA levels was found in colorectal tumors, compared to normal colon mucosa. These results suggest that alterations in topoisomerase I expression in humans are tumor type specific and that the increase in topoisomerase I levels results from either increased transcription of the topoisomerase I gene or increased mRNA stability.

PMID: 8275492 [PubMed - indexed for MEDLINE]

Expression of calcyclin in human melanocytic lesions.

Weterman MA, van Muijen GN, Bloemers HP, Ruiter DJ.

Department of Biochemistry, University of Nijmegen, The Netherlands.

When comparing two subsequent stages of melanocytic tumor progression we identified calcyclin as a new potential progression marker, the expression of which was correlated with metastatic behavior of various human melanoma cell lines in nude mice. In this study, we describe a good correlation between RNA and protein levels in the xenografts of these cell lines and extended these experiments to a panel of 120 routinely processed human melanocytic cutaneous lesions. Northern blot analysis demonstrated that calcyclin RNA expression was elevated in melanoma metastases as compared to several types of nevocellular nevi. Calcyclin staining using a specific polyclonal antiserum showed a more complex pattern. A stronger staining in a higher percentage of positive cells was observed in thick primary melanoma (≥ 1.5 mm) as compared to thin primary melanoma (< 1.5 mm). Calcyclin expression was also present in a higher percentage of cells showing a stronger staining in melanomas with higher Clark levels ($> II$) corresponding to the vertical growth phase of primary melanomas. Protein expression in nevocellular nevi was confined to the dermal part and was highest in the lower parts of the dermis. Remarkably, dysplastic nevi (atypical moles), potential precursors of melanoma, did not show any expression at all, either in junctional or dermal parts. Confinement of the expression to the dermal part of nondysplastic nevi and primary melanomas may reflect interactions with the microenvironment of the reticular dermis that occurs with vertical growth.

PMID: 8261423 [PubMed - indexed for MEDLINE]

FREE full text article at
endo.endojournals.org

Induction of the estrogen receptor by growth hormone and glucocorticoid substitution in primary cultures of rat hepatocytes.

Freyschuss B, Stavreus-Evers A, Sahlin L, Eriksson H.

Department of Reproductive Endocrinology, Karolinska Hospital, Stockholm, Sweden.

Hepatic estrogen receptors (ER) mediate estrogenic effects on mammalian liver metabolism and are thereby involved in the regulation of important physiological/pathological processes, such as coagulation, atherosclerosis, and hypertension. The regulation of the formation of the ER in primary cultures of rat hepatocytes was studied by assaying ER and ER mRNA under different endocrine conditions. The ER concentration was measured using two different methods, a ligand-binding technique and an ER enzyme immunoassay. The results obtained by the two methods showed good correlation, and linear regression analysis gave a correlation coefficient of 0.95. ER concentrations fell to low steady state levels within 16 h after establishing the cell culture and remained low in the absence of hormonal substitution. Upon medium supplementation with pituitary GH and the glucocorticoid dexamethasone (DEX) in combination, the ER concentration increased 6-fold from 4.2 ± 1.0 to 25.8 ± 7.0 fmol/mg cytosolic protein. ER mRNA was measured by solution hybridization. Substitution with GH and DEX in combination increased ER mRNA to $210 \pm 14\%$ of control levels. No effect on ER mRNA stability was seen after hormone treatment. It is concluded that the regulatory effects of GH and DEX on the hepatic ER in this in vitro system are very similar to the effects of these hormones under in vivo conditions. The inducible expression of the ER has never before, to our knowledge, been demonstrated in any mammalian liver cell culture system.

PMID: 8404593 [PubMed - indexed for MEDLINE]

Developmental regulation of acidic fibroblast growth factor (aFGF) expression in bovine retina.

Jacquemin E, Jonet L, Oliver L, Bugra K, Laurent M, Courtois Y, Jeanny JC.

Unite de Recherches Gerontologiques, U. 118 INSERM, Paris, France.

Acidic fibroblast growth factor (aFGF) is a signalling molecule implicated in a wide variety of biological processes such as cell growth, differentiation and survival. It has been purified from bovine retina. The present study was carried out to detect which cells in the bovine retina expressed aFGF at the different stages of embryonic and post-natal development. The specific aFGF mRNA and protein were detected by in situ hybridization employing riboprobes and immunocytochemistry using affinity purified polyclonal human recombinant aFGF antibodies respectively. No signal was detected by either technique until 4-5 months and then there was progressive expression of aFGF with terminal morphogenesis of the retina. By 8-9 months of embryonic development, nuclei of the 3 neuronal layers (ganglion cell layer, inner and outer nuclear layers) were all uniformly and intensely labeled. A slight labeling of the pigmented epithelium of the retina was also visible throughout development and maturation. These results showed a good correlation between message and protein expression in these cell types. In contrast, glial cells in the nerve fiber layer and vascular endothelial cells displayed a nuclear immunostaining for the protein in the absence of message. These data suggest that aFGF plays a role in the late steps of retinal differentiation by autocrine and paracrine mechanisms.

PMID: 7507349 [PubMed - indexed for MEDLINE]

Severely decreased MARCKS expression correlates with ras reversion but not with mitogenic responsiveness.

Wojtaszek PA, Stumpo DJ, Blackshear PJ, Macara IG.

Department of Pathology, University of Vermont College of Medicine, Burlington 05405.

Phorbol ester-inducible phosphorylation of MARCKS, the '80-kDa' substrate of protein kinase C, was undetectable in several phenotypically dominant, non-transformed revertants independently derived from the ras-transformed cell line NIH3T3 DT-ras. Extremely low expression of MARCKS protein accounted for this apparent lack of phosphorylation. MARCKS-encoding mRNA levels were correspondingly decreased relative to normal and ras-transformed cells in all four ras revertant cell lines studied: C-11 and F-2, derived by 5-azacytidine treatment and selection with ouabain; CHP 9CJ, derived by ethylmethane sulfonate mutagenesis and selection with cis-hydroxy-L-proline; and 12-V3, derived by transfection with the human Krev-1 gene. However, re-expression of MARCKS after transfection of a cloned MARCKS cDNA into the C-11 ras revertant cells was not sufficient to induce retransformation. In fact, no significant difference in sensitivity to mitogenic stimulation by phorbol esters was observed among several cell lines expressing widely varying levels of MARCKS. This evidence argues against a direct role for MARCKS in mitogenic signaling. However, the strong correlation between attenuation of MARCKS expression and phenotypically dominant ras reversion suggests that a common negative regulatory mechanism might be responsible for both effects, presenting a potentially useful strategy for identifying factors involved in transducing the ras signal.

PMID: 8437859 [PubMed - indexed for MEDLINE]

Induction of class 3 aldehyde dehydrogenase in the mouse hepatoma cell line Hepa-1 by various chemicals.

Torronen R, Korkalainen M, Karenlampi SO.

Department of Physiology, University of Kuopio, Finland.

The mouse hepatoma cell line Hepa-1 was shown to express an aldehyde dehydrogenase (ALDH) isozyme which was inducible by TCDD and carcinogenic polycyclic aromatic hydrocarbons. The induced activity could be detected with benzaldehyde as substrate and NADP as cofactor (B/NADP ALDH). As compared with rat liver and hepatoma cell lines, the response was moderate (maximally 5-fold). There was an apparent correlation between this specific form of ALDH and aryl hydrocarbon hydroxylase (AHH) in the Hepa-1 wild-type cell line--in terms of inducibility by several chemicals. However, the magnitude of the response was clearly smaller for ALDH than for AHH. Southern blot analysis showed that a homologous gene (class 3 ALDH) was present in the rat and mouse genome. The gene was also expressed in Hepa-1 and there was a good correlation between the increase of class 3 ALDH-specific mRNA and B/NADP ALDH enzyme activity after exposure of the Hepa-1 cells to TCDD. It is concluded that class 3 ALDH is inducible by certain chemicals in the mouse hepatoma cell line, although the respective enzyme is not inducible in mouse liver *in vivo*.

PMID: 1505055 [PubMed - indexed for MEDLINE]

FREE full text article at
jds.fass.org

Mammary-derived growth inhibitor protein and messenger ribonucleic acid concentrations in different physiological states of the gland.

Politis I, Gorewit RC, Muller T, Grosse R.

Department of Animal Science, Cornell University, Ithaca 14853.

Expression of mammary-derived growth inhibitor in tissue from lactating and involuting bovine mammary glands was investigated. Seventeen lactating, pregnant (220 to 272 d in gestation) cows were divided in two groups of 8 and 9 cows each. Cows of the first group were slaughtered while in lactation. Cows of the second group (9 involuting cows) were slaughtered at 13 to 52 d following sudden cessation of milking. High concentrations of mammary-derived growth inhibitor (.63% of the total protein) were detected in mammary tissue of lactating cows. Mammary-derived growth inhibitor (less than .10% of the total protein) was dramatically reduced during most of the involution period (13 to 45 d following cessation of milking). Mammary-derived growth inhibitor was again detected (.28% of the total protein) during the last stage of the involution (46 to 53 d after cessation of milking), which coincided with colostrum formation. When steady state concentrations of mammary-derived growth inhibitor mRNA were examined, the results obtained mirrored those obtained at the protein concentration. These data suggest that regulation of mammary-derived growth inhibitor occurs via modulation of the steady state concentration of its mRNA. Furthermore, there is a strong correlation between mammary-derived growth inhibitor expression and lactation in dairy cows.

PMID: 1500548 [PubMed - indexed for MEDLINE]

Neu oncogene expression in ovarian tumors: a quantitative study.

Huettner PC, Carney WP, Naber SP, DeLellis RA, Membrino W, Wolfe HJ.

Department of Pathology, Tufts University School of Medicine, Massachusetts.

We studied neu mRNA expression by slot blot analysis and protein product expression by capture ELISA and immunohistochemistry in 57 primary and metastatic ovarian neoplasms, two paraovarian leiomyosarcomas, and eight normal ovaries. Some 61% of ovarian tumors but none of the paraovarian neoplasms or normal ovaries overexpressed neu mRNA. A total of 96% of the ovarian tumors that overexpressed neu were of epithelial type. Epithelial ovarian tumors had significantly higher amounts of the neu oncogene product as determined by capture ELISA than either germ cell and stromal tumors or normal ovaries (p less than 0.025). Different subtypes of ovarian carcinomas had significantly different amounts of neu oncogene product as measured by capture ELISA; endometrioid tumors had the highest, and poorly differentiated carcinomas not otherwise specified had the lowest (p less than 0.025). ELISA values, mRNA overexpression, and immunohistochemical staining intensity did not correlate with stage at diagnosis or architectural or nuclear grade in ovarian tumors. We conclude that capture ELISA is a simple, effective way to measure the neu oncogene protein product and that there is a good correlation between ELISA levels and immunohistochemical staining intensity. However, ELISA values did not correlate with stage or histologic prognostic factors in ovarian neoplasms.

PMID: 1353878 [PubMed - indexed for MEDLINE]

Oncogene and growth factor expression in ovarian cancer.

Kommoss F, Bauknecht T, Birmelin G, Kohler M, Tesch H, Pfleiderer A.

Department of Gynaecology, Albert-Ludwig University, Freiburg, Germany.

The varying tumor-biological behavior of ovarian carcinomas probably influences both their operability and response to chemotherapy, which are the most relevant prognostic factors. The phenotype of different ovarian carcinomas is obviously associated with an activation of the EGF/TGF-alpha signal pathway, including c-myc and c-jun expression. Analysis of EGF-R, TGF-alpha, c-myc and c-jun expression in 33 stage III/IV, and 2 stage I/II ovarian carcinomas with biochemical, molecular-chemical and immunohistochemical methods showed a correlation between the mRNA and protein levels of EGF-R and TGF-alpha for tumors with low or high expressing rates. However, the concentration of measurable free EGF-Rs seems to depend on the amount of TGF-alpha expression by the tumors. The EGF-R binding ligand TGF-alpha is produced by epithelial tumor cells; stromal cells are usually TGF-alpha-negative, as shown by immunohistochemistry. High expression rates of EGF-R, TGF-alpha and c-myc were detected in 6, 7, and 10 out of 35 ovarian carcinomas, respectively. C-jun mRNA was detected in 18/19 cases studied. Non-malignant tissues originating from myometrium or ovary expressed no (or only small amounts of) EGF-R or TGF-alpha mRNA, whereas a high c-myc expression was found in 1/7 normal myometria, and in 2/5 normal ovaries. There was no strong correlation between EGF-R/TGF-alpha and c-myc/c-jun expression.(ABSTRACT TRUNCATED AT 250 WORDS)

PMID: 1502888 [PubMed - indexed for MEDLINE]

FREE full text article at
mcb.asm.org

FREE full text article
in PubMed Central

A sampling of the yeast proteome.

Futcher B, Latter GI, Monardo P, McLaughlin CS, Garrels JI.

Cold Spring Harbor Laboratory, Cold Spring Harbor, New York 11724, USA.
futcher@cshl.org

In this study, we examined yeast proteins by two-dimensional (2D) gel electrophoresis and gathered quantitative information from about 1,400 spots. We found that there is an enormous range of protein abundance and, for identified spots, a good correlation between protein abundance, mRNA abundance, and codon bias. For each molecule of well-translated mRNA, there were about 4,000 molecules of protein. The relative abundance of proteins was measured in glucose and ethanol media. Protein turnover was examined and found to be insignificant for abundant proteins. Some phosphoproteins were identified. The behavior of proteins in differential centrifugation experiments was examined. Such experiments with 2D gels can give a global view of the yeast proteome.

PMID: 10523624 [PubMed - indexed for MEDLINE]

FREE full text article at
www.jbc.org

Overexpression of a DEAD box protein (DDX1) in neuroblastoma and retinoblastoma cell lines.

Godbout R, Packer M, Bie W.

Department of Oncology, Cross Cancer Institute and University of Alberta, 11560 University Ave., Edmonton, Alberta T6G1Z2, Canada.

The DEAD box gene, DDX1, is a putative RNA helicase that is co-amplified with MYCN in a subset of retinoblastoma (RB) and neuroblastoma (NB) tumors and cell lines. Although gene amplification usually involves hundreds to thousands of kilobase pairs of DNA, a number of studies suggest that co-amplified genes are only overexpressed if they provide a selective advantage to the cells in which they are amplified. Here, we further characterize DDX1 by identifying its putative transcription and translation initiation sites. We analyze DDX1 protein levels in MYCN/DDX1-amplified NB and RB cell lines using polyclonal antibodies specific to DDX1 and show that there is a good correlation with DDX1 gene copy number, DDX1 transcript levels, and DDX1 protein levels in all cell lines studied. DDX1 protein is found in both the nucleus and cytoplasm of DDX1-amplified lines but is localized primarily to the nucleus of nonamplified cells. Our results indicate that DDX1 may be involved in either the formation or progression of a subset of NB and RB tumors and suggest that DDX1 normally plays a role in the metabolism of RNAs located in the nucleus of the cell.

PMID: 9694872 [PubMed - indexed for MEDLINE]



Expression of somatostatin receptor types 1-5 in 81 cases of gastrointestinal and pancreatic endocrine tumors. A correlative immunohistochemical and reverse-transcriptase polymerase chain reaction analysis.

Papotti M, Bongiovanni M, Volante M, Allia E, Landolfi S, Helboe L, Schindler M, Cole SL, Bussolati G.

Department of Biomedical Sciences and Oncology, University of Turin, Via Santena 7, 10126 Turin, Italy. mauro.papotti@unito.it

Somatostatin receptors (SSTRs) have been extensively mapped in human tumors by means of autoradiography, reverse-transcriptase polymerase chain reaction (RT-PCR), in situ hybridization (ISH) and immunohistochemistry (IHC). We analyzed the SSTR type 1-5 expression by means of RT-PCR and/or IHC in a series of 81 functioning and non-functioning gastroenteropancreatic (GEP) endocrine tumors and related normal tissues. Moreover, we compared the results with clinical, pathological and hormonal features. Forty-six cases (13 intestinal and 33 pancreatic) were studied for SSTR 1-5 expression using RT-PCR, IHC with antibodies to SSTR types 2, 3, 5 and ISH for SSTR2 mRNA. The vast majority of tumors expressed SSTR types 1, 2, 3 and 5, while SSTR4 was detected in a small minority. Due to the good correlation between RT-PCR and IHC data on SSTR types 2, 3, and 5, thirty-five additional GEP endocrine tumors were studied with IHC alone. Pancreatic insulinomas had an heterogeneous SSTR expression, while 100% of somatostatinomas expressed SSTR5 and 100% gastrinomas and glucagonomas expressed SSTR2. Pre-operative biopsy material showed an overlapping immunoreactivity with that of surgical specimens, suggesting that the SSTR status can be detected in the diagnostic work-up. It is concluded that SSTRs 1-5 are heterogeneously expressed in GEP endocrine tumors and that IHC is a reliable tool to detect SSTR types 2, 3 and 5 in surgical and biopsy specimens.

PMID: 12021920 [PubMed - indexed for MEDLINE]



Expression of deoxycytidine kinase in leukaemic cells compared with solid tumour cell lines, liver metastases and normal liver.

van der Wilt CL, Kroep JR, Loves WJ, Rots MG, Van Groenigen CJ, Kaspers GJ, Peters GJ.

Department of Medical Oncology, VU University Medical Center, Amsterdam, The Netherlands.

Deoxycytidine kinase (dCK) is required for the phosphorylation of several deoxyribonucleoside analogues that are widely employed as chemotherapeutic agents. Examples include cytosine arabinoside (Ara-C) and 2-chlorodeoxyadenosine (CdA) in the treatment of acute myeloid leukaemia (AML) and gemcitabine to treat solid tumours. In this study, expression of dCK mRNA was measured by a competitive template reverse transcriptase polymerase chain reaction (CT RT-PCR) in seven cell lines of different histological origin, 16 childhood and adult AML samples, 10 human liver samples and 11 human liver metastases of colorectal cancer origin. The enzyme activity and protein expression levels of dCK in the cell lines were closely related to the mRNA expression levels ($r=0.75$, $P=0.026$ and $r=0.86$, $P=0.007$). In AML samples, dCK mRNA expression ranged from 1.16 to 35.25 ($\times 10^{-3}$) dCK/beta-actin. In the cell line panel, the range was 2.97-56.9 ($\times 10^{-3}$) dCK/beta-actin of dCK mRNA expression. The enzyme activity in liver metastases was correlated to dCK mRNA expression ($r=0.497$, $P=0.05$). In the liver samples, these were not correlated. dCK mRNA expression showed only a 36-fold range in liver while a 150-fold range was observed in the liver metastases. In addition, dCK activity and mean mRNA levels were 2.5-fold higher in the metastases than in the liver samples. Since dCK is associated with the sensitivity to deoxynucleoside analogues and because of the good correlation between the different dCK measurements in malignant cells and tumours, the CT-RT PCR assay will be useful in the selection of patients that can be treated with deoxycytidine analogues.

PMID: 12628850 [PubMed - indexed for MEDLINE]



Galanin in pituitary adenomas.

Grenback E, Bjellerup P, Wallerman E, Lundblad L, Anggard A, Ericson K, Aman K, Landry M, Schmidt WE, Hokfelt T, Hulting AL.

Department of Molecular Medicine, Endocrine and Diabetes Unit, Karolinska Hospital, S-17176 Stockholm, Sweden. Eva.Grenback@ks.se

Tumor galanin content was measured in extracts from human pituitary adenomas using a specific RIA method for monitoring human galanin. Twenty-two out of twenty-four tumors contained galanin with notably high levels in corticotroph adenomas, varying levels in clinically inactive tumors, and low levels in GH secreting adenomas. Tumor galanin and ACTH contents were closely correlated in all tumors. In four young patients with microadenomas and highly active Mb Cushing tumor galanin was inversely related to tumor volume. The molecular form of tumor galanin, studied with reverse-phase HPLC, was homogeneous with the majority of tumor galanin coeluting with standard human galanin. In the tumors analysed with in situ hybridization there was a good correlation between galanin peptide levels and galanin mRNA expression. In some tumors galanin mRNA and POMC levels coexisted, in others they were essentially in different cell populations. Levels of plasma galanin-LI were not related to tumor galanin concentration, and galanin levels were in the same range in sinus petrosus close to the pituitary venous drainage as in peripheral blood. Corticotrophin releasing hormone injections in two patients caused ACTH, but no detectable galanin release into sinus petrosus. Our results demonstrate that corticotroph, but not GH adenomas, express high levels of galanin, in addition to ACTH, and that in some tumors both polypeptides are synthesised in the same cell population. However, galanin levels in plasma were not influenced by the tumor galanin content.

PMID: 14700749 [PubMed - indexed for MEDLINE]

Full text article at
www.bloodjournal.org

BCL2 protein expression parallels its mRNA level in normal and malignant B cells.

Shen Y, Iqbal J, Huang JZ, Zhou G, Chan WC.

Department of Pathology and Microbiology, University of Nebraska Medical Center, Omaha, USA.

The regulation of B-cell lymphoma 2 (BCL2) protein expression in germinal center (GC) B cells has been controversial. Previous reports have indicated posttranscriptional regulation plays a dominant role. However, a number of recent studies contradicted these reports. Using real-time polymerase chain reaction (PCR) and Standardized Reverse Transcriptase-PCR (StaRT-PCR), we measured the level of mRNA expression in GC, mantle zone (MNZ), and marginal zone (MGZ) cells from laser capture microdissection. Both quantitative RT-PCR measurements of microdissected GC cells from tonsils showed that GC cells had low expression of BCL2 transcripts commensurate with the low protein expression level. These results are in agreement with microarray studies on fluorescence-activated cell sorter (FACS)-sorted cells and microdissected GC cells. We also examined BCL2 mRNA and protein expression on a series of 30 cases of diffuse large B-cell lymphoma (DLBCL) and found, in general, a good correlation. The results suggested that BCL2 protein expression is regulated at the transcriptional level in normal B cells and in the neoplastic cells in most B-cell lymphoproliferative disorders.

PMID: 15242877 [PubMed - indexed for MEDLINE]

Full text article at
www.bloodjournal.org

Cyclin D1-negative mantle cell lymphoma: a clinicopathologic study based on gene expression profiling.

Fu K, Weisenburger DD, Greiner TC, Dave S, Wright G, Rosenwald A, Chiorazzi M, Iqbal J, Gesk S, Siebert R, De Jong D, Jaffe ES, Wilson WH, Delabie J, Ott G, Dave BJ, Sanger WG, Smith LM, Rimsza L, Braziel RM, Muller-Hermelink HK, Campo E, Gascoyne RD, Staudt LM, Chan WC; Lymphoma/Leukemia Molecular Profiling Project.

Department of Pathology and Microbiology, University of Nebraska Medical Center, 983135
Nebraska Medical Center, Omaha, NE 68198-3135, USA. kfu@unmc.edu

Cyclin D1 overexpression is believed to be essential in the pathogenesis of mantle cell lymphoma (MCL). Hence, the existence of cyclin D1-negative MCL has been controversial and difficult to substantiate. Our previous gene expression profiling study identified several cases that lacked cyclin D1 expression, but had a gene expression signature typical of MCL. Herein, we report the clinical, pathologic, and genetic features of 6 cases of cyclin D1-negative MCL. All 6 cases exhibited the characteristic morphologic features and the unique gene expression signature of MCL but lacked the t(11;14)(q13; q32) by fluorescence in situ hybridization (FISH) analysis. The tumor cells also failed to express cyclin D1 protein, but instead expressed either cyclin D2 (2 cases) or cyclin D3 (4 cases). There was good correlation between cyclin D protein expression and the corresponding mRNA expression levels by gene expression analysis. Using interphase FISH, we did not detect chromosomal translocations or amplifications involving CCND2 and CCND3 loci in these cases. Patients with cyclin D1-negative MCL were similar clinically to those with cyclin D1-positive MCL. In conclusion, cases of cyclin D1-negative MCL do exist and are part of the spectrum of MCL. Up-regulation of cyclin D2 or D3 may substitute for cyclin D1 in the pathogenesis of MCL.

PMID: 16123218 [PubMed - indexed for MEDLINE]

full text article at
vir.sgmjournals.org

The alpha(v)beta6 integrin receptor for Foot-and-mouth disease virus is expressed constitutively on the epithelial cells targeted in cattle.

Monaghan P, Gold S, Simpson J, Zhang Z, Weinreb PH, Violette SM, Alexandersen S, Jackson T.

Institute for Animal Health, Pirbright Laboratory, Ash Road, Pirbright, Surrey GU24 0NF, UK.

Field strains of Foot-and-mouth disease virus (FMDV) use a number of alpha(v)-integrins as receptors to initiate infection on cultured cells, and integrins are believed to be the receptors used to target epithelial cells in animals. In this study, immunofluorescence confocal microscopy and real-time RT-PCR were used to investigate expression of two of the integrin receptors of FMDV, alpha(v)beta6 and alpha(v)beta3, within various epithelia targeted by this virus in cattle. These studies show that alpha(v)beta6 is expressed constitutively on the surfaces of epithelial cells at sites where infectious lesions occur during a natural infection, but not at sites where lesions are not normally formed. Expression of alpha(v)beta6 protein at these sites showed a good correlation with the relative abundance of beta6 mRNA. In contrast, alpha(v)beta3 protein was only detected at low levels on the vasculature and not on the epithelial cells of any of the tissues investigated. Together, these data suggest that in cattle, alpha(v)beta6, rather than alpha(v)beta3, serves as the major receptor that determines the tropism of FMDV for the epithelia normally targeted by this virus.

PMID: 16186231 [PubMed - in process]



Somatostatin receptors in primary human breast cancer: quantitative analysis of mRNA for subtypes 1–5 and correlation with receptor protein expression and tumor pathology.

Kumar U, Grigorakis SI, Watt HL, Sasi R, Snell L, Watson P, Chaudhari S.

Fraser Laboratories For Diabetes Research, Department of Medicine, McGill University, Royal Victoria Hospital, 687 Pine Avenue West, H3A 1A1 Montreal, Quebec, Canada. ujendra.kumar@muhc.mcgill.ca

Somatostatin receptors (SSTRs) have been identified in most hormone-producing tumors as well as in breast cancer. In the present study, we determined SSTR1-5 expression in primary ductal NOS breast tumors through semi-quantitative RT-PCR and immunocytochemistry. The results from the analysis of 98 samples were correlated with several key histological markers and receptor expression. All five SSTR subtypes are variably expressed at the mRNA level in breast tumors with 91% of samples showing SSTR1, 98% SSTR2, 96% SSTR3, 76% SSTR4, and 54% SSTR5. SSTR1-5 are localized to both tumor cells and the surrounding peritumoral regions as detected by immunocytochemistry. Levels of SSTR mRNA, when corrected for beta-actin levels, were highest for SSTR3 followed by SSTR1, SSTR2, SSTR5, and SSTR4. Furthermore, there was good correlation between mRNA and protein expression with 84% for SSTR1, 79% for SSTR2, 89% for SSTR3, 68% for SSTR4, 68% for SSTR5, and 78% for all five receptors. SSTR1, 2 and 4 were correlated with ER levels whereas SSTR2 showed an additional correlation with PR levels. These correlations were independent of patient age and histological grade. Moreover, using immunocytochemistry, blood vessels exhibited receptor-specific localization for SSTR2 and SSTR5. Our results indicate significant correlations between mRNA and protein expression along with receptor-specific correlations with histological markers as well as ER and PR levels. Differential distribution of SSTR subtypes in tumors and receptor-specific expression in vascular structures may be considered as a novel diagnosis for breast tumors with receptor subtype agonists.

Publication Types:

- Evaluation Studies

PMID: 15986128 [PubMed - indexed for MEDLINE]



Human chorionic gonadotrophin beta expression in malignant Barrett's oesophagus.

Couvelard A, Paraf F, Vidaud D, Dubois S, Vidaud M, Flejou JF, Degott C.

Service d'Anatomie Pathologique, Hopital Beaujon, 92118 Clichy cedex, France.
anne.couvelard@bjn.ap-hop-paris.fr

BACKGROUND: Human chorionic gonadotrophin beta (hCGbeta) is expressed in several non-trophoblastic tumours, and this is usually associated with aggressive behaviour. Little is known about hCGbeta expression in Barrett's adenocarcinoma. **MATERIALS AND METHODS:** We determined the hCGbeta profile in a large series of surgically resected Barrett's adenocarcinoma (a) at mRNA level using real-time quantitative reverse-transcription polymerase chain reaction analysis and (b) at protein level using immunohistochemistry with a polyclonal antibody and with a monoclonal antibody specific for free hCGbeta. We then sought links between the hCGbeta protein expression pattern and clinical and pathological parameters, including patient outcome as well as vascular endothelial growth factor (VEGF) expression. **RESULTS:** hCGbeta protein expression was observed in 43 of 76 (57%) Barrett's adenocarcinomas. We showed a strong correlation between hCGbeta protein abundance and CGB mRNA level. We observed a statistical link between hCGbeta protein expression and infiltrative tumour type ($P=0.023$), perineural neoplastic invasion ($P=0.007$) and VEGF protein expression ($P=0.016$). hCGbeta expression tended to be associated with a poor outcome (16% versus 36% survival 8 years after resection). **CONCLUSION:** Expression of hCGbeta correlates with specific infiltrative characteristics and is associated with higher VEGF expression. Both molecules may play a co-ordinated role in the development of Barrett's adenocarcinomas.

PMID: 15309632 [PubMed - indexed for MEDLINE]

full text article at
www.jpet.org

Estrogen regulation of the cytochrome P450 3A subfamily in humans.

Williams ET, Levk M, Wrighton SA, Davies PJ, Loose DS, Shipley GL, Strobel HW.

Department of Biochemistry, Medical School, University of Texas Health Science Center at Houston, 6431 Fannin, MSB 6.200, Houston, TX 77030, USA.

This study examines the possible role of estrogen in regulating the expression of the human CYP3A subfamily: CYP3A4, CYP3A5, CYP3A7, and CYP3A43. To accomplish this goal, mRNA was quantified from human livers and endometrial samples, and total CYP3A protein levels were evaluated by Western immunoblot analysis of the liver samples. The human endometrial samples were from premenopausal and postmenopausal women. The premenopausal endometrium was either in the proliferative or secretory phase, whereas for the postmenopausal endometrium samples, the women had been treated with either a placebo or estropipate, an estrogen substitute. After analyses, CYP3A4 mRNA was shown to have lower hepatic expression in females than in males. In the endometrium, CYP3A4 and CYP3A43 are down-regulated by estrogen, whereas CYP3A5 is expressed at higher levels during the secretory phase. CYP3A7 was not detected in the endometrium. In addition, the CYP3A subfamily showed increased mRNA expression in the liver as age increased. The expression levels of total CYP3A protein and total CYP3A mRNA showed good correlation. Despite apparent regulation of CYP3A4 mRNA expression by estrogen, the effects of estrogen may be overshadowed by additional regulators of gene expression.

PMID: 15282264 [PubMed - indexed for MEDLINE]



FREE full text article at
www.jbc.org

Discordant regulation of granzyme H and granzyme B expression in human lymphocytes.

Sedelies KA, Sayers TJ, Edwards KM, Chen W, Pellicci DG, Godfrey DI, Trapani JA.

Cancer Immunology Laboratory, Peter MacCallum Cancer Centre, Locked Bag 1, A'Beckett Street, East Melbourne, 8006, Australia.

We analyzed the expression of granzyme H in human blood leukocytes, using a novel monoclonal antibody raised against recombinant granzyme H. 33-kDa granzyme H was easily detected in unfractionated peripheral blood mononuclear cells, due to its high constitutive expression in CD3(-)CD56(+) natural killer (NK) cells, whereas granzyme B was less abundant. The NK lymphoma cell lines, YT and Lopez, also expressed high granzyme H levels. Unstimulated CD4(+) and particularly CD8(+) T cells expressed far lower levels of granzyme H than NK cells, and various agents that classically induce T cell activation, proliferation, and enhanced granzyme B expression failed to induce granzyme H expression in T cells. Also, granzyme H was not detected in NK T cells, monocytes, or neutrophils. There was a good correlation between mRNA and protein expression in cells that synthesize both granzymes B and H, suggesting that gzmH gene transcription is regulated similarly to gzmB. Overall, our data indicate that although the gzmB and gzmH genes are tightly linked, expression of the proteins is quite discordant in T and NK cells. The finding that granzyme H is frequently more abundant than granzyme B in NK cells is consistent with a role for granzyme H in complementing the pro-apoptotic function of granzyme B in human NK cells.

PMID: 15069086 [PubMed - indexed for MEDLINE]



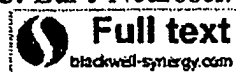
Expression level of Ubc9 protein in rat tissues.

Golebiowski F, Szulc A, Sakowicz M, Szutowicz A, Pawelczyk T.

Department of Molecular Medicine, Medical University of Gdansk, 80-211 Gdansk, Poland.

Ubc9 is a homologue of the E2 ubiquitin conjugating enzyme and participates in the covalent linking of SUMO-1 molecule to the target protein. In this report we describe a simple and efficient method for obtaining pure human recombinant Ubc9 protein. The purified Ubc9 retained its native structure and was fully active in an in vitro sumoylation assay with the promyelocytic leukaemia (PML) peptide as a substrate. In order to better understand the physiology of Ubc9 protein we examined its levels in several rat tissues. Immunoblot analyses performed on tissue extracts revealed quantitative and qualitative differences in the expression pattern of Ubc9. The Ubc9 protein was present at a high level in spleen and lung. Moderate level of Ubc9 was detected in kidney and liver. Low amount of Ubc9 was observed in brain, whereas the 18 kDa band of Ubc9 was barely visible or absent in heart and skeletal muscle. In heart and muscle extracts the Ubc9 antibodies recognized a 38 kDa protein band. This band was not visible in extracts of other rat tissues. A comparison of the relative levels of Ubc9 mRNA and protein indicated that the overall expression level of Ubc9 was the highest in spleen and lung. In spleen, lung, kidney, brain, liver and heart there was a good correlation between the 18 kDa protein and Ubc9 mRNA levels. In skeletal muscle the Ubc9 mRNA level was unproportionally high comparing to the level of the 18 kDa protein. The presented data indicate that in the rat the expression of the Ubc9 protein appears to have some degree of tissue specificity.

PMID: 14739995 [PubMed - indexed for MEDLINE]



Neurokinin 1 receptor and relative abundance of the short and long isoforms in the human brain.

Caberlotto L, Hurd YL, Murdock P, Wahlin JP, Melotto S, Corsi M, Carletti R.

Department of Biology, Psychiatry CEDD, GlaxoSmithKline Medicine Research Centre, Verona, Italy. Laura.L.Caberlotto@gsk.com

Substance P exerts its various biochemical effects mainly via interactions through neurokinin-1 receptors (NK1). Recently, the NK1 receptor has attracted considerable interest for its possible role in a variety of psychiatric disorders including depression and anxiety. However, little is known regarding the anatomical distribution of NK1 in the human central nervous system (CNS). Riboprobe in situ hybridization, quantitative PCR and in vitro autoradiography were performed. Highest NK1 mRNA levels were localized in the locus coeruleus and ventral striatum, while moderate hybridization signals were observed in the cerebral cortex (most abundant in the visual cortex), hippocampus and different amygdaloid nuclei. Very low levels of the NK1 mRNA were detected in the cerebellum and thalamus. In view of the existence of a long and short isoform of the NK1 receptor, it was of interest to assess whether there was a differential distribution of the two splice variants in the human CNS and peripheral tissues. A quantitative TaqMan PCR analysis showed that the long NK1 isoform was the most prevalent throughout the human brain, while in peripheral tissues the truncated form was the most represented. 3H-Substance P autoradiography revealed a good correlation between receptor binding sites and NK1 mRNA expression throughout the brain, with the highest levels of binding in the locus coeruleus. These results provide the anatomical evidence that the NK1 receptors have a strong association with neuronal systems relevant to mood regulation and stress in the human brain, but do not suggest a region-specific role of the two isoforms in the CNS.

PMID: 12752772 [PubMed - indexed for MEDLINE]



Transcriptional activity of potent glucocorticoids: relevance of glucocorticoid receptor isoforms and drug metabolites.

Spika I, Hammer S, Kleuser B, Korting HC, Schafer-Korting M.

Institut für Pharmazie, Abteilung für Pharmakologie und Toxikologie, Freie Universität Berlin, Berlin, Germany.

As compared to standard glucocorticoids (GC), prednicarbate (PC) is favorable in the treatment of eczema due to its high benefit/risk ratio. The remarkable anti-inflammatory effects of PC are in strong contrast to its reported low glucocorticoid receptor (GR) binding affinity. In transfected COS-7 cells we related the transcriptional potencies of PC, its metabolites and conventional GC to their receptor binding properties. Moreover, the expression pattern of the human GR isoform hGRalpha and its mutual dominant negative inhibitor hGRbeta in skin cells have been investigated as well as the influence of hGRbeta on receptor binding and transactivation. hGRalpha mRNA and protein was largely overexpressed in skin cells. hGRbeta showed no influence on hGRalpha binding and transactivation. Concentration response curves indicated the greater transactivation potency of betamethasone 17-valerate followed by dexamethasone and prednisolone 17-ethylcarbonate. Native PC appeared almost as potent as dexamethasone. With both a strong correlation was observed between transactivation and GR binding. Copyright 2003 S. Karger AG, Basel

PMID: 12677094 [PubMed - indexed for MEDLINE]



Comment in:

- [Blood. 2003 Aug 15;102\(4\):1550-1.](#)

FREE full text article at
www.bloodjournal.org

Transcript profiling of human platelets using microarray and serial analysis of gene expression.

Gnatenko DV, Dunn JJ, McCorkle SR, Weissmann D, Perrotta PL, Bahou WF.

Department of Medicine, Program in Genetics, State University of New York, Stony Brook 11794-8151, USA.

Human platelets are anucleate blood cells that retain cytoplasmic mRNA and maintain functionally intact protein translational capabilities. We have adapted complementary techniques of microarray and serial analysis of gene expression (SAGE) for genetic profiling of highly purified human blood platelets. Microarray analysis using the Affymetrix HG-U95Av2 approximately 12 600-probe set maximally identified the expression of 2147 (range, 13%-17%) platelet-expressed transcripts, with approximately 22% collectively involved in metabolism and receptor/signaling, and an overrepresentation of genes with unassigned function (32%). In contrast, a modified SAGE protocol using the Type IIS restriction enzyme MmeI (generating 21-base pair [bp] or 22-bp tags) demonstrated that 89% of tags represented mitochondrial (mt) transcripts (enriched in 16S and 12S ribosomal RNAs), presumably related to persistent mt-transcription in the absence of nuclear-derived transcripts. The frequency of non-mt SAGE tags paralleled average difference values (relative expression) for the most "abundant" transcripts as determined by microarray analysis, establishing the concordance of both techniques for platelet profiling. Quantitative reverse transcription-polymerase chain reaction (PCR) confirmed the highest frequency of mt-derived transcripts, along with the mRNAs for neurogranin (NGN, a protein kinase C substrate) and the complement lysis inhibitor clusterin among the top 5 most abundant transcripts. For confirmatory characterization, immunoblots and flow cytometric analyses were performed, establishing abundant cell-surface expression of clusterin and intracellular expression of NGN. These observations demonstrate a strong correlation between high transcript abundance and protein expression, and they establish the validity of transcript analysis as a tool for identifying novel platelet proteins that may regulate normal and pathologic platelet (and/or megakaryocyte) functions.

PMID: 12433680 [PubMed - indexed for MEDLINE]

Comment in:

- [Equine Vet J. 2002 Jul;34\(4\):326-7.](#)

Molecular characterisation of carbohydrate digestion and absorption in equine small intestine.

Dyer J, Fernandez-Castano Merediz E, Salmon KS, Proudman CJ, Edwards GB, Shirazi-Beechey SP.

Department of Veterinary Preclinical Sciences, University of Liverpool, UK.

Dietary carbohydrates, when digested and absorbed in the small intestine of the horse, provide a substantial fraction of metabolisable energy. However, if levels in diets exceed the capacity of the equine small intestine to digest and absorb them, they reach the hindgut, cause alterations in microbial populations and the metabolite products and predispose the horse to gastrointestinal diseases. We set out to determine, at the molecular level, the mechanisms, properties and the site of expression of carbohydrate digestive and absorptive functions of the equine small intestinal brush-border membrane. We have demonstrated that the disaccharidases sucrase, lactase and maltase are expressed diversely along the length of the intestine and D-glucose is transported across the equine intestinal brush-border membrane by a high affinity, low capacity, Na⁺/glucose cotransporter type 1 isoform (SGLT1). The highest rate of transport is in duodenum > jejunum > ileum. We have cloned and sequenced the cDNA encoding equine SGLT1 and alignment with SGLT1 of other species indicates 85-89% homology at the nucleotide and 84-87% identity at the amino acid levels. We have shown that there is a good correlation between levels of functional SGLT1 protein and SGLT1 mRNA abundance along the length of the small intestine. This indicates that the major site of glucose absorption in horses maintained on conventional grass-based diets is in the proximal intestine, and the expression of equine intestinal SGLT1 along the proximal to distal axis of the intestine is regulated at the level of mRNA abundance. The data presented in this paper are the first to provide information on the capacity of the equine intestine to digest and absorb soluble carbohydrates and has implications for a better feed management, pharmaceutical intervention and for dietary supplementation in horses following intestinal resection.

PMID: 12117106 [PubMed - indexed for MEDLINE]

FREE full text article at
circ.ahajournals.org

Vascular endothelial growth factor enhances cardiac allograft arteriosclerosis.

Lemstrom KB, Krebs R, Nykanen AI, Tikkanen JM, Sihvola RK, Aaltola EM, Hayry PJ, Wood J, Alitalo K, Yla-Herttuala S, Koskinen PK.

Cardiopulmonary Research Group, Transplantation Laboratory, University of Helsinki and Helsinki University Central Hospital, Helsinki, Finland. Karl.Lemstrom@helsinki.fi

BACKGROUND: Cardiac allograft arteriosclerosis is a complex process of alloimmune response, chronic inflammation, and smooth muscle cell proliferation that includes cross talk between cytokines and growth factors. **METHODS AND RESULTS:** Our results in rat cardiac allografts established alloimmune response as an alternative stimulus capable of inducing vascular endothelial growth factor (VEGF) mRNA and protein expression in cardiomyocytes and graft-infiltrating mononuclear inflammatory cells, which suggests that these cells may function as a source of VEGF to the cells of coronary arteries. Linear regression analysis of these allografts with different stages of arteriosclerotic lesions revealed a strong correlation between intragraft VEGF protein expression and the development of intimal thickening, whereas blockade of signaling downstream of VEGF receptor significantly reduced arteriosclerotic lesions. In addition, in cholesterol-fed rabbits, intracoronary perfusion of cardiac allografts with a clinical-grade adenoviral vector that encoded mouse VEGF(164) enhanced the formation of arteriosclerotic lesions, possibly secondary to increased intragraft influx of macrophages and neovascularization in the intimal lesions. **CONCLUSIONS:** Our findings suggest a positive regulatory role between VEGF and coronary arteriosclerotic lesion formation in the allograft cytokine microenvironment.

PMID: 12034660 [PubMed - indexed for MEDLINE]



Expression and distribution of laminin alpha1 and alpha2 chains in embryonic and adult mouse tissues: an immunochemical approach.

Sasaki T, Giltay R, Talts U, Timpl R, Talts JF.

Max-Planck-Institute for Biochemistry, Martinsried, D-82152, Germany.

Protein levels, mRNA expression, and localization of laminin alpha1 and alpha2 chains in development and in adult mice were examined. Recombinant fragments were used to obtain high-titer-specific polyclonal antibodies for establishing quantitative radioimmuno-inhibition assays. This often demonstrated an abundance of alpha2 chain, but also distinct amounts of alpha1 chain for adult tissues. The highest amounts of alpha1 were found in placenta, kidney, testis, and liver and exceeded those of alpha2. All other tissue extracts showed a higher content of alpha2, which was particularly high in heart and muscle when compared to alpha1. Content of gamma1 chain, shared by most laminins, was also analyzed. This demonstrated gamma1 chain levels being equal to or moderately exceeding the sum of alpha1 and alpha2 chains, indicating that these isoforms represent the major known laminin isoforms in most adult mouse tissues so far examined. Moreover, we found good correlation between radioimmuno-inhibition data and mRNA levels of adult tissues as measured by quantitative real-time reverse transcriptase-PCR. Embryonic tissues were also analyzed by radioimmuno-inhibition assays. This demonstrated for day 11 embryos comparable amounts of alpha1 and gamma1 and a more than 25-fold lower content of alpha2. This content increased to about 10% of alpha1 in day 13 embryos. The day 18 embryo showed in heart, kidney, and liver, but not yet in brain and lung, alpha1/alpha2 chain ratios comparable to those in adult tissues. Immunostaining demonstrated alpha1 in Reichert's membrane (day 7.5), while alpha2 could not be detected before day 11.5. These data were compared with immunohistochemical localization results on several more embryonic and adult tissue sections. Our results regarding localization are consistent with those of earlier work with some notable exceptions. This was in part due to epitope masking for monoclonal antibodies commonly used in previous studies in esophagus, intestine, stomach, liver, kidney, and spleen.

PMID: 11969289 [PubMed - indexed for MEDLINE]



Modulation of glucagon receptor expression and response in transfected human embryonic kidney cells.

Ikegami T, Cypess AM, Bouscarel B.

Department of Medicine, George Washington University Medical Center, Washington, District of Columbia 20037, USA.

The modulation of glucagon receptor (GR) expression and biological response was investigated in human embryonic kidney cell (HEK-293) clones permanently expressing the GR with different densities. The GR mRNA expression level in these clones was upregulated by cellular cAMP accumulation and presented a good correlation with both the protein expression level and the maximum number of glucagon binding sites. However, the determination of glucagon-induced cAMP accumulation in these cell lines revealed that the enhancement of receptor expression did not lead to a proportional increase in cAMP formation. Under these conditions, the maximum cAMP production induced by NaF and forskolin was not significantly different among selected clones, regardless of the receptor expression level. High receptor-expressing clones showed the greatest susceptibility for agonist-induced desensitization compared with clones with lower GR expression levels. The results of the present study suggest that the GR can recruit non-GR-specific desensitization mechanism(s). Furthermore, the partial inhibition or alteration of the overall cAMP synthesis pathway at the receptor level may be a necessary adaptive step for a cell in response to a massive increase in membrane receptor expression level.

PMID: 11546678 [PubMed - indexed for MEDLINE]

Assessment of proliferative activity in colorectal carcinomas by quantitative reverse transcriptase-polymerase chain reaction (RT-PCR).

Duchrow M, Hasemeyer S, Broll R, Bruch HP, Windhovel U.

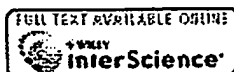
Surgical Research Laboratory, Surgical Clinic, Medical University of Lubeck, Ratzeburger Allee 160, D-23538 Lubeck, Germany.

The monoclonal antibody Ki-67 and the isospecific monoclonal antibody MIB-1 are routinely used in oncology to assess the proliferation index of tumor cells. A more objective and sensitive method is the determination of the of Ki-67 protein-specific mRNA by quantitative reverse transcriptase-polymerase chain reaction (RT-PCR). In 25 resected colorectal adenocarcinomas of different stages and grades we determined between 0.2 and 4.4 amol (10(-18) mol) Ki-67 protein-specific mRNA per microgram total RNA (median = 0.88 amol). The corresponding Ki-67 indices (expressing the percentage of Ki-67/MIB-I positive tumor cells) ranged from 41 to 81% (median = 61%). We found a good correlation between Ki-67 index and mRNA expression ($r = 0.75$), a significant correlation between both data and tumor stage (primary tumor, regional nodes, metastasis [pTNM] staging classification) ($p < 0.001$), but not between both data and tumor grade. Both Ki-67 indices ($p = 0.05$) and mRNA levels ($p = 0.014$) correlated significantly to the patients' survival. These results demonstrate that the Ki-67 protein-specific quantitative RT-PCR is a useful method for the characterization of tumor cell proliferation.

PMID: 11486701 [PubMed - indexed for MEDLINE]

Erratum in:

- Int J Cancer 2002 Feb 20;97(6):878.



Immunohistochemical analysis of NY-ESO-1 antigen expression in normal and malignant human tissues.

Jungbluth AA, Chen YT, Stockert E, Busam KJ, Kolb D, Iversen K, Coplan K, Williamson B, Altorki N, Old LJ.

Ludwig Institute for Cancer Research, Memorial Sloan-Kettering Cancer Center, New York, NY, USA. jungblua@mskcc.org

NY-ESO-1, a member of the CT (cancer/testis) family of antigens, is expressed in normal testis and in a range of human tumor types. Knowledge of NY-ESO-1 expression has depended on RT-PCR detection of mRNA and there is a need for detecting NY-ESO-1 at the protein level. In the present study, a method for the immunochemical detection of NY-ESO-1 in paraffin-embedded tissues has been developed and used to define the expression pattern of NY-ESO-1 in normal tissues and in a panel of human tumors. No normal tissue other than testis showed NY-ESO-1 reactivity, and expression in testis was restricted to germ cells particularly spermatogonia. In human tumors, the frequency of NY-ESO-1 antigen expression corresponds with past analysis of NY-ESO-1 mRNA expression e.g., 20-30% of lung cancers, bladder cancers and melanoma, and no expression in colon and renal cancer. Co-typing of NY-ESO-1 antigen and mRNA expression in a large panel of lung cancers showed a good correlation. There is great variability in NY-ESO-1 expression in individual tumors, ranging from an infrequent homogeneous pattern of staining to highly heterogeneous antigen expression. Copyright 2001 Wiley-Liss, Inc.

PMID: 11351307 [PubMed - indexed for MEDLINE]

Expression of superoxide dismutases, catalase, and glutathione peroxidase in glioma cells.

Zhong W, Yan T, Lim R, Oberley LW.

Radiation Research Laboratory, Department of Radiology, The University of Iowa, Iowa City 52242, USA.

Four primary antioxidant enzymes were measured in both human and rat glioma cells. Both manganese-containing superoxide dismutase (MnSOD) and copper-zinc-containing superoxide dismutase (CuZnSOD) activities varied greatly among the different glioma cell lines. MnSOD was generally higher in human glioma cells than in rat glioma cells and relatively higher than in other tumor types. High levels of MnSOD in human glioma cells were due to the high levels of expression of MnSOD mRNA and protein. Heterogeneous expression of MnSOD was present in individual glioma cell lines and may be due to subpopulations or cells at different differentiation stages. Less difference in CuZnSOD, catalase, or glutathione peroxide was found between human and rat glioma cells. The human glioma cell lines showed large differences in sensitivity to the glutathione modulating drugs 1,3-bis (2-chloroethyl)-1-nitrosourea (BCNU) and buthionine sulfoximine (BSO). A good correlation was found between sensitivity to BCNU and the activities of catalase in these cell lines. Only one cell line was sensitive to BSO and this line had low CuZnSOD activity.

PMID: 10641728 [PubMed - indexed for MEDLINE]

Protein abundancy and mRNA levels of the adipocyte-type fatty acid binding protein correlate in non-invasive and invasive bladder transitional cell carcinomas.

Gromova I, Gromov P, Wolf H, Celis JE.

Department of Medical Biochemistry and Danish Centre for Human Genome Research, The University of Aarhus, Aarhus C, Denmark.

The adipocyte type fatty acid-binding protein (A-FABP) is a small molecular weight fatty acid-binding protein whose expression correlates both with the grade of atypia and the stage of bladder transitional cell carcinomas (TCCs). To determine if the protein abundancy correlates with the mRNA levels in non-invasive and invasive lesions, we have analysed fresh TCCs (grade II, Ta; grade III, T2-4) by two-dimensional polyacrylamide gel electrophoresis (2D-PAGE) and measured the mRNA levels using the reverse transcription linked polymerase chain reaction (RT-PCR). Overall, the results showed a good correlation between protein abundancy and mRNA levels, indicating that the lack of expression of the protein observed in some lesions reflects low levels of transcription of the A-FABP gene rather than translational regulation. In addition, our studies showed that the loss of A-FABP protein observed in some tumors is not compensated by an increase in the skin fatty acid-binding protein PA-FABP, as is the case in the A-FABP knockout mice.

PMID: 9664136 [PubMed - indexed for MEDLINE]



[3H]MK-801 binding and the mRNA for the NMDAR1 subunit of the NMDA receptor are differentially distributed in human and rat forebrain.

Meoni P, Mugnaini M, Bunnemann BH, Trist DG, Bowery NG.

Department of Pharmacology, Medical School, University of Birmingham, UK.
meonip@novell5.bham.ac.uk

The distributions of [3H]MK-801 binding and the NMDA NR1 subunit mRNA were studied using receptor autoradiography and in-situ hybridization in rat and human brain whole-hemisphere coronal sections. Receptor protein detected by radioligand autoradiography and the mRNA for the key subunit of the receptor presented similar distributions in the forebrain, with a few areas showing an imbalance between the levels of mRNA and receptor protein. Human frontal cortex showed a relative abundance of NMDAR1 mRNA as compared to [3H]MK-801 binding. The same area in rat brain did not show any difference in the two distributions. In comparison, the rat claustrum presented a relative excess of NMDAR1 mRNA which was not detected in human sections. Human caudate nucleus exhibited relatively high levels of [3H]MK-801 binding that were unmatched in rat caudate. The hippocampi of either species presented similar levels of [3H]MK-801 binding and NMDAR1 mRNA, but when the two signals were measured in specific subfields of the hippocampal formation, the differential distribution of the two signals reflected the anatomy of hippocampal connections assuming a preferential dendritic distribution for MK-801 binding. Interestingly, rat and human hippocampi also showed some important species-dependent difference in the relative distribution of the receptor protein and mRNA. The data presented show an overall good correlation between the mRNA for the key subunit of the NMDA receptor and the functional receptor detected with radioligand binding and highlight the presence of local differences in their ratio. This may reflect different splicing of the mRNA for the NMDAR1 subunit in specific brain areas of rat and human. The species-dependent differences in the relative distribution of the mRNA for the key subunit of the NMDA receptor and that of a marker of functional receptors also highlights important differences in the NMDA function in rat and human brain.

PMID: 9526033 [PubMed - indexed for MEDLINE]

Quantitative determinations of the steady state transcript levels of hexokinase isozymes and glucose transporter isoforms in normal rat tissues and the malignant tumor cell line AH130.

Shinohara Y, Yamamoto K, Inoo K, Yamazaki N, Terada H.

Faculty of Pharmaceutical Sciences, University of Tokushima, Japan.
yasuo@ph.tokushima-u.ac.jp

The steady state transcript levels of the four hexokinase (HK) isozymes and four glucose transporter (GLUT) isoforms were determined quantitatively by Northern analysis of RNA samples from rat tissues using synthetic fragments of the RNAs encoding the HK isozymes and GLUT isoforms. Results showed that the levels of HK isozyme transcripts were low in rat tissues, the level of that most highly expressed, the type I isozyme (HKI), in the brain being 0.025% of the total poly(A)+ RNA. A good correlation was found between the reported HK activities and the total amounts of transcripts encoding all HK isozymes in various tissues, showing that the HK activities in tissues can be estimated from the total amount of transcripts encoding HK isozymes. The proposed associated expressions of HK isozymes and GLUT isoforms in particular tissues were confirmed at their transcript levels. The steady state transcript levels of type II HK and the type 1 GLUT isoform in the malignant tumor cell line AH130 were also determined quantitatively.

PMID: 9459591 [PubMed - indexed for MEDLINE]

Expression of the multidrug resistance-associated protein (MRP) mRNA and protein in normal peripheral blood and bone marrow haemopoietic cells.

Legrand O, Perrot JY, Tang R, Simonin G, Gurbuxani S, Zittoun R, Marie JP.

Laboratoire de Cinetique et de Cultures Cellulaires, Hotel Dieu, Paris, France.

We studied the expression of multidrug resistance-associated protein (MRP) in normal haemopoietic cells from peripheral blood and bone marrow. The MRP mRNA levels were estimated by RT/PCR and in situ hybridization (ISH) assay, and the protein levels by flow cytometry. 21 samples of peripheral blood and 21 samples of bone marrow (11 normal bone marrow donors, 10 patients in complete remission after chemotherapy for large cell lymphoma or acute myeloid leukaemia) were analysed. In peripheral blood the mean MRP mRNA level in CD3+ cells was statistically higher than in the other cells (3-fold by the methods used). The levels of MRP in CD3+ varied from one individual to another (4.5-34.8 units by RT/PCR and 5-23 grains/cell by ISH); however, this was proportional to the variation in all the cell lineages of same individual ($r = 0.84$). In bone marrow the mean MRP levels of the various cell lineages (including CD34+) were similar to the basal level in HL60 cells. Individual expression levels were again variable; however, there was no difference between untreated normal bone marrow and post chemotherapy normal bone marrow. MRP protein expression was determined by flow cytometry with the monoclonal antibody MRPM6. The CD4+ lymphocytes exhibited a higher MRP protein expression than the other cell lineages, including CD8+ cells. There was a good correlation between the three methods used (RT/PCR and ISH, $P = 0.0001$, $r = 0.87$; RT/PCR and flow cytometry, $P = 0.0001$, $r = 0.85$; ISH and flow cytometry, $P = 0.002$, $r = 0.67$).

PMID: 8757504 [PubMed - indexed for MEDLINE]



Rat kidney glutamyl aminopeptidase (aminopeptidase A): molecular identity and cellular localization.

Song L, Ye M, Troyanovskaya M, Wilk E, Wilk S, Healy DP.

Department of Pharmacology, Mount Sinai School of Medicine, City University of New York, New York 10029.

Glutamyl aminopeptidase [aminopeptidase A (EAP), EC 3.4.11.7] is an ectoenzyme that selectively hydrolyzes acidic amino acid residues from the amino terminus of oligopeptides. EAP activity is highest within the kidney and small intestine. The murine pre-B cell BP-1/6C3 and the human kidney glycoprotein gp160 differentiation antigens have been reported to have biochemical properties indistinguishable from EAP. It is not known, however, if rat kidney EAP is a homologue of these antigens or molecularly distinct. Using the reverse transcription-polymerase chain reaction method with oligonucleotide primers based on the BP-1/6C3 nucleotide sequence, we isolated a 450-bp partial cDNA from rat kidney poly(A)+ RNA. The partial cDNA encoded a predicted protein that was 92% and 86% identical to the murine BP-1/6C3 and human gp160 antigens, respectively; the amino acid sequence within the zinc-binding domain was completely conserved. Purification of EAP from rat kidney and microsequence analysis of a tryptic digest peptide fragment (18-mer) indicated that the fragment was highly similar to a region within the BP-1/6C3 and gp160 proteins. Northern blot hybridization and immunoblot analyses were also consistent with labeling of products the same size as reported for the BP-1/6C3 and gp160 antigens. There was a good correlation between the cellular distribution of EAP mRNA and EAP immunoreactivity, with proximal tubules and glomerular mesangial cells having the highest densities. These results indicate that rat kidney EAP is a species homologue of the murine BP-1/6C3 and human gp160 antigens. Furthermore, on the basis of its cellular localization, rat kidney EAP is likely to be involved in degradation of oligopeptides within the glomerulus and the glomerular filtrate. Since cells that express EAP also express receptors for angiotensin II, an intrarenal vasoactive hormone that is a substrate for EAP, these results further suggest that EAP may play a role in modulating the activity of intrarenal angiotensin II.

PMID: 7943354 [PubMed - indexed for MEDLINE]

Differential expression of the short and long forms of the gamma 2 subunit of the GABAA/benzodiazepine receptors.

Miralles CP, Gutierrez A, Khan ZU, Vitorica J, De Blas AL.

Division of Molecular Biology and Biochemistry, School of Biological Sciences,
University of Missouri-Kansas City 64110-2499.

The distribution of the mRNAs encoding the gamma 2S and gamma 2L subunits of the GABAA receptor in the rat brain has been revealed by in situ hybridization, northern blot and dot blot analysis using specific antisense oligonucleotides. In addition, the quantitative distribution of the gamma 2S and gamma 2L subunit peptides participating in the fully assembled GABAA receptors/benzodiazepine receptors has been mapped by immunoprecipitation with specific anti-gamma 2S and anti-gamma 2L antibodies. Several neuronal types and brain regions are enriched in gamma 2L such as neurons of the layer II of striate cortex and cerebellar Purkinje cells as well as the inferior colliculus, superior colliculus, deep cerebellar nuclei, medulla and pons. Other neuronal types and regions are enriched in gamma 2S such as the mitral cells of the olfactory bulb, pyramidal neurons of the pyriform cortex, layer VI of the neocortex, granule cells of the dentate gyrus and pyramidal cells of the hippocampus. Other cortical areas and cerebellar granule cells express both gamma 2S and gamma 2L in comparable amounts. There is a good correlation between the relative expression of gamma 2S and gamma 2L mRNAs and the relative presence of these protein subunits in fully assembled and mature receptors in the studied brain regions. The differential distribution of gamma 2S and gamma 2L might result in differential ethanol sensitivity of the neurons expressing these GABAA receptor subunits.

PMID: 7968350 [PubMed - indexed for MEDLINE]

Cell proliferation in human soft tissue tumors correlates with platelet-derived growth factor B chain expression: an immunohistochemical and in situ hybridization study.

Wang J, Coltrera MD, Gown AM.

Department of Pathology, University of Washington, Seattle 98195.

The authors tested the hypothesis that the B chain of the platelet-derived growth factor (PDGF), a known connective tissue mitogen and growth factor, could be expressed by human soft tissue tumors, and that its expression could play a role in the control of cell proliferation in these tumors. Using a set of 56 soft tissue tumors, including benign tumors and all three grades of sarcomas, PDGF-B chain protein was localized using immunohistochemistry and PDGF-B mRNA was localized using in situ hybridization. The hypothesis that PDGF-B expression was related to cell proliferation was tested by simultaneously demonstrating the expression of the proliferating cell nuclear antigen in sequential tissue sections of the same tumors. Sixty and 82% of tumors had demonstrable PDGF-B mRNA and protein, respectively, with a strong correlation between their degrees of expression ($P = 0.0001$). Among the sarcomas, a strong correlation between PDGF-B expression and increasing malignant tumor grade ($P = 0.006$), and between PDGF-B expression and increasing proliferating cell nuclear antigen index ($P = 0.01$) was found. All tumors were also demonstrated to express the beta receptor of PDGF via immunohistochemistry. These studies suggest that PDGF-B expression may be an important mediator of cell proliferation control, via an autocrine mechanism, in human soft tissue tumors and may correlate with clinical outcome in the sarcomas.

PMID: 7903911 [PubMed - indexed for MEDLINE]

Expression of cytokines and growth factors in human glomerulonephritides.

Waldherr R, Noronha IL, Niemir Z, Kruger C, Stein H, Stumm G.

Department of Pathology, University of Heidelberg, Germany.

Numerous experimental studies point to the potential role of cytokines and growth factors in the pathogenesis of renal disease. However, from the various autocrine and paracrine mediators identified in vitro and in animal models, so far only a few have been demonstrated in selected human glomerulopathies. We examined two types of glomerulonephritis (GN): extracapillary GN with anti-neutrophil cytoplasmic autoantibodies (ANCA), an example of an acute form of GN, and mesangial IgA GN, usually a chronic form of GN, with immunocytochemistry, in situ hybridization and the polymerase chain reaction. Normal renal tissue from tumour nephrectomies served as a control. In ANCA-positive GN with active renal lesions (crescents, glomerular and vascular necrosis), infiltrating mononuclear cells in glomeruli and in the interstitium expressed interleukin (IL)-1 beta, tumour necrosis factor (TNF)-alpha, IL-2, interferon (IFN)-gamma, platelet-derived growth factor (PDGF) and transforming growth factor (TGF)-beta. Cytokine expression was also observed in activated resident cells, including endothelial cells, capsular epithelial cells, smooth muscle cells of vessel walls, fibroblasts and some tubular epithelial cells. In addition, we noted an increase in the cytokine and growth factor receptors TNF-R, IL-1R type II, IL-2R, IFN-gamma R and PDGF beta-R. In contrast, in mesangial IgA-GN, IL-1 beta, TNF-alpha, IFN-gamma and IL-2 were usually absent in glomeruli. Mesangial expansion in this disorder was accompanied by an increased expression of PDGF, PDGF beta-R, TGF-beta and IL-6 in mesangial areas. In both conditions a good correlation was observed between cytokine expression at the mRNA (in situ hybridization) and protein level (immunocytochemistry). (ABSTRACT TRUNCATED AT 250 WORDS)

Publication Types:

- Review
- Review, Tutorial

PMID: 8398664 [PubMed - indexed for MEDLINE]

Comment in:

- J Invest Dermatol. 1994 Nov;103(5):742-4.

T-cell receptor V beta-family usage in primary cutaneous and primary nodal T-cell non-Hodgkin's lymphomas.

Preesman AH, Hu HZ, Tilanus MG, de Geus B, Schuurman HJ, Reitsma R, van Wichen DF, van Vloten WA, de Weger RA.

Department of Pathology, University Hospital Utrecht, The Netherlands.

To evaluate whether the expression of T-cell receptor (TCR) V beta families in eight cases of malignant T-cell lymphomas took place in a preferential manner, we analyzed four cases of mycosis fungoides (MF), the most common form of primary cutaneous T-cell non-Hodgkin's lymphomas (NHL), and four cases of primary nodal T-cell NHL. The usage of V beta families in T-cell populations was investigated on mRNA that was transcribed to cDNA using a C beta primer and reverse transcriptase. Subsequently, the specific usage of the families was analyzed by polymerase chain reaction (PCR) using combinations of the selected C beta-oligonucleotide primer and one of the family-specific V beta primers. Peripheral blood lymphocytes from four healthy volunteers and 1 "reactive" lymph node served as a control and expressed all 20 V beta families tested for. In T-cell lines, with restricted V beta expression, and in three patients with advanced MF, only one or two V beta families were expressed at the mRNA level. In an early MF lesion this monoclonal expression was absent: several V beta families were expressed with a weak intensity. This may indicate either a polyclonal origin of MF, or that too few monoclonal neoplastic cells were present in the tissue specimen. In the four nodal T-cell NHL, only one family could be clearly distinguished, whereas some of the other V beta families showed only a weak expression. These latter families represent the reactive T-cell component in the nodal T-cell NHL. Both in nodal T-cell NHL and in MF there was no preferential expression of a particular V beta family. There was a good correlation between PCR data and the expression of V beta-family protein products observed by immunohistochemistry on tissue sections of the T-cell lymphomas. All T-cell lines, three cases of MF, and three cases of nodal T-cell NHL showed a rearrangement of the TCR beta chain on DNA level.

PMID: 1331246 [PubMed - indexed for MEDLINE]

Expression of the pS2 gene in breast tissues assessed by pS2-mRNA analysis and pS2-protein radioimmunoassay.

Hahnel E, Robbins P, Harvey J, Sterrett G, Hahnel R.

Department of Pathology, University of Western Australia, Queen Elizabeth II Medical Centre, Nedlands.

The expression of the pS2 gene in breast tissues was assessed by measuring pS2-protein using a radioimmunoassay, and by determining pS2-mRNA using Northern blotting. There was a good correlation between the two measurements, indicating that expression of the pS2 gene in breast tissues may be assessed by either method. Since radioimmunoassay is technically easier and more efficient than Northern blotting, radioimmunoassay will be the method of choice in routine applications.

PMID: 1463873 [PubMed - indexed for MEDLINE]



Modulation of the glutamatergic receptors (AMPA and NMDA) and of glutamate vesicular transporter 2 in the rat facial nucleus after axotomy.

Eleore L, Vassias I, Vidal PP, de Waele C.

LNRS (CNRS-Paris V), ESA 7060, Centre Universitaire des Saints-Peres, 45 rue des Saints-Peres, 75270 Paris Cedex 06, France.

Facial nerve axotomy is a good model for studying neuronal plasticity and regeneration in the peripheral nervous system. We investigated in the rat the effect of axotomy on the different subunits of excitatory glutamatergic AMPA (GLuR1-4), NMDA (NR1, NR2A-D) receptors, post-synaptic density 95, vesicular glutamate transporter 2, beta catenin and cadherin. mRNA levels and/or protein production were analyzed 1, 3, 8, 30 and 60 days after facial nerve axotomy by in situ hybridization and immunohistochemistry. mRNAs coding for the GLuR2-4, NR1, NR2A, B, D subunits of glutamatergic receptors and for post-synaptic density 95, were less abundant after axotomy. The decrease began as early as 1 or 3 days after axotomy; the mRNAs levels were lowest 8 days post-lesion, and returned to normal or near normal 60 days after the lesion. The NR2C subunit mRNAs were not detected in either lesioned or intact facial nuclei.

Immunohistochemistry using specific antibodies against GLuR2-3 subunits and against NR1 confirmed this down-regulation. There was also a large decrease in vesicular glutamate transporter 2 immunostaining in the axotomized facial nuclei at early stages following facial nerve section. In contrast, no decrease of NR2A subunit and of post-synaptic density 95 could be detected at any time following the lesion. beta Catenin and cadherin immunoreactivity pattern changed around the cell body of facial motoneuron by day 3 after axotomy, and then, tends to recover at day post-lesion 60 days. Therefore, our results suggest a high correlation between restoration of nerve/muscle synaptic contact, synaptic structure and function in facial nuclei. To investigate the mechanisms involved in the change of expression of these proteins following axotomy, the facial nerve was perfused with tetrodotoxin for 8 days. The blockade of action potential significantly decreased GLuR2-3, NR1 and NR2A mRNAs in the ipsilateral facial nuclei. Thus, axotomy-induced changes in mRNA abundance seemed to depend partly on disruption of activity.

PMID: 16182453 [PubMed - in process]



High-level mRNA quantification of proliferation marker pKi-67 is correlated with favorable prognosis in colorectal carcinoma.

Ihmann T, Liu J, Schwabe W, Hausler P, Behnke D, Bruch HP, Broll R, Windhovel U, Duchrow M.

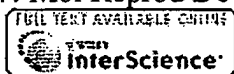
St. Elisabeth Klinik, Klinik fur Anesthesiologie, Schmerztherapie und Intensivmedizin, Saarlouis, Germany.

PURPOSE: The present study retrospectively examines the expression of pKi-67 mRNA and protein in colorectal carcinoma and their correlation to the outcome of patients. **METHODS:** Immunohistochemistry and quantitative RT-PCR were used to analyze the expression of pKi-67 in 43 archival specimens of patients with curatively resected primary colorectal carcinoma, who were not treated with neo-adjuvant therapy. **RESULTS:** We determined a median pKi-67 (MIB-1) labeling index of 31.3% (range 10.3-66.4%), and a mean mRNA level of 0.1769 (DeltaC(T): range 0.01-0.69); indices and levels did not correlate. High pKi-67 mRNA DeltaC(T) values were associated with a significantly favorable prognosis, while pKi-67 labeling indices were not correlated to prognostic outcome. A multivariate analysis of clinical and biological factors indicated that tumor stage (UICC) and pKi-67 mRNA expression level were independent prognostic factors. **CONCLUSION:** Quantitatively determined pKi-67 mRNA can be a good and new prognostic indicator for primary resected colorectal carcinoma.

Publication Types:

- [Evaluation Studies](#)

PMID: 15449182 [PubMed - indexed for MEDLINE]



c-fos and estrogen receptor gene expression pattern in the rat uterine epithelium during the estrous cycle.

Mendoza-Rodriguez CA, Merchant-Larios H, Segura-Valdez ML, Moreno-Mendoza N, Cruz ME, Arteaga-Lopez P, Camacho-Arroyo I, Dominguez R, Cerbon M.

Facultad de Quimica, Universidad Nacional Autonoma de Mexico, Ciudad Universitaria, Coyoacan 04510, Mexico, D.F., Mexico.

Different studies in ovariectomized estrogen treated animals support the idea that c-fos plays a role in the proliferation of uterine epithelial cells. However, these studies invite us to reassess the role played by c-fos in epithelial cell types of the endometrium during the estrous cycle. The present study was undertaken to determine the c-fos and estrogen receptor (ER) gene expression pattern in the rat uterine epithelium during the estrous cycle in which natural and cyclic changes of steroid hormones occur, and correlate these changes with the proliferation status of this cellular types. Proliferation was assessed during the estrous cycle using bromodeoxyuridine incorporation to DNA. ERalpha and beta proteins were assessed by immunohistochemistry. The regulation of c-fos gene expression in the uterus of intact animals during the estrous cycle was evaluated using both in situ hybridization and immunohistochemistry. Estradiol (E(2)) and progesterone (P(4)) plasma levels were assessed by radioimmunoassay. The results indicated that luminal (LE) and glandular epithelia (GE) presented maximal proliferation during the metestrus (M) and the diestrus (D) days. However, during the proestrus (P) day only LE presented proliferation, and during the estrus (E) day only the stromal cells proliferated. A marked immunostaining for ERalpha was detected in both LE and GE cells during the early phases of the cycle but diminished on the P and the E day. In contrast, ERbeta was undetectable in both epithelia during all stages of the cycle. The highest c-fos mRNA level was detected in both epithelia on the M day, followed by a significant reduction during the other days of the cycle. The highest protein content was observed on the M and D days, and the minimal value was detected on the E day. The c-Fos protein level in LE was increased during M and D days, presenting a high correlation with the cellular proliferation pattern of this cell type. In conclusion, the overall results indicate that c-Fos protein presented a good correlation with uterine epithelial cell proliferation of LE. In the case of GE, the same tendency was observed, although no significant correlation was found. Both in LE and GE, c-fos mRNA did not strictly correlate with its protein levels. c-fos seems to have a postranscriptional regulation in uterine epithelial cells during the rat's estrous cycle. Copyright 2003 Wiley-Liss, Inc.

PMID: 12589649 [PubMed - indexed for MEDLINE]

FREE full text article at
clincancerres.aacrjournals.org

Thymidine kinase, thymidylate synthase, and dihydropyrimidine dehydrogenase profiles of cell lines of the National Cancer Institute's Anticancer Drug Screen.

Grem JL, Danenberg KD, Behan K, Parr A, Young L, Danenberg PV, Nguyen D, Drake J, Monks A, Allegra CJ.

Developmental Therapeutics Department, Medicine Branch, Division of Clinical Sciences, National Cancer Institute at the National Naval Medical Center, Bethesda, Maryland 20889, USA.

PURPOSE: To determine the expression of three targets of 5-fluorouracil (5-FU) and 5-fluoro-2'-deoxyuridine (FdUrd) in human tumor cell lines and to compare these with the 50% growth inhibition concentrations (GI(50)) from the National Cancer Institute database. **EXPERIMENTAL DESIGN:** Thymidine kinase (TK) activity was assessed by conversion of [(3)H]thymidine to [(3)H]TMP. Thymidylate synthase (TS) protein expression was determined by Western analysis. TS and dihydropyrimidine dehydrogenase (DPD) mRNA expression were measured by quantitative reverse transcription-PCR. **RESULTS:** The median (range) for the targets were as follows: 5-FU GI(50), 20.8 microM (0.8-536); FdUrd GI(50), 0.75 microM (0.25-237); TK, 0.93 nmol/min/mg (0.16-5.7); in arbitrary units: TS protein, 0.41 (0.05-2.95); TS mRNA, 1.05 (0.12-6.41); and DPD mRNA, 1.09 (0.00-24.4). A moderately strong correlation was noted between 5-FU and FdUrd GI(50)s ($r = 0.60$), whereas a weak-moderate correlation was seen between TS mRNA and protein expression ($r = 0.45$). Neither TS expression nor TK activity correlated with 5-FU or FdUrd GI(50)s, whereas lines with lower DPD expression tended to be more sensitive to 5-FU. Cell lines with faster doubling times and wild-type p53 were significantly more sensitive to 5-FU and FDURD. **CONCLUSIONS:** The lack of correlation may in part be attributable to the influence of downstream factors such as p53, the observation that the more sensitive cell lines with faster doubling times also had higher TS levels, and the standard procedure of the screen that uses a relatively short (48-h) drug exposure.

PMID: 11309351 [PubMed - indexed for MEDLINE]

FREE full text article at
bjo.bmjournals.com

Intravitreal invading cells contribute to vitreal cytokine milieu in proliferative vitreoretinopathy.

El-Ghrably IA, Dua HS, Orr GM, Fischer D, Tighe PJ.

Larry A Donoso Laboratory for Eye Research, Department of Ophthalmology, University of Nottingham, UK.

AIM: To examine the contribution of infiltrating cells in the local production of cytokines within the vitreous of patients with proliferative vitreoretinopathy (PVR). **METHODS:** The presence of mRNA coding for IL-6, IL-8, IL-1beta, IL-1alpha, TNFalpha, IFNgamma, IL-12, and HPRT was investigated in 25 vitreous samples from patients with PVR, 11 vitreous samples from patients with retinal detachment (RD) not complicated by PVR, and 10 vitreous samples from patients with macular hole (MH). A quantitative reverse transcriptase polymerase chain reaction (RT-PCR) using an internal competitor was used to investigate these samples. From these samples, 15 PVR, 8 RD, and 8 MH were analysed for the protein levels of the same cytokines using enzyme linked immunosorbent assay (ELISA). Spearman correlation was used to test any association between mRNA and cytokine protein levels, as an indicator of the contribution these cells make to the intravitreal cytokine milieu. **RESULTS:** A strong correlation was found between mRNA and their respective cytokine levels (protein products) for IL-6, IL-8, IL-1beta, IL-1alpha, TNFalpha, IFNgamma (Spearman $r = 0.83, 0.73, 0.67, 0.91, 0.73,$ and 0.73 respectively), but not for IL-12. The median levels of IL-6, IL-8, IL-1beta, and IFNgamma mRNA and their respective cytokines were significantly higher ($p < 0.05$) in patients with PVR than in those with macular hole. There was no statistically significant difference in the median levels of IL-1alpha mRNA between PVR and MH but the cytokine IL-1alpha was detected at a significantly higher level in PVR compared with MH patients. Between PVR and RD patients, there was no statistically significant difference in mRNA levels for all the investigated cytokines ($p > 0.05$) except for IL-6 where there was a statistical significance ($p = 0.038$). In contrast, the median levels of IL-6, IL-8, and IL-1beta cytokines were significantly higher ($p < 0.05$) in patients with PVR than in those with RD, whereas for IL-1alpha and IFNgamma no significant statistical difference was detected between PVR and RD patients ($p > 0.05$). When results of RD and MH patients were compared, a statistical difference was only detected in mRNA levels of IFNgamma ($p = 0.008$). However, no difference was detected for IFNgamma (protein product) or for any of the other cytokines between RD and MH patients. **CONCLUSION:** Levels of both protein and mRNA encoding IL-6, IL-8, IL-1beta, and IFNgamma is significantly increased in vitreous samples from patients with PVR. The strong correlation between ELISA detectable cytokines (protein products) and their respective mRNA levels suggest that intravitreal, invasive cells are the major source of these cytokines, with the exception of IL-12. Cells invading the vitreous do not appear to locally produce IL-12 mRNA. This would appear to implicate cells peripheral to the

vitreal mass as the major source of this cytokine.

PMID: 11264138 [PubMed - indexed for MEDLINE]



Human hepatic microsomal epoxide hydrolase: comparative analysis of polymorphic expression.

Hassett C, Lin J, Carty CL, Laurenzana EM, Omiecinski CJ.

Department of Environmental Health, University of Washington, Seattle 98105-6099, USA.

Interindividual variation in the expression of human microsomal epoxide hydrolase (mEH) may be an important risk factor for chemically induced toxicities, including cancer and teratogenesis. In this study, phenotypic variability and mEH genetic polymorphisms were examined in a bank of 40 transplant-quality human liver samples. Immunochemically determined protein content, enzymatic activities, polymorphic amino acids, as well as mEH RNA levels were evaluated in parallel. Enzymatic activity was assessed using (+/-)-benzo[a]pyrene-4,5-epoxide at 2 substrate concentrations. The relative hydrolyzing activities obtained using saturating substrate levels were highly correlated ($r = 0.85$) with results derived from limiting substrate concentrations and exhibit approximately an 8-fold range in activity levels across the panel of 40 liver samples. mEH enzyme activity also demonstrated strong correlation ($r > \text{or} = 0.74$) with an 8.4-fold variation determined for mEH protein content within the same samples. However, these protein/activity measurements were poorly correlated ($r < \text{or} = 0.23$) with mEH RNA levels, which exhibited a 49-fold variation. Two common polymorphic amino acid loci in the mEH protein did not exclusively account for variation in enzymatic activity, although this conclusion is confounded by heterozygosity in the samples. These data demonstrate the extent of hepatic mEH functional variability in well-preserved human tissues and suggest that polymorphism of mEH protein expression is regulated in part by posttranscriptional controls, which may include nonstructural regulatory regions of the mEH transcript.

PMID: 9016823 [PubMed - indexed for MEDLINE]



401: Biochem Biophys Res Commun. 1995 Sep 25;214(3):1009-14.

[Related Articles](#), [Links](#)



Differential expression of heat shock protein 70 in well healing and chronic human wound tissue.

Oberringer M, Baum HP, Jung V, Welter C, Frank J, Kuhlmann M, Mutschler W, Hanselmann RG.

Department of Traumatology, University of Saarland, Germany.

Heat shock protein 70 (hsp 70) is an important member of the heat shock protein family, which is induced by different forms of stress. We attempted to find out if hsp 70 is also involved in wound healing, which likewise resembles a stress situation for cells too. Therefore we collected tissue samples from well healing and chronic human wound tissue. We used Northern- and Western-blot analysis to study the expression of hsp 70. At the protein level we found a strong correlation between well healing wounds and high expression of hsp 70, whereas chronic wounds showed no or weak expression. Interestingly hsp 70 mRNA did not show this significant correlation, displaying a variant expression pattern in the same kind of wound tissue, possibly due to unknown posttranscriptional regulating step, which has to be investigated in further studies. To localize hsp 70 mRNA and protein was used insitu hybridization and immunohistochemistry. Both displayed an overexpression in endothelial cells of capillary vessels.



Pre-translational regulation of cytochrome P450 genes is responsible for disease-specific changes of individual P450 enzymes among patients with cirrhosis.

George J. Liddle C, Murray M, Byth K, Farrell GC.

Department of Gastroenterology and Hepatology, University of Sydney at Westmead Hospital, NSW, Australia.

We have recently reported that disease-specific differential alterations in the hepatic expression of xenobiotic-metabolizing cytochrome P450 (CYP P450) enzymes occur in patients with advanced liver disease. In order to determine whether the observed changes in CYP proteins are modulated at pre- or post-translational levels, we have now examined the hepatic levels of mRNA for CYPs 1A2, 2C9, 2E1 and 3A4 by solution hybridization in the same livers of 20 controls (surgical waste from histologically normal livers), 32 cases of hepatocellular and 18 of cholestatic severe chronic liver disease. CYP1A2 mRNA and CYP1A immunoreactive protein were both reduced in livers with hepatocellular and cholestatic types of cirrhosis. In contrast, CYP3A4 mRNA and protein were reduced only in livers from patients with hepatocellular diseases. For 1A2 and 3A4 there were significant correlations between mRNA species and the respective protein contents ($r_{S1A2} = 0.74$, $r_{S3A4} = 0.64$, $P < 0.0001$). CYP2C9 mRNA was reduced in patients with both cholestatic and hepatocellular types of liver disease, but 2C protein was reduced only in patients with cholestatic dysfunction. The correlation between CYP2C9 mRNA and protein, was also significant ($r_s = 0.36$, $P < 0.005$) but mRNA levels accounted for only 13% of the variability in protein rankings. This is probably a consequence of other CYP2C proteins apart from 2C9 being detected by the anti-2C antibody. CYP2E1 mRNA and protein were reduced in patients with cholestatic liver disease, but in hepatocellular disease the expression of only CYP2E1 mRNA was decreased. CYP2E1 mRNA was significantly correlated with CYP2E1 protein but accounted for only 18% of the variability in protein rankings ($r_s = 0.43$, $P < 0.0005$). Taken collectively these data indicate that the disease-specific alterations of xenobiotic-metabolizing CYP enzymes among patients with cirrhosis is due, at least in part, to pre-translational mechanisms. The lack of a strong correlation between CYP2E1 mRNA and protein suggests that this gene, like its rat orthologue, may be subject to pre-translational as well as translational and/or post-translational regulation.

PMID: 7741759 [PubMed - indexed for MEDLINE]

Cell localization and regulation of expression of cytochrome P450 1A1 and 2B1 in rat lung after induction with 3-methylcholanthrene using mRNA hybridization and immunohistochemistry.

Pairon JC, Trabelsi N, Buard A, Fleury-Feith J, Bachelet CM, Poron F, Beaune P, Brochard P, Laurent P.

INSERM Unite 139, Hopital Henri Mondor, Creteil, France.

In order to characterize the response of various pulmonary cell types to polycyclic aromatic hydrocarbons, the expression of cytochrome P450 (CYP) 1A1 and 2B1 mRNA in the lung of rats, with or without induction by 3-methylcholanthrene (3MC), was analyzed by in situ hybridization using appropriate 35S-labeled riboprobes. The expression of the corresponding proteins was investigated immunohistochemically. Following induction with 3MC, the kinetics of mRNA expression differed considerably between Clara cells and type II pneumocytes and venous endothelial cells. In Clara cells, mRNA expression was detected as early as 1 h after induction, peaked between 2 and 4 h, and was completely undetectable at 14 h. In contrast, venous endothelial cells and type II pneumocytes exhibited permanent mRNA expression of CYP 1A1 in 3MC-pretreated rats. These kinetic results explain the striking absence of correlation between mRNA and protein expression observed in Clara cells 24 h after the end of the induction protocol, as these cells exhibited intense protein expression with no mRNA. In contrast, a good correlation was observed for mRNA and protein expression of CYP 2B1, with similar expressions for Clara cells and type II pneumocytes, but no expression in endothelial cells. This study clearly distinguished the regulation of CYP 1A1 expression in the rat lung from that described in the liver. The differences observed in the various lung cell types, whatever the post-transcriptional mechanisms involved, emphasize that studies must be performed at the cellular level in order to understand the specific response to xenobiotics, not only of this organ as a whole but also of its various anatomic structures.

PMID: 7917307 [PubMed - indexed for MEDLINE]

Cellular location and age-dependent changes of the regulatory subunits of cAMP-dependent protein kinase in rat testis.

Landmark BF, Oyen O, Skalhegg BS, Fauske B, Jahnsen T, Hansson V.

Institute of Medical Biochemistry, University of Oslo, Norway.

This study was undertaken to examine the expression and cellular location of the various cAMP-dependent protein kinase (PKA) subunits in different testicular cell types, using cDNA probes, isoenzyme-specific antibodies and activity measurements. Amounts of mRNA and protein were examined in cultured Sertoli cells, cultured peritubular cells, germ cells (pachytene spermatocytes, round spermatids), Leydig cell tumours as well as whole testes from rats of various ages. In Sertoli cells, there was a good correlation between the amount of mRNA and the respective immunoreactive proteins. In other types of cell, such as germ cells and Leydig tumour cells, this was not always the case. Large amounts of RII beta mRNA were found in Leydig tumour cells, whereas the amount of immunoreactive protein was low. Furthermore, large amounts of small-sized, germ cell-specific mRNAs for RI alpha (1.7 kb) and RII alpha (2.2 kb) were also found in the developing rat testis after 30 to 40 days of age, but the large amounts of mRNA were only partially reflected at the protein level. Pachytene spermatocytes and round spermatids were practically devoid of both RII alpha and RII beta protein. During spermatid differentiation, there was a decrease in RI alpha and an increase in RII alpha protein. Cell specific distribution of the various PKA subunits in testicular cell types is described. In some types of cell, discrepancies between mRNA and protein were demonstrated, which clearly suggest cell specific differences in translational efficiencies for some of these mRNAs, particularly the small-sized mRNAs for RI alpha and RII alpha in meiotic and post-meiotic germ cells.

PMID: 8107013 [PubMed - indexed for MEDLINE]

**This Page is Inserted by IFW Indexing and Scanning
Operations and is not part of the Official Record**

BEST AVAILABLE IMAGES

Defective images within this document are accurate representations of the original documents submitted by the applicant.

Defects in the images include but are not limited to the items checked:

- ☐ **BLACK BORDERS**
- ☐ **IMAGE CUT OFF AT TOP, BOTTOM OR SIDES**
- ☐ **FADED TEXT OR DRAWING**
- ☐ **BLURRED OR ILLEGIBLE TEXT OR DRAWING**
- ☐ **SKEWED/SLANTED IMAGES**
- ☐ **COLOR OR BLACK AND WHITE PHOTOGRAPHS**
- ☐ **GRAY SCALE DOCUMENTS**
- ☒ **LINES OR MARKS ON ORIGINAL DOCUMENT**
- ☐ **REFERENCE(S) OR EXHIBIT(S) SUBMITTED ARE POOR QUALITY**
- ☐ **OTHER:** _____

IMAGES ARE BEST AVAILABLE COPY.

As rescanning these documents will not correct the image problems checked, please do not report these problems to the IFW Image Problem Mailbox.